PHOSPHONIC-BASED HF ACID: INTERACTIONS WITH CLAY MINERALS AND FLOW IN SANDSTONE CORES

A Dissertation

by

LIJUN ZHOU

Submitted to the Office of Graduate and Professional Studies of
Texas A&M University
in partial fulfillment of the requirements for the degree of

DOCTOR OF PHILOSOPHY

Chair of Committee,	Hisham A. Nasr-El-Din
Committee Members,	Maria A. Barrufet
	Robert H. Lane
	Mahmoud El-Halwagi
Head of Department,	A. Daniel Hill

May 2015

Major Subject: Petroleum Engineering

ABSTRACT

Regular mud acid, which is composed of HCl and HF, has been extensively used to remove the formation damage in sandstone reservoirs; however, many problems may occur during stimulation treatments with this acid. To overcome many of these drawbacks, phosphonic-based HF acid systems (HF and a phosphonic acid) have been used as an alternative to mud acid. However, very limited research has been performed to investigate the interactions of phosphonic-based acid systems with clay minerals in sandstone reservoirs.

Phosphonic-based acid has been used in the field. Reactions of this acid with clays and its propagation in sandstone cores have not been examined previously. Therefore, the main objectives of this study are to: 1) investigate the reaction of phosphonic-based acid systems with clay minerals; 2) evaluate the effect of acid concentration, temperature, and reaction time on the acid performance; 3) determine the nature of precipitate that might form during the reaction of this acid system with various clay minerals, and 4) conduct coreflood tests to determine the impact of this acid system on core permeability.

In this study, a phosphonic-based HF acid system with two HF concentrations (1.5 and 3 wt %) was used to evaluate the solubility of various clay minerals (kaolinite, bentonite, chlorite, and illite) as a function of time and temperature. Scanning electron microscopy (SEM) and energy-dispersive X-ray spectroscopy (EDS) were used to identify the reaction products. The pH of the solutions was measured using a HF

resistant electrode. The concentrations of key cations in the supernatant were analyzed using inductively coupled plasma optical emission spectrometry (ICP-OES). ^{19}F, ^{31}P, and ^{27}Al liquid nuclear magnetic resonance (NMR) spectroscopy were used for the first time to evaluate the reaction of this phosphonic-based HF acid system with clay minerals. Coreflood experiments on Berea sandstone cores were conducted at 300°F at a flow rate of 2 cm^3 /min using full strength phosphonic-based HF acid (3 wt% HF) and mud acid (12 wt% HCl/ 3 wt% HF).

No AlF_3 precipitate was identified by EDS and XRD analyses of the solid samples after kaolinite, bentonite, and illite reacted with full strength phosphonic-based HF acid system. Large amounts of AlF_3 were noticed in the chlorite samples after being treated with a full strength phosphonic-based HF acid system. The concentration of soluble Si decreases in the spent acid after full strength phosphonic-based HF acid reacted with clay minerals at 302°F. This indicated a secondary reaction that occurred at high temperatures decreasing the ratio of Si/Al. This result was further confirmed by the ^{19}F NMR results at high temperature. ^{19}F NMR results also showed that HF acid in the full strength phosphonic-based HF acid solution was completely consumed in 30 minutes when it reacted with clay minerals at a weight ratio of 10:1 at both 77 and 302°F. Coreflood tests showed significant permeability improvement to Berea sandstone when using full strength phosphonic-based HF acid systems compared to regular mud acid.

DEDICATION

TO MY PARENTS, MY FAMILY

ACKNOWLEDGEMENTS

I would like to express my sincere thanks to my supervising professor Dr. Hisham A. Nasr-El-Din. I am grateful for his assistance and guidance throughout my studies and research. I wish to extend my appreciation to Dr. Barrufet, Dr. Lane, and Dr. El-Halwagi for devoting their invaluable time to review my research work and evaluate its results.

Thanks also go to lab technicians, Joevan Beladi, and administrative officer, Kristina Hansen. I also want to extend my gratitude to my friends and colleagues and the department faculty and staff for making my time at Texas A&M University a great experience. I also want to extend my gratitude to Saudi Aramco for funding this research project.

Finally, thanks to my parents, my husband, Pengxi Li and my lovely kids for their encouragement, patient and endless love.

NOMENCLATURE

HF	Hydrofluoric Acid
HCl	Hydrochloric Acid
DI	Deionized Water
PV	Pore Volume
ICP	Inductively Coupled Plasma
wt%	Weight Percent
md	Millidarcy
CEC	Cation Exchange Capacity

TABLE OF CONTENTS

Page

ABSTRACT ii

DEDICATION iv

ACKNOWLEDGEMENTS v

NOMENCLATURE vi

TABLE OF CONTENTS vii

LIST OF FIGURES ix

LIST OF TABLES xv

CHAPTER I INTRODUCTION: THE IMPORTANCE OF RESEARCH 1

- Sandstone Acidizing 1
- Problems Associated with Mud Acid Treatments 4
  - Precipitation of Fluorides 4
  - Precipitation of Fluosilicate and Fluoaluminate Salts 5
  - Precipitation of Silica Gel 6
- Organic Acids/Chelating Agents in Sandstone Stimulation 10
- Clay Mineralogy 12
- Selection of Treatment Fluid for Sandstone Acidizing 22

CHAPTER II SANDSTONE ACIDIZING USING A PHOSPHONIC-BASED HF ACID SYSTEM 28

- Introduction 28
- Theory of HF-Based Acid Reactions 30
- NMR Analysis 32
- Objectives 36

CHAPTER III INTERACTIONS BETWEEN A PHOSPHONIC-BASED HF ACID AND CLAY MINERALS: SOLUBILITY TESTS 38

- Introduction 38
- Experiment Studies 38
  - Materials 38
  - Clay Particle Size Selection 40
  - Clay Solubility Tests 44

NMR Analysis 46
SEM/EDS Analysis 49
Results and Discussion 50
Effect of Reaction Time 50
Effect of Temperature 59
Effect of HF Acid Concentration 64
Effect of Acid to Clay Weight Ratio on Solubility 67
NMR Results 70
SEM/EDS and XRD Analyses 81
Conclusions 88

CHAPTER IV EVALUATION OF SANDSTONE ACIDIZING USING PHOSPHONIC-BASED HF ACID: COREFLOOD STUDIES 90

Introduction 90
Experimental Studies 91
Materials 91
Experimental Procedure 93
Results and Discussion 97
Stimulating Berea Sandstone Core Using Full Strength Phosphonic-based HF Acid without Preflush 97
Stimulation of Bandera Sandstone Using Phosphonic-based HF Acid 102
Coreflood Experiments on Berea Sandstone Cores Using Phosphonic-based HF Acid under Different Temperatures 104
Effect of Preflush on the Stimulation of Bandera Sandstone Using Phosphonic-based HF Acid 109
Stimulating Berea Sandstone Cores with Preflush Using Phosphonic-based HF Acid and 12:3 Mud Acid 118
Conclusions 129

CHAPTER V CONCLUSIONS 131

REFERENCES 133

LIST OF FIGURES

Page

Fig. 1—Components of sandstone (Civan 2000). 2

Fig. 2—Structure of the octahedral sheet (Murray 2007). 15

Fig. 3—Structure of the tetrahedral sheet (Murray 2007). 16

Fig. 4—Crystal structure of kaolinite (Civan 2000). 18

Fig. 5—Scanning electron micrograph of kaolinite (Murray 2007). 19

Fig. 6—Structure of Montmorillonite (Murray 2007) 20

Fig. 7—Crystal structure of illite (Murray 2007). 21

Fig. 8—Crystal Structure of Chlorite (Murray 2007). 22

Fig. 9—Chemical Structure of HEDPA (Lacour *et al. 1998*). 29

Fig. 10—^{19}F NMR spectrum of 13.5% HCl– 1.5 wt% HF reacted with kaolinite at room temperature (Shuchart and Gdanski 1996) 33

Fig. 11—^{19}F NMR spectra of aluminum solutions containing varying F/Al ratio (0.2 to 6.26) 35

Fig. 12—^{19}F NMR spectra of HF acid reacted with $Si(OH)_4$ at variable temperature (Shuchart and Gdanski 1996). 36

Fig. 13—Kaolinite particle size distribution histogram. 41

Fig. 14—Bentonite particle size distribution histogram. 42

Fig. 15—Chlorite particle size distribution histogram. 43

Fig. 16—Illite particle size distribution histogram. 44

Fig. 17—Optima 7000 DV Inductively Coupled Plasma (ICP) 45

Fig. 18—OFITE Aging Cell 46

Fig. 19—NMR Spectrometer 49

Fig. 20—Evex Mini- Scanning Electron Microscope (SEM) with MSC-1000 Mini Sputter Coater and energy-dispersive X-ray spectroscopy (EDS). 50

Fig. 21— Ion concentrations in the spent acids after full strength phosphonic-based HF acid reacted with kaolinite at 77°F. 51

Fig. 22— Ion concentrations in the spent acids after full strength phosphonic-based HF acid reacted with bentonite at 77°F. 52

Fig. 23— Ion concentrations in the spent acids after full strength phosphonic-based HF acid reacted with chlorite at 77°F. 53

Fig. 24— Ion concentrations in the spent acids after full strength phosphonic-based HF acid reacted with illite at 77°F. 54

Fig. 25—Ion concentrations in the spent acids after full strength phosphonic-based HF acid reacted with kaolinite at 302°F. 55

Fig. 26—Ion concentrations in the spent acids after full strength phosphonic-based HF acid reacted with bentonite at 302°F. 56

Fig. 27—Ion concentrations in the spent acids after full strength phosphonic-based HF acid reacted with chlorite at 302°F. 57

Fig. 28—Ion concentrations in the spent acids after full strength phosphonic-based HF acid reacted with illite at 302°F. 59

Fig. 29—Concentrations of key cations in the spent acid solutions after full strength phosphonic-based HF acid reacted with kaolinite at different temperatures for 30 minutes. 60

Fig. 30—Concentrations of key cations in the spent acid solutions after full strength phosphonic-based HF acid reacted with bentonite at different temperatures for 30 minutes. 61

Fig. 31—Concentrations of key cations in the spent acid solutions after full strength phosphonic-based HF acid reacted with chlorite illite at different temperatures for 30 minutes. 62

Fig. 32—Concentrations of key cations in the spent acid solutions after full strength phosphonic-based HF acid reacted with illite at different temperatures for 30 minutes. 63

Fig. 33—Si/Al molar ratio in the spent acids after full strength phosphonic-based HF acid reacted with clay minerals at different temperatures for 30 minutes. 64

Fig. 34—Si/Al molar ratio in the spent acids after full and half strength phosphonic-based HF acid reacted with clay minerals at 77°F for 30 minutes. 67

Fig. 35–Solubility of clays treated with full strength phosphonic-based HF acid system for 30 minutes at room temperature at different weight ratio. 68

Fig. 36–Si/Al molar ratio in the reaction precipitates when full strength phosphonic-based HF acid reacted with clay minerals at room temperature at different weight ratio, reaction time is 30 minutes. 69

Fig. 37—^{19}F NMR spectra after full strength phosphonic-based HF acid reacted with kaolinite for 24 hours at 77°F. 71

Fig. 38—^{19}F NMR spectra after full strength phosphonic-based HF acid reacted with bentonite for 24 hours at 77°F. 72

Fig. 39—^{19}F NMR spectra after full strength phosphonic-based HF acid reacted with chlorite for 24 hours at 77°F. 73

Fig. 40—^{19}F NMR spectra after full strength phosphonic-based HF acid reacted with illite for 24 hours at 77°F. 75

Fig. 41—Relative intensities of the ^{19}F NMR signals in the spent acid solutions after full strength phosphonic-based HF acid reacted with kaolinite for 30 minutes as a function of temperature. Relative intensities were determined by integrating the SiF_6^{2-}, SiF_5^-, AlF_3, AlF_2^+, and AlF^{2+} ^{19}F NMR peaks for each sample using $CFCl_3$ as internal reference. 78

Fig. 42—Liquid ^{31}P NMR spectra of (a) full strength phosphonic-based HF acid and (b) spent acid after the full strength phosphonic-based HF acid reacted with kaolinite for 24 hours. 79

Fig. 43—^{31}P NMR spectrum of full strength phosphonic-based HF acid mixed with 8,000 ppm $AlCl_3$. 80

Fig. 44— Elemental analysis of kaolinite after treated with full strength phosphonic-based HF acid at 77°F for 24 hours. 82

Fig. 45— Elemental analysis of bentonite after treated with full strength phosphonic-based HF acid at 77°F for 24 hours. 83

Fig. 46— Elemental analysis of chlorite after treated with the full strength phosphonic-based HF acid at 77°F for 24 hours. 84

Fig. 47— Elemental analysis of illite after treated with the full strength phosphonic-based HF acid at 77°F for 24 hours. 85

Fig. 48—Elemental analysis of chlorite before treated with full strength phosphonic-based HF acid. 86

Fig. 49—X-ray powder diffraction pattern of chlorite (a) before treated with the full strength phosphonic-based HF acid and (b) after treated with full strength phosphonic-based HF acid..... 87

Fig. 50—Coreflood Experiment Setup..... 94

Fig. 51—pH Meter and HF Resistant Submersible Electrode. 95

Fig. 52—Pressure drop across the Berea core treated by 2.5 PV of full strength phosphonic-based HF acid without preflush at 2 cm^3/min and 250°F. 98

Fig. 53—Analysis of coreflood effluent samples for Berea sandstone core treated without preflush and 2.5 PV of full strength phosphonic-based HF as main flush at 300°F and 2 cm^3/min. 100

Fig. 54—Analysis of coreflood effluent samples for Berea sandstone core treated without preflush and 3 PV of half strength phosphonic-based HF acid as main flush at 300°F and 2 cm^3/min. 101

Fig. 55—Pressure drop across the Bandera core treated by 2 PV of full strength phosphonic-based HF acid without preflush at 2 cm^3/min and 300°F 102

Fig. 56—Ions concentrations in the coreflood effluent samples for Bandera sandstone core treated by 2 PV of full strength phosphonic-based HF acid without preflush at 2 cm^3/min and 300°F 104

Fig. 57—Analysis of coreflood effluent samples for Berea sandstone core treated without preflush and 3PV of full strength phosphonic-based HF acid as main flush at 150°F and 3 cm^3/min 106

Fig. 58—Analysis of coreflood effluent samples for Berea sandstone core treated without preflush and 3PV of full strength phosphonic-based HF acid as main flush at 250°F and 3 cm^3/min. 107

Fig. 59—Analysis of coreflood effluent samples for Berea sandstone core treated without preflush and 3PV of full strength phosphonic-based HF acid as main flush at 300 °F and 3 cm^3/min 108

Fig. 60—Pressure drop across the Bandera cores treated by 0.6M GLDA (pH = 3.8), 0.6M HEDTA (pH = 3.8), and 9 wt% formic acid (pH = 1.75) at 2 cm^3/min and 300°F.....110

Fig. 61—Analysis of coreflood effluent samples for Bandera sandstone core treated with 10 PV of 0.6M GLDA (pH = 3.8) at 300°F and 2 cm^3/min. 111

Fig. 62—Analysis of coreflood effluent samples for Bandera sandstone core treated with 10PV of 0.6M HEDTA (pH = 4) at 300°F and 2 cm^3/min.....112

Fig. 63—Analysis of coreflood effluent samples for Bandera sandstone core treated with 10PV of 9 wt% formic acid (pH =1.75) at 300°F and 2 cm^3/min. 113

Fig. 64—Weight loss of Bandera cores after the coreflood experiments using 0.6M GLDA (pH = 3.8), 0.6M HEDTA (pH = 3.8), and 9 wt% formic acid (pH =1.75) at 2 cm^3/min and 300°F.....114

Fig. 65—Comparison between 0.6M GLDA (pH = 3.8), 0.6 M HEDTA (pH = 3.8), and 9 wt% formic Acid (pH =1.75) in stimulating Bandera sandstone cores.....115

Fig. 66—Amount of different cations, calcium, iron, and magnesium, in the coreflood effluent for Bandera cores treated by 0.6M GLDA (pH = 3.8), 0.6 M HEDTA (pH = 3.8), and 9 wt% formic Acid (pH =1.75) at 2 cm^3/min and 300°F. 116

Fig. 67—Analysis of coreflood effluent samples for Bandera sandstone core treated with 5 PV of 0.6M GLDA (pH =3.8) at 300°F and 2 cm^3/min. Shut in 2 hours after 5 PV GLDA.....118

Fig. 68—Pressure drop in the Berea coreflood experiment with 3 PV of 12:3 mud acid in the main flush at 300°F.....119

Fig. 69—Pressure drop across the core in the Berea coreflood experiment with 3 PV of full strength phosphonic-based HF acid as the main acid at 300°F. 120

Fig. 70—CT number across the Berea sandstone core before and after the acid treatment using HCl as a preflush and 3 PV of full strength phosphonic-based HF acid as the main flush at 300°F and 2 cm^3/min. 121

Fig. 71—CT number across the Berea sandstone core before and after treatment using HCl as a preflush and 3 PV of 12:3 mud acid as the main flush at 300°F and 2 cm^3/min. 123

Fig. 72—Ion concentrations in the effluent samples from the Berea coreflood experiment with 3 PV of 12:3 mud acid in the main flush at 300°F. 124

Fig. 73—Ion concentrations in the effluent samples from the Berea coreflood experiment with 3 PV of full strength phosphonic-based HF acid in the main flush at 300°F.....125

Fig. 74—pH values of the effluent samples from the Berea coreflood experiment with 3 PV of 12:3 mud acid in the main flush at 300°F. 126

Fig. 75—pH values of the effluent samples from the Berea coreflood experiment with 3 PV of full strength phosphonic-based HF acid in the main flush at 300°F. 127

Fig. 76—Phosphorus concentrations of the effluent samples from the Berea coreflood experiment with 3 PV of full strength phosphonic-based HF acid in the main flush at 300°F.....128

LIST OF TABLES

Page

TABLE 1—Chemical composition of typical sandstone minerals 3

TABLE 2—Solubility of different minerals in HCl and HCl/HF acids 8

TABLE 3—Surface area and chemical structure of clay minerals 13

TABLE 4—Possible precipitates in sandstone acidizing 23

TABLE 5—Guidelines for the proper design of acid treatments 26

TABLE 6—The dissociation constants of HEDP 30

TABLE 7—Formula of full and half strength phosphonic-based HF acids / 1000 gallons solutions 39

TABLE 8—Elemental analysis of clay minerals using SEM/EDS 40

TABLE 9—NMR acquisition parameters 48

TABLE 10—Ion concentrations in spent acid after clays reacted with full and half strength phosphonic-based HF acids for 24 hours at 77°F[a] 65

TABLE 11—Fluorine chemical shifts assignment in ^{19}F NMR spectra[a] 75

TABLE 12—Relative intensities of the ^{19}F NMR peaks in the spent acid as a function of reaction temperature [b] 76

TABLE 13—Formula of 12:3 mud acid 92

TABLE 14—Mineral composition for Berea and Bandera sandstone cores based on weight 92

TABLE 15—Coreflood experiments on Berea sandstone cores at different temperatures 105

CHAPTER I

INTRODUCTION: THE IMPORTANCE OF RESEARCH

Sandstone Acidizing

Sandstones are sedimentary rocks composed mainly of quartz and/or feldspar. These sands are cemented together by a combination of any of feldspar, carbonates, clays and/or silica. Sandstones account for about 30% of the world's petroleum reserves. The most common carbonates found in sandstone reservoirs are limestone, dolomite and siderite while the most common clays are kaolinite, montmorillonite, chlorite and illite. Feldspars occur in various forms. **Fig. 1** shows the various components of sandstone.

The objective of matrix stimulation treatments in sandstone formations is to remove formation damage caused by drilling, work over, or completion processes, and improve well productivity. Due to their complex mineralogy and acid/rock interaction, sandstone acidizing is a very sensitive procedure. The most commonly used treating fluids for sandstones have been mud acid mixtures, which have been used to stimulate sandstone reservoirs since 1930s. Three main steps are involved, including preflush, mainflush, and postflush. In the main stage, mixtures of HF and HCl have been extensively employed in the field (Smith and Hendrickson 1965; Gidley 1985). The role of hydrofluoric acid (HF) is to dissolve aluminosilicates and silica, while hydrochloric acid lowers pH, thus keeps reaction products soluble in spent acids.

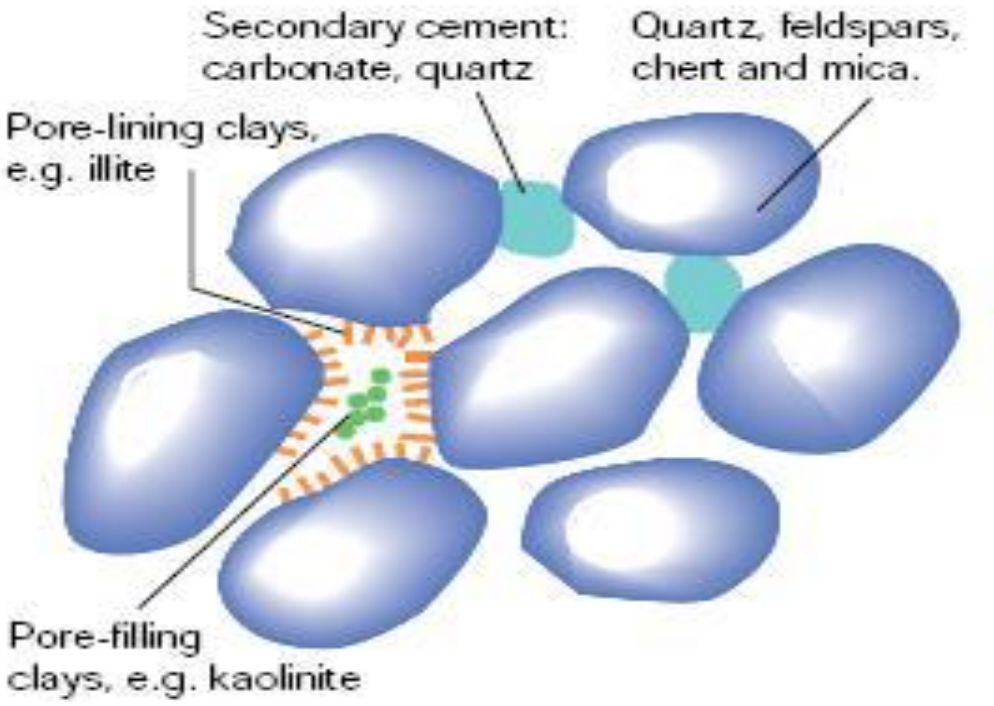

Fig. 1—Components of sandstone (Civan 2000).

Formation damage was reported in some cases (Simon and Anderson 1990; Thomas et al. 2001), these dissatisfactory results were attributed to the drawbacks of this conventional full strength mud acid system. First, in the zones that are not adequately covered by preflush, there is high risk of secondary and tertiary reactions. Second, HCl-sensitive clays (e.g., illite) can cause formation damage and decrease the permeability. Third, the high reaction and corrosion rates also cause many problems (Simon and Anderson 1990; Gdanski and Shuchart 1996; Thomas *et al*. 2002). The major drawback of mud acid is its rapid reaction rate with clays and cementing material at high

bottomhole temperatures, which results in the precipitation of reaction products following the secondary and tertiary reactions.

The mineralogy of sandstone formations is complicated, numerous mineral species react with HF, and generate aluminum silica fluoride complexes as showed in **Table 1**.

TABLE 1—Chemical composition of typical sandstone minerals

Classification	**Mineral**	**Chemical Composition**
Quartz		SiO_2
Feldspar	Microcline	$KAlSi_3O_8$
	Orthoclase	$KAlSi_3O_8$
	Albite	$NaAlSi_3O_8$
	Plagioclase	$(Na,Ca)Al(Si,Al)Si_2O_8$
Mica	Biotite	$K(Mg,Fe^{2+})3(Al,Fe^{3+})Si_3O_{10}(OH)_2$
	Muscovite	$KAl_2(AlSi_3)O_{10}(OH)_2$
	Chlorite	$(Mg,Fe^{2+},Fe^{3+})AlSi_3O_{10}(OH)_8$
Clay	Kaolinite	$Al_2Si_2O_5(OH)_4$
	Illite	$(H_3,O,K)y(Al_4{\cdot}Fe_4{\cdot}Mg_4{\cdot}Mg_6)(Si_{8-y}{\cdot}Aly)O_{20}(OH)_4$
	Smectite	$(Ca_{0.5}Na)_{0.7}(Al,Mg,Fe)_4(Si,Al)_8O_{20}(OH)_4 \cdot nH_2O$
	Chlorite	$(Mg,Fe^{2+},Fe^{3+})AlSi_3O_{10}(OH)_8$

TABLE1 Continued

Classification	Mineral	Chemical Composition
Carbonate	Calcite	$CaCO_3$
	Dolomite	$CaMg(CO_3)_2$
	Ankerite	$Ca(Fe,Mg,Mn)(CO_3)_2$
	Siderite	$FeCO_3$
Sulfate	Gypsum	$CaSO_4 \cdot 2H_2O$
	Anhydrite	$CaSO_4$
Chloride	Halite	NaCl
Metallic oxide	Iron oxides	FeO, Fe_2O_3, Fe_3O_4

Problems Associated with Mud Acid Treatments

Many problems may occur during sandstone acidizing with regular mud acid, including decomposition of clays in HCl acids, precipitation caused by the presence of fluoride, and silica gel precipitation. As a result, mud acid might significant damage to sandstone reservoirs, especially for those with a high content of calcium or clays such as illite. In general, the following material may precipitate during sandstone acidizing treatments by mud acid:

Precipitation of Fluorides

Calcite reacts very quickly and completely with HCl acid, but in the presence of HF, the

reaction proceeds as follow:

$CaCO_3 + 2HF \rightarrow CaF_2 + H_2O + CO_2$ ……. (1)

Calcium fluoride (CaF_2) has very low solubility, consequently, a high potential for precipitation. This precipitation can be eliminated by a preflush of HCl or organic acid to remove carbonate minerals prior to HF injection stage. AlF_3 is another potential precipitation which might be produced from tertiary reactions, precipitation of AlF_3 occurs at high HF to HCl ratios or when the HF concentration exceeds 4 wt% (Mahmoud *et al*. 2011)

$3F^- + Al^{3+} \rightarrow AlF_3$……..……. (2)

Precipitation of Fluosilicate and Fluoaluminate Salts

The silicon or aluminum fluoride species can react with metal ions released into the solution from clays that are highly substituted or alkali feldspars as soon as their concentration becomes sufficiently high to form insoluble alkali fluosilicates and fluoaluminate as follow:

$2Na^+ + H_2SiF_6 \rightarrow Na_2SiF_6 + 2H_2O$…….……...….. (3)

$2K^+ + H_2SiF_6 \rightarrow K_2SiF_6 + 2H_2O$…….……...….. (4)

$3Na^+ + AlF_3 + 3F^- \rightarrow Na_3AlF_6$……..…….... (5)

$2K^+ + AlF_4^- + F^- \rightarrow K_2SiF_5$…….……...….. (6)

To avoid these possible precipitations, a preflush ammonium chlorite brine has to be injected in sandstones to displace the formation brine prior to the main flush stage of HF acid. In addition, sodium-based additives should not be used with HF-based acids.

Precipitation of Silica Gel

$Si(OH)_4$ or silica gel is formed due to the secondary reaction of fluosilic acid formed from the primary reaction reacted with alumino-silicates (Gdanski 1999).

$$x/5\ HSiF_5 + M–Al–Si + (3 – x + 1)\ H^+ + H_2O \rightarrow AlF_x^{(3-x)+} + M^+ + Si(OH)_4 \quad \text{……} \quad (7)$$

Where: x is the average F/Al ratio, M^+ stands for cations, such as Na^+ and K^+.

The reaction rate of secondary reaction was found to be very fast and goes to completion very quickly at temperatures above 125°F (Gdanski 1999, 2000). To avoid precipitation of silica gel, HCl or an organic acid can be added to the main acid stage containing HF acid.

Equations mentioned above indicated that sandstone formations acidizing is complicated due to the various chemical reactions involved during the treatment. Due to the variation in mineral composition of the formations, there is always an inherent risk

involved in sandstone acidizing. This risk is high during high temperature sandstone acidizing operations (Nasr-El-Din *et al*. 2007).

In sandstone containing HCl sensitive clays, HCl cannot be used to remove carbonates in the formations as discussed previously. All clay minerals are unstable in HCl at temperature higher than 300°F (Gdanski and Shuchart 1998), so it is important to find out stimulation fluids other than HCl to remove carbonate minerals from sandstone formations. HCl can be used mixed with organic acids for better performance. Though research has been done regarding the organic-acid/carbonates system (Buijse *et al*. 2004; Chang *et al.* 2008). Very little research has been performed to remove the carbonates in sandstone reservoirs. Mahmoud *et al.* 2011 evaluated three chelate agents at different pH values in chelating calcium minerals in sandstone cores with different compositions. Acetic or formic acid is usually used as an alternative of HCl acid, Nasr-El-Din *et al.* (2009) reported the calcium dissolving power of typical organic acids used in acidizing treatments, and stated that the solubility of their calcium salt should be considered. Both calcium acetate and formate salts have limited solubility, so the maximum concentration of acetic acid or formic acid is below 13 wt% and 9 wt%, respectively. Yang *et al.* (2012) compared the effectiveness of 9 wt% formic acid in removing carbonates in Berea sandstone reservoirs at various temperatures. But there is no study to show the effectiveness of formic acid in removing carbonates in Bandera sandstone reservoirs, especially at high temperatures.

The reaction products of fluosilicic acid from the primary reaction and fluoaluminic acid from the secondary reaction are water soluble, but their potassium,

sodium, and calcium salts formed by the reactions of **Eqs. 3** to **6** are partially insoluble. Therefore, calcium, potassium, and sodium ions should not be blended with either spent or unspent HF acid. Formation brines that contain calcium chloride, potassium chloride, and sodium chloride should not be used. The only brine solution compatible with HF is ammonium chloride (NH_4Cl).

HF acid can dissolve quartz, clays, and feldspar. The main reason using HF acid is to remove clay minerals. If there are carbonates sandstone formation, they should be removed via a preflush of HCl to avoid CaF_2 precipitation. If a sandstone formation contains more than 20% carbonate, the formation should be acidized with HCl acid only. **Table 2** shows different minerals that are typically present in sandstone formations and the solubility of the different types of minerals in mud acid (Economides and Nolte (2000).

TABLE 2—Solubility of different minerals in HCl and HCl/HF acids

Minerals	**Solubility**	
	HCl	**HCl/HF**
Quartz	No solubility	Very low
Feldspar	No solubility	Low to moderate
Kaolinite	No solubility	High
Illite	No solubility	High
Smectite	No solubility	High

TABLE 2 Continued.

Chlorite	Low to moderate	High
Calcite	High	High, CaF_2 precipitate
Dolomite	High	High, CaF_2 precipitate

After Economides and Nolte (2000)

Reaction rate of HF with sand and clays depends on two factors, one is the surface area of the rock and another one is the volume of acid in sandstone formations, the ratio between two factors affects the reaction rate significantly. The fluosilicic acid produced by the primary reaction of HF acid with sand or clay minerals will react with Na^+, K^+, and Ca^{2+} and produce an insoluble precipitation. We should use ammonium chloride solution as a preflush or postflush in HF treatment. Chlorite which contain Fe^{2+}, so that HCl can leach Fe^{2+} from chlorite leaving an amorphous silica residue.

Attempts have been made to overcome the problems associated with regular mud acid. These include the use of retarded mud acid systems (Gdanski and Shuchart 1996; Gdanski 1985, 1998; Al-Dahlan et al. 2001). However, these systems still have the same problems as regular mud acid at high temperatures. For example, an aluminum chloride retarded HF system is susceptible to aluminum fluoride precipitation (Al-Dahlan et al. 2001). Fluoboric-based retarded mud acid will form potassium-based precipitate (KBF4) when it reacts with illite, K-feldspars, or KCl brines used in well completion (Bertaux 1989; Al-Dahlan *et al*. 2001; Al-Harbi *et al*. 2012). Several studies have used organic-HF acids to improve the efficient of sandstone acidizing treatment (Gdanski and Shuchart 1997; Shuchart and Gdanski 1996; Shuchart 1997; Al-Harbi *et al*. 2011; 2013;

Yang *et al*. 2012), especially for formations with HCl-sensitive clay minerals such as illites (Abrams *et al. 1983*; Shuchart 1997; Taylor *et al*. 2005).

Organic Acids/Chelating Agents in Sandstone Stimulation

Matrix stimulation of high temperature sandstone formations is challenging due to the very fast reaction rates and instability of clays at high temperatures. The ideal treating fluids should remove the near-wellbore damage without depositing precipitates in the formation, and prevent well production declines due to solids movements.

Organic acids, with and without HF, have been widely used to treat carbonate and sandstone formations, respectively. They were preferred over many other acid systems because of their retarded nature and low corrosion rates, especially in high temperatures formations. In addition, organic acids are often used as an additive to control iron and aluminum precipitation by buffering or chelating action. In the formations containing HCl-sensitive clays, such as illite, organic-HF acids have become imperative substitute. Acetic and formic based acids are two main organic-HF acids. Al-Harbi *et al.* (2011) reported that the acetic and formic acids are used at concentrations less than 13 wt% and 9 wt%, respectively. This is because these acids are expensive and some of their reaction products can precipitate at high concentrations. Besides acetic-HF and formic-HF acid, citric mud acid also has been used. All these acids rely on the same retardation mechanism, which is the slow release of HF acid through their reaction with ammonium bifluoride (NH_4HF_2) salt.

Laboratory tests and field results have shown that organic acid with HF can be excellent alternatives to regular mud acid. Simon (1980) test a 12% acetic- 3% HF acid mixture for stimulating sandstone core plugs and the results demonstrated that acetic-HF acid mixture can effectively increase permeability. Wehunt et al. (1993) tested several acids using flow tests including three organic acids, namely acetic, propanoic and butanoic acid. Among these acids, acetic-HF acid was the most effective one. The 10% acetic-0.05% HF acid and 10% acetic-0.1% HF acid worked better than systems with higher HF acid concentrations, i.e., 10% acetic-1.5% HF acid. However, formation damages were also reported by organic acid system. Yang et al. (2012) reported the results of coreflood tests using formic-HF acid mixtures to stimulate Berea sandstone cores. During the preflush stage, formic was not effective in leaching aluminum. At higher HF acid concentrations, more aluminosilicate were removed from the sandstone core but more calcium fluoride precipitate was noticed. The optimum HF acid concentration was 0. 5 wt% in 9 wt% formic acid.

Chelating agents have been used widely as iron control agents and as stand-alone stimulation fluids in carbonate and sandstone stimulation (Fredd and Fogler 1998; Frenier *et al*. 2000; 2004). Frenier *et al*. (2000, 2004) studied the reaction of HEDTA with the calcium, magnesium, and iron carbonate minerals and the results showed that HEDTA can remove the above minerals without inducing damage through clay degradation and extra precipitation. Chelating agents can also be used for high temperature sandstone stimulation in the field; they can remove the scale and stimulate the high temperature wells.

Parkinson *et al*. (2010) studied the effectiveness of a low-pH chelating agents to stimulate carbonate rich sandstone formations at high temperature. The studied area is a multilayered formation with a wide range of carbonate content (varying from 2% to 100%) and the formation temperature is nearly 300°F. Na_3HEDTA at pH 4 was compared with 9:1 mud acid (9 wt% HCl + 1 wt% HF) to stimulate Berea sandstone cores. The results showed that Na_3HEDTA was much more effective in stimulating Berea core than 9:1 mud acid.

Ali *et al*. (2008) used a chelate-based fluid to stimulate sandstone reservoirs at 300°F. A significant increase in the rock permeability was obtained with this fluid. Ali *et al*. (2002) also reported that EDTA containing no HF performed better than HCl and organic acid for stimulating damaged sandstone formations containing carbonate and acid sensitive clays. Additionally, Na_3HEDTA was used to stimulate Berea core and better results were obtained compared to HCl and almost similar results to acetic acid followed by 9:1 mud acid. Sopngwi et al. (2014) discussed the successful application of a new chelant-based HF acid to remove formation damage and enhance oil production in the field, and an increase of 305% in oil production was achieved as a result of the application of the APCA/HF acid treatment.

Clay Mineralogy

Clay minerals are extremely small, platy-shaped materials that may be present in sedimentary rocks as packs of crystals. The maximum dimension of a typical clay particle is less than 0.005mm. The clay minerals can be classified into three main

groups: (1) Kaolinite group, (2) Smectite (or Montmorillonite) group, and (3) Illite group. In addition, there are mixed-layer clay minerals formed from several of these three basic groups. The chemical structure of different clay minerals is described in **Table 3** (Civan 2000).

TABLE 3—Surface area and chemical structure of clay minerals

Mineral	**Specific Surface Area, m^2/gm**	**Chemical Structure**
Kaolinite	20	$Al_4[Si_4O_4](OH)_8$
Montmorillonite Or Smectite	700	$(½Ca, Na)_{0.7}$ $(Al, Mg, Fe)_4$ $[(Si, Al)_8O_{20}]\cdot$ $nH2O$
Chlorite	100	$(Mg, Al, Fe)_{12}[(Si, Al)_8O_{20}](OH)_{16}$
Illite	100	$K_{1-1.5}Al_4[Si_{7-6.5}\ Al_{\ 1-1.5}O_{20}](OH)_4$

After Civan (2000)

Amaefule *et al*. (1988) stated that rock-fluid interactions in sedimentary formations can be classified in two groups: (1) chemical reactions resulting from the contact of rock minerals with incompatible fluids, and (2) physical process caused by excessive flow rates and pressure gradients. The interactions of the clay minerals with

aqueous solutions are the primary culprit for the damage of petroleum-bearing formations.

The primary factors that might affect the mineralogical sensitivity of sedimentary formations were summarized by Amaefule *et al*. (1988). Mineralogy and chemical composition determine the dissolution or swelling of minerals, and precipitation of new minerals. Mineral abundance, size, morphology, and location also play an important role since the mineral sensitivity is proportional to the minerals surface area, and mineral size determines the ratio of the surface area to the volume of particles. Mineral morphology determine the grain shape, and therefore determine the surface to volume ratios. Moreover, Mungan (1989) stated that the damage caused by clay minerals mainly depends on the type and amount of the exchangeable cations, such as K^+, Na^+, Ca^{2+}, and the layered structure existing in the clay minerals.

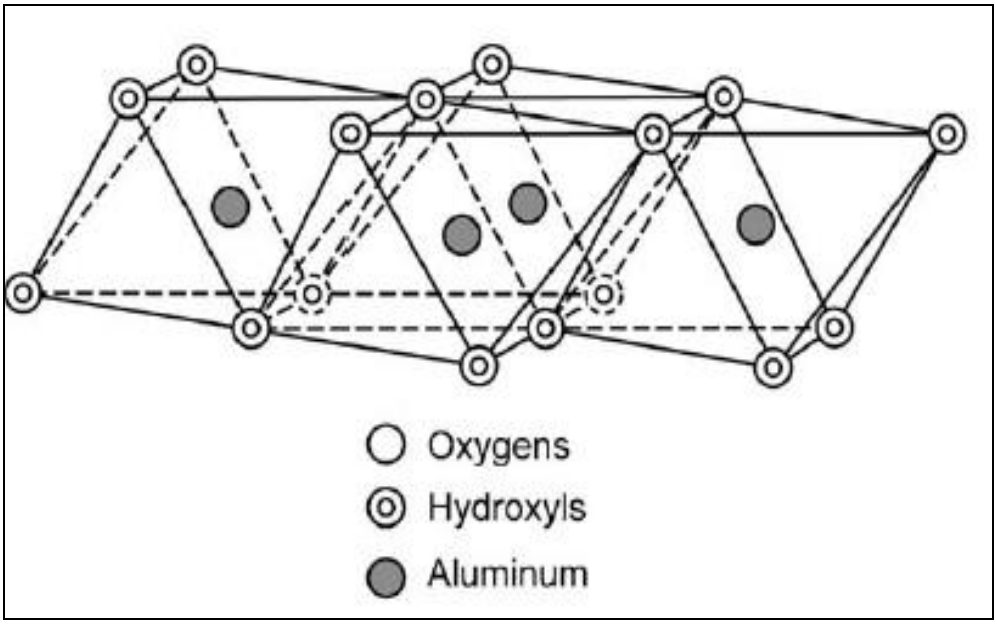

Fig. 2—Structure of the octahedral sheet (Murray 2007).

The atomic structure of the clay minerals consists of two basic units, an octahedral sheet and a tetrahedral sheet (Murray 2007). The octahedral sheet is comprised of closely packed oxygens and hydroxyls between which aluminum, magnesium or iron atoms are arranged in octahedral coordination. **Fig. 2** shows the crystal structure of octahedral sheet.

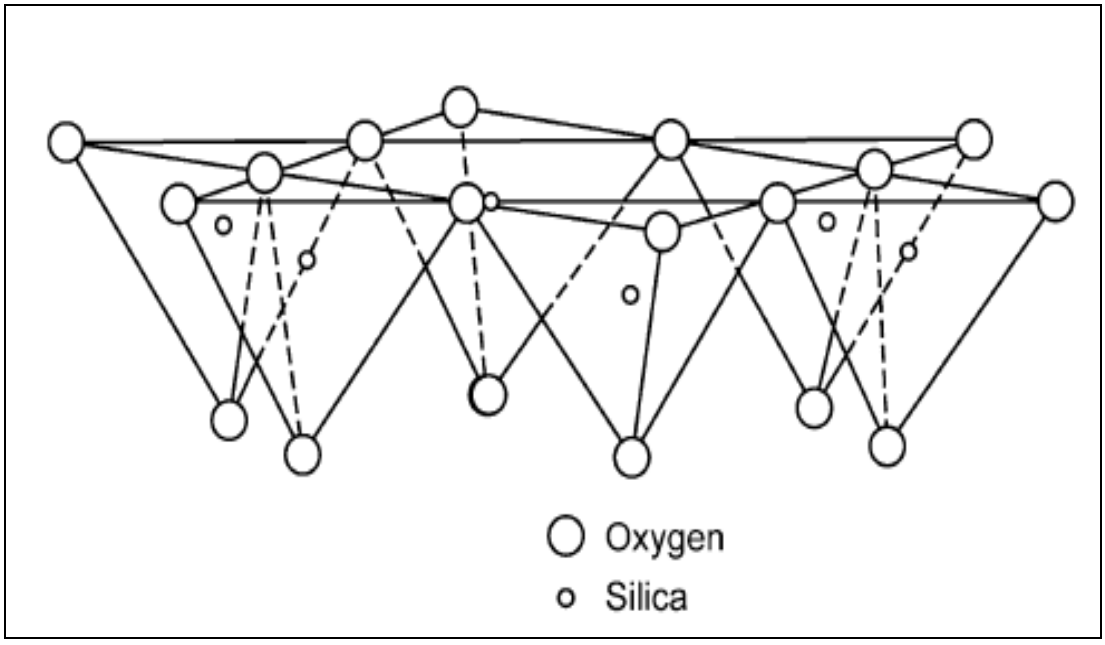

Fig. 3—Structure of the tetrahedral sheet (Murray 2007).

The second structure unit is the tetrahedral layer of silica in which the silicon atom is packed equally from four oxygens or possibly hydroxyls arranged in the form of a tetrahedron with the silicon atom in the center. These tetrahedrons are arranged to form a hexagonal structure repeated infinitely in two horizontal directions to form the silica tetrahedral sheet (**Fig. 3**). The silica tetrahedral sheet and the octahedral sheet are joined by sharing the oxygens or hydroxyls to form what is called the 1:1 layer structure (e.g. kaolinite) or the 2:1 layer structure (e.g. illite). The arrangement and composition of the octahedral and tetrahedral sheets account for most of the differences in their physical and chemical properties (Murray. 2007).

The properties and damage processes of the clay groups can be classified as the follows (Civan 2000):

1. Kaolinite has a 1:1 layered structure (**Figs. 4 and 5**), that is each layer consists of one tetrahedral silicate sheet and one octahedral sheet. The exchange cation is K^+, with a small Cation Exchange Capacity (CEC). It is geneally a non-swelling clay but it will disperse and move easily. Kaolinite can adsorb some water, the adsorbed water is held tightly to the clay surfaces. The ideal structural formula of kaolinite is $Al_4Si_4O_{10}(OH)_8$ and the theoretical chemical composition is SiO_2, 46.54%; Al_2O_3, 39.50%; and H_2O, 13.96%.
2. Smectite/Montmorillonite is composed of two silica tetrahedral sheet with central octahedral sheet (**Fig. 6**). It has a large Cation Exchange Capacity (CEC) of 90 to 150 meq/100 g and will readily adsorb Na^+, all leading to a high degree of swelling and dispersion. Smectite swells by taking water into its structure. It can increase its volume up to 600%, significantly reducing permeability, creating impermeable barrier to flow. The removal of these clays can be accomplished during HF treatment if the depth of penetration was small. If the depth of the penetration was large, the best treatment is to fracture the well to bypass the damage. The theoretical formula of smectite is $(OH)_4Si_8Al_4O_{20}\cdot n$H2O and the theoretical chemical composition without the interlayer material is SiO_2, 66.7%; Al_2O_3, 28.3%; and H_2O, 5%.

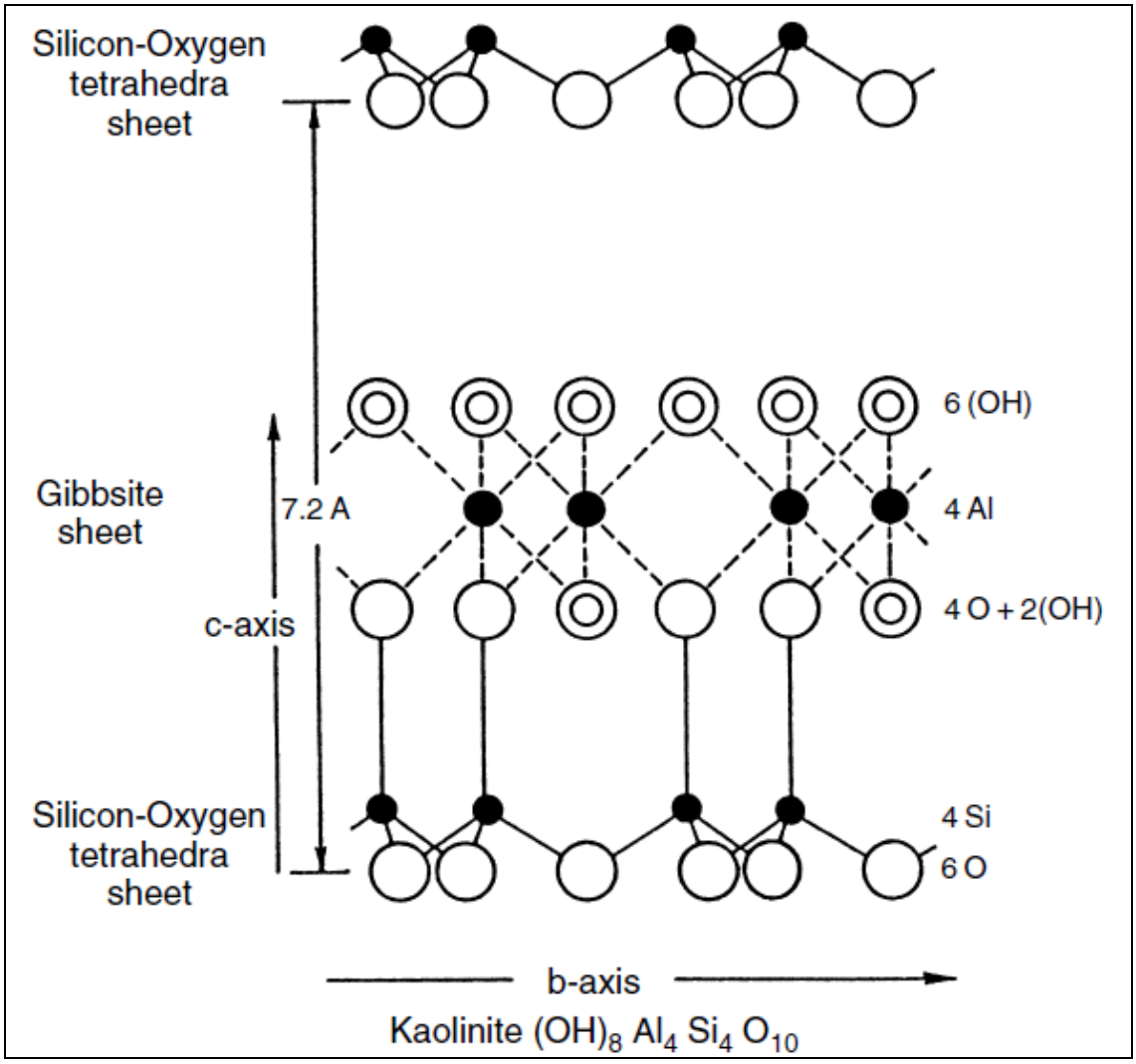

Fig. 4—Crystal structure of kaolinite (Civan 2000).

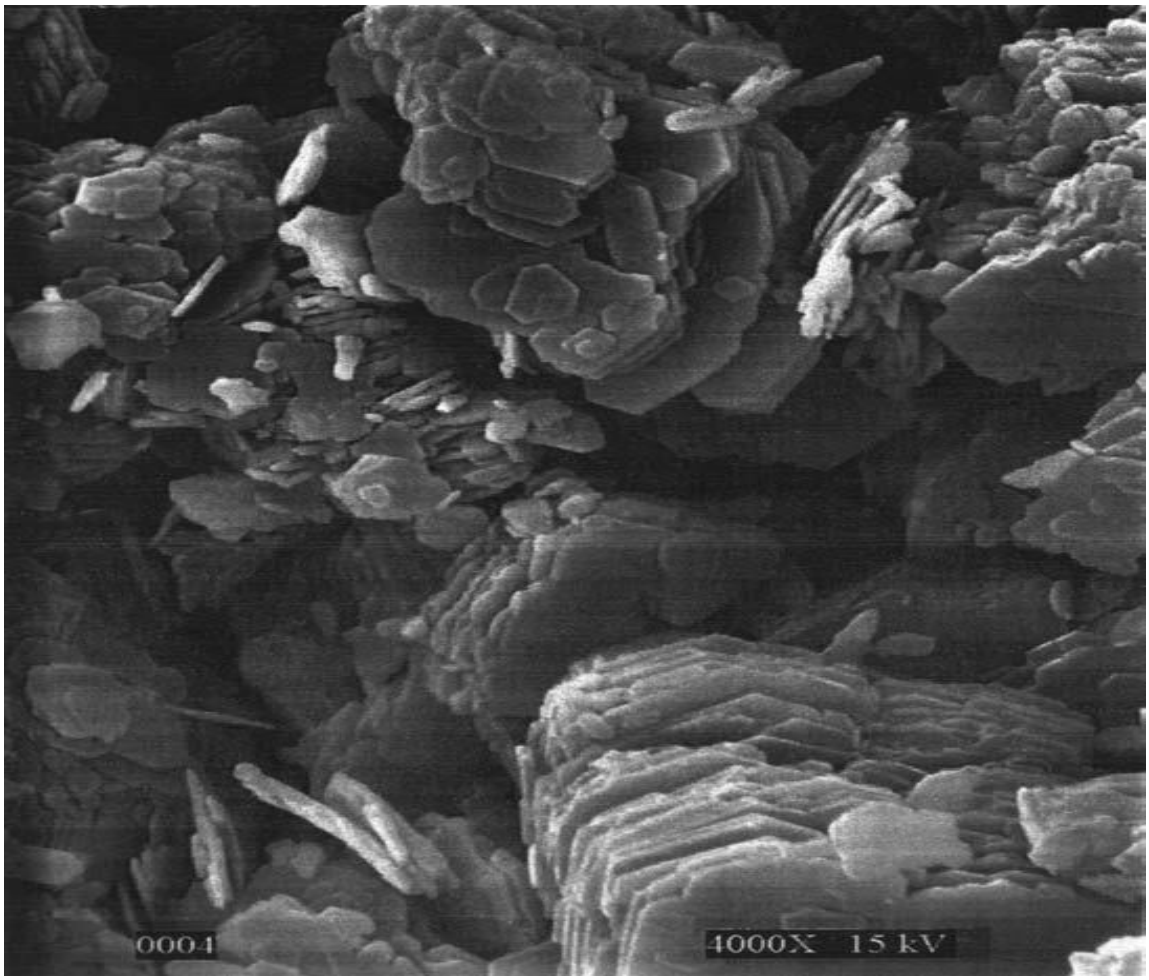

Fig. 5—Scanning electron micrograph of kaolinite (Murray 2007).

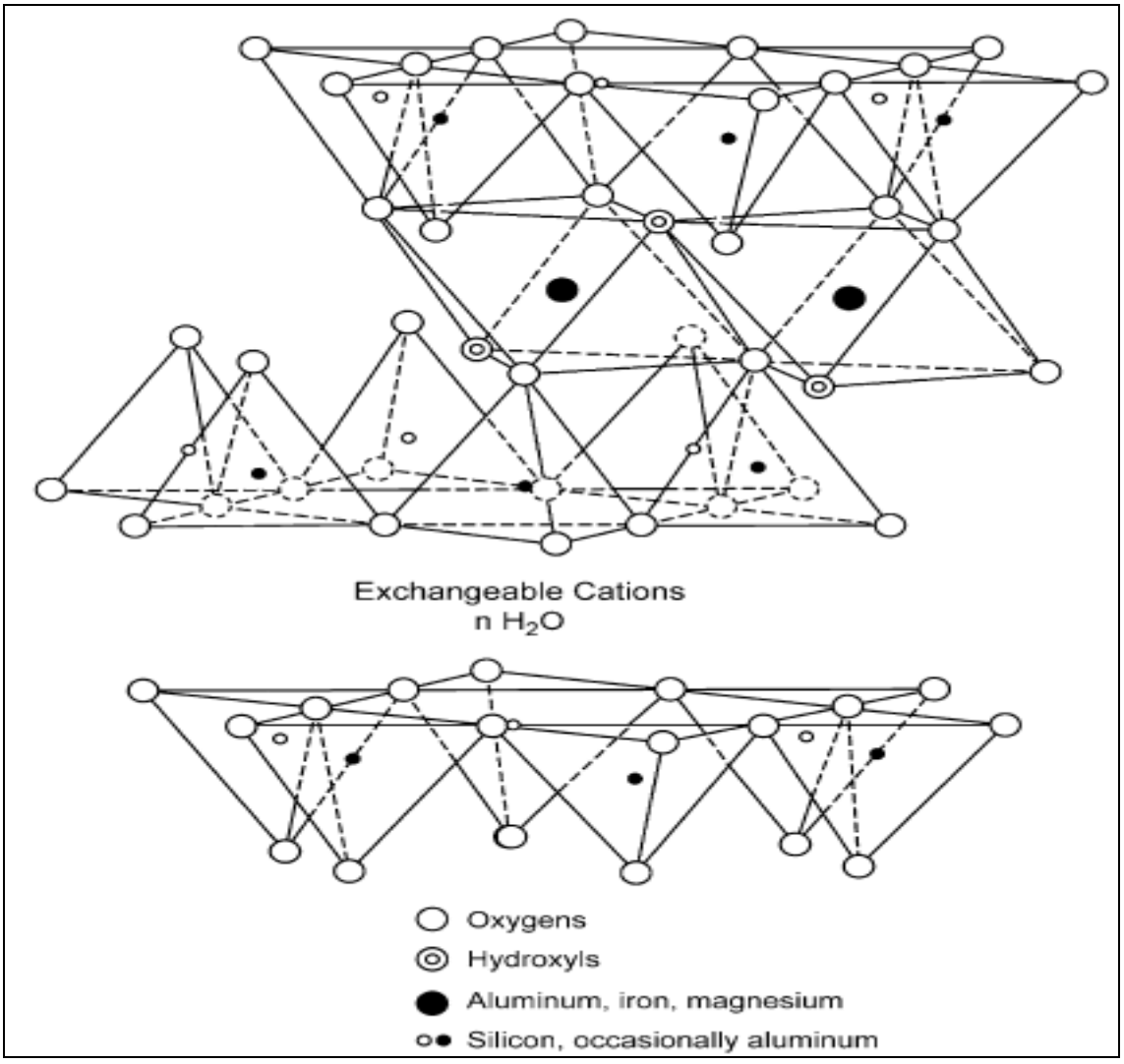

Fig. 6—Structure of Montmorillonite (Murray 2007).

3. Illite is interlayered, the interlay cation is potassium (**Fig. 7**). Potassium bonds the layer in a fixed position so that water and other compound cannot readily enter the interlayer position and the K ion is not easily exchangeable. Therefore, illites combine the worst characterization of the dispersible and the swellable clays. These characteristics make illite the most difficult to stabilize.

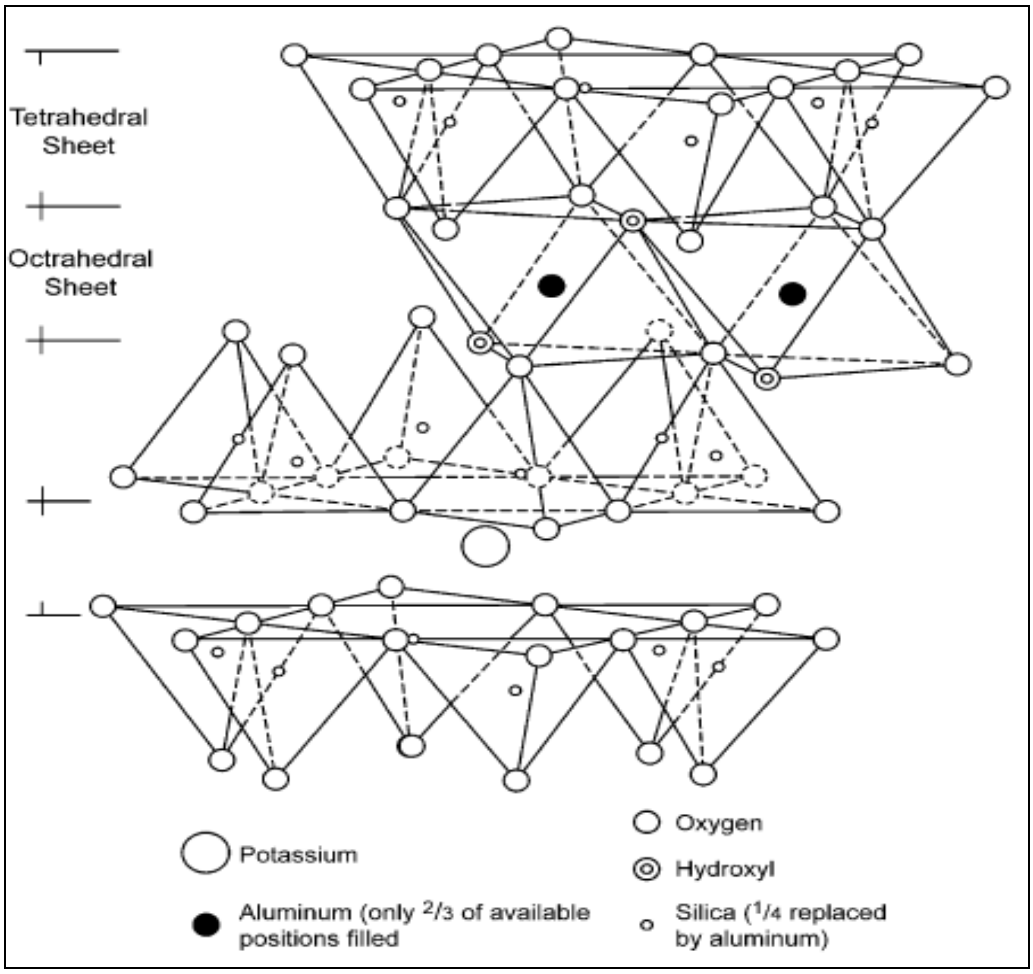

Fig. 7—Crystal structure of illite (Murray 2007).

4. **Chlorites** are a 2:1 layer minerals with an interlayer brucite sheet ($Mg(OH)_2$) (**Fig. 8**). There are various substitutions in chlorites, most commonly Mg^{2+}, Fe^{2+}, Al^{3+}, and Fe^{3+}. The composition of chlorite is generally shown as $(OH)_4(SiAl)_8(Mg\text{-}Fe)_6O_{20}$. The brucite-like sheet in the interlayer position has the general composition $(MgAl)_6(OH)_{12}$.

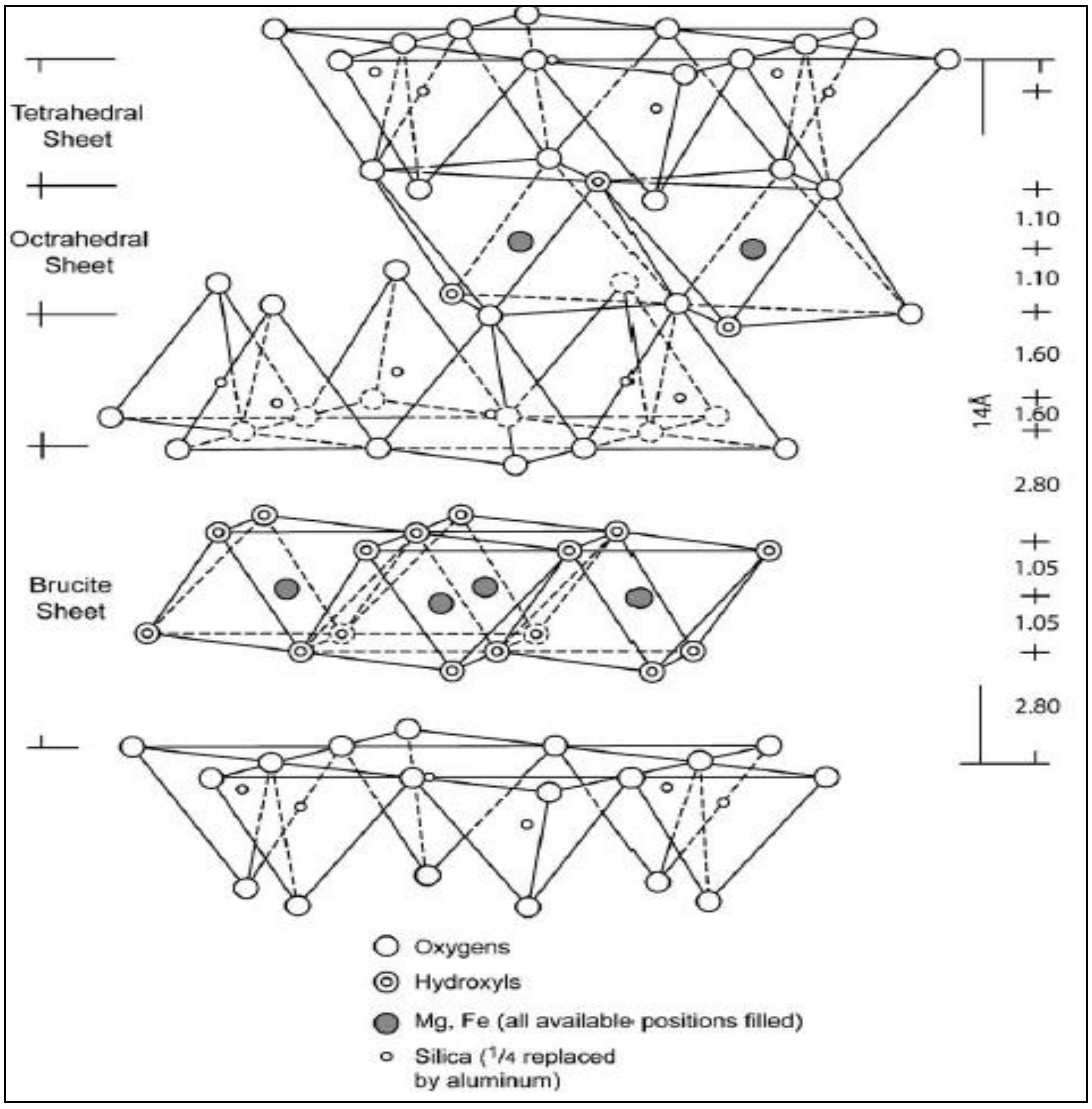

Fig. 8—Crystal Structure of Chlorite (Murray 2007).

Selection of Treatment Fluid for Sandstone Acidizing

As mentioned previously, sandstone acidizing is to dissolve clay minerals and remove the plugging materials near the well bore and restore original permeability or increase

permeability. During acidizing, treatment fluid is injected into the formation under pressure below the fracture pressure to dissolve the material present in the formation. The mostly common used treatment fluid in sandstone acidizing is a mixture of HF and HCl, However, the reactions occurring in sandstone acidizing are much more complicated because of the complicated mineral composition in sandstone formation. Treatment fluid selection in sandstone formations acidizing is very important, which is highly dependent on the mineralogy of the rock as well as the damage mechanism. HF acid is typically used to dissolve the damaging silicate particles.

The main sources and causes of precipitates formed during sandstone matrix acidizing are summarized in **Table 4 (**Schlumberger, 2003**)**. The formation of these potentially damaging precipitates is affected by the complex mineralogy of the sandstones.

TABLE 4—Possible precipitates in sandstone acidizing

Precipitate	**Origin**
Calcium fluoride (CaF_2)	Carbonate-HF reaction CaF_2 can be caused by an inadequate HCl preflush to remove calcium ions from calcite cementing materials or to flush calcium chloride completion fluids away from the near wellbore.
Amorphous silica	Clay and silicate dissolution in HF. Amorphous silica results from both secondary and tertiary HF acidizing reactions.

TABLE 4 Continued.

Precipitate	**Origin**
Sodium and potassium fluosilicates	Feldspar and illite clay dissolution in HF produce these primary reaction products. They can also form if seawater or sodium or potassium brines are mixed with spent HF.
Sodium and potassium fluoaluminates	Silico-aluminate dissolution in HF. Fluoaluminates, like fluosilicates, occur when spent mud acid (H_2SiF_6) reacts with the formation. They can also form if seawater or sodium or potassium brines are mixed with spent HF.
Aluminium hydroxides and fluorides	Clay and feldspar dissolution in HF can cause these precipitates.
Iron compounds	Iron minerals or iron oxides (rust) can react with HCl-HF to produce these compounds.

After Schlumberger (2003).

The treating fluid must remove existing damage without creating additional damage through the reaction between the formation rock and fluids. Therefore, the criteria for selecting the treating fluid are generally mineralogy, formation damage mechanism, petrophysics and well conditions. Based on the formation mineralogy and original rock permeability, McLeod presented a guideline for acid selection (McLeod, 1984), which is a very important consideration for any acid treatment as acid-formation interaction/ compatibility is very crucial to the success or failure of any acid job. Acid type and concentration are often selected according to this guideline.

To prevent the damage caused by precipitated byproducts and rock deconsolidation during acidizing treatment, small concentrations of HF were generally recommended since the reaction rates between HF acid and the minerals are proportional to the acid concentration. The 9:1 mud acid has been extensively used in the field to minimize the precipitation during sandstone acidizing. Several studies also found that the HCl/HF ratio is an important factor that might affect the possible precipitation and the overall stimulation efficiency (Thomas et al., 2002). Also some research shows that there are many sandstone formations cannot be stimulated successfully using HF systems, such as those with a high content of carbonate minerals or highly reaction sensitive clays. For these kinds of formations, non-HF systems can work successfully without causing further damage of precipitation byproducts (Martin 2004, Nwoke *et al*. 2004).

A formation is sensitive if the reaction between the rock minerals and a given fluid induces damage to the formation. Sandstones can be sensitive to acid depending on temperature and mineralogy. Sensitivity depends on the overall reactivity of the formation minerals with the acid, and reactivity depends on the structure of the rock and the distribution of minerals within the rock. The sensitivity of sandstone also depend on the permeability of the formation. Low permeability sandstones are more sensitive than high-permeability sandstones for a given mineralogy.

Kalfayan and Metcalf 2000 presented a modification of McLeod's guideline. Kalfayan and Metcalf's treatments were based on the assessment of formation damage contributors, an in depth evaluation of production and stimulation histories, and the

flexibility of production and continuous improvement in stimulation procedure and execution practices. Kalfayan and Metcalf's modification based on McLeod's work, which is summarized in **Table 5** (Kalfayan and Metcalf 2000).

TABLE 5—Guidelines for the proper design of acid treatments

Formation	Suggested Acid Formulation	Preflush
Solubility in HCl > 15-20%	Avoid use of HF	
Calcite or dolomite	15% HCl only	5% NH_4Cl
High iron carbonate (siderite, ankerite)	15% HCl +iron control	5% NH_4Cl + 3% Acetic
High permeability (> 100mD)		
High quartz (> 80%); low clay (<5%)	12 HCl, 3% HF	15% HCl
Mod Clay(5-8%); low feldspar (<10%)	7.5 HCl, 1.5 HCl	10% HCl
High feldspar (>15%)	13.5% HCl, 1.5% HCl	15% HCl
High feldspar (>15%) and clay(>10%)	9% HCl, 1%HF	10% HCl
High iron chlorite clay (>8%)	3% HCl, 0.5% HF	5% HCl
Medium permeability (10-100mD)		
High clay (>5-7%)	6% HCl, 1%HF	10% HCl
Lower clay (<5-7%)	9% HCl, 1%HF	10% HCl
High feldspar (>10-15%)	12% HCl, 1.5%HF	10-15% HCl
High feldspar (>10-15%)	9% HCl, 1.5%HF	10%HCl

TABLE 5 Continued

Formation	**Suggested Acid Formulation**	**Preflush**
High iron chlorite clay (>8%)	3%HCl,0.5%HF	5%HCl
High iron carbonate (>5-7%)	9%HCl, 1%HF	5% HCl
K< 25mD	5% HCl, 0.5%HF	10% HCl
Low permeability (1-10mD)		
Lower clay (<5%); low HCl	6% HCl, 1.5%HF	5% HCl
High clay (>8-10%)	3% HCl, 0.5%HF	5% HCl
High feldspar (>10%)	9% HCl, 1%HF	10%HCl
High iron chlorite clay (>5%)	10% acetic,0.5%HF	10% acetic +5%NH_4Cl
Very low permeability (<1mD)	Avoid HF acidizing, non or hydraulic fracturing is	HF matrix simulation preferred

After Kalfayan and Metcalf (2000).

CHAPTER II

SANDSTONE ACIDIZING USING A PHOSPHONIC-BASED HF ACID SYSTEM

Introduction

The phosphonic-based HF acid has been used as an alternative to regular mud acid (Di Lullo and Rae 1996; Rae and Di Lullo 2007). Field applications have shown that phosphonic-based HF acid can be effective sandstone stimulation fluids (Nwoke *et al*. 2004), however, very limited research has been performed to investigate the interactions of this phosphonic-based HF acid with clay minerals in sandstone reservoirs. The chemistry involved in HF acidizing is complicated, due to the complexity of reaction products, mineralogy, reaction mechanism, and so on. A deep understanding of the chemistry between sandstone minerals and acid formulation is essential for its field application.

In the present study, a phosphonic-based HF acid formulation was used as an alternate version of regular mud acids. The pH of the fresh phosphonic-based acid system 2.14, which corresponds to the release of two protons from phosphonic acid groups. The diprotonated phosphonic acid has strong chelating properties, so the phosphonic acid in the mixtures can effectively sequester Ca^{2+} ions, and prevent the subsequent precipitation of calcium fluoride, therefore, eliminating the potential formation damage caused by calcium fluoride precipitation. It can also chelate with Fe^{3+} and Al^{3+} ions and form stable compounds. The chelating property of phosphonic acid

has been studied by Nasr-El-Din et al. (2002). Their results showed that HF based phosphonic acid minimized iron precipitation over a narrow pH range (4.7-5.3). Di Lullo and Rae (1996) and Ross and Di Lullo (1998) developed a HF acid mixture using a phosphonic acid complex to hydrolyzed fluoride salts instead of HCl. They concluded that phosphonic acid can sequester iron and other multivalent cations effectively.

The active component of the phosphonic-based HF acid system used in this study is 1-Hydroxyethane-1, 1-diphosphonic Acid (HEDP), one of the most widely used diphosphonic acid. The chemical structure of HEDPA is showed in **Fig. 9**. HEDP acid, like most other bisphosphonates, is a tetraprotic acid and therefore has various forms having different degrees of protonation, such as H_4L, H_3L^-, H_2L^{2-}, HL^{3-}, L^{4-}, where L = $[CH_3C(OH)(PO_3)_2]^{4-}$, that are pH-dependent and whose dissociation constants, pKa, have been experimentally determined (**Table 6**).

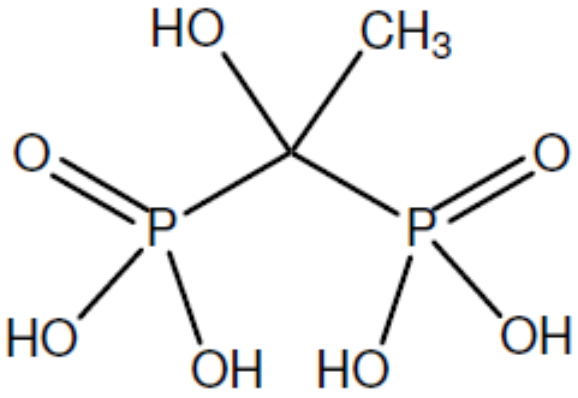

Fig. 9—Chemical Structure of HEDPA (***Lacour et al. 1998***).

TABLE 6—The dissociation constants of HEDP	
Equilibrium reaction	**Dissociation constant at 25°C, pK_a**
$H_4L \leftrightarrow H_3L^- + H^+$	**2.43**
$H_3L^- \leftrightarrow H_2L^{2-} + H^+$	**2.97**
$H_2L^{2-} \leftrightarrow HL^{3-} + H^+$	**6.81**
$HL^{3-} \leftrightarrow L^{4-} + H^+$	**10.11**

After Lacour *et al.* (1998).

Theory of HF-Based Acid Reactions

The reactions of HF acid with sandstone minerals are very complex, due to the mineralogical diversity of sandstone formations. Most sandstone formations consist primarily of quartz or sand particles bonded together by cementing materials which are typically calcite ($CaCO_3$), silicates and alumino-silicates (clay and feldspar). The reactivity of different clay minerals with HF varies due to the difference in their structure and specific surface area (Gidley 1985). The reaction of HF with quartz is expressed in **Eq. 8**

$$6HF + SiO_2 \rightarrow H_2SiF_6 + 2H_2O \quad \text{.....(8)}$$

The reaction kinetic between HF and alumino-silicates has been reported in detail by Gdanski (1998, 1999, and 2000). The reactions kinetics of different clays with HF can be generalized from previous research. For example, for kaolinite, the primary reaction can be written in the form of **Eq. 9**.

$$Al_2Si_2O_5(OH)_4 + 16HF + 2H^+ \rightarrow 2Al^{3+} + 4F^- + 2H_2SiF_6 + 9H_2O \quad \text{.....(9)}$$

All the reaction products of HF primary reaction with kaolinite, show in Eq. 9, are soluble. Therefore, the primary reaction results in complete dissolution of clay minerals. Fluorosilicates can be especially problematic because re-dissolution can be difficult. Fluorosilicates are thought to be soluble as long as the pH is below about 2 and the F/Al ratio is maintained below about 2.5 (Shuchart and Gdanski 1996). If precipitated, their dissolution typically requires strong hydroxide concentration of more than 5 wt%.

The secondary reaction is the one between H_2SiF_6 and clay minerals, for example for kaolinite (**Eq. 10**)

$$H_2SiF_6 + Al_2Si_2O_5(OH)_4 + 2H^+ + 3H_2O \rightarrow 2F^- + 2AlF_2^+ + 3SiO_2 \cdot 2H_2O \quad \text{.....(10)}$$

Fluosilicic acid that formed from the primary reaction was consumed; whereas silica gel and aluminum fluoride complexes were formed during the secondary reaction. The reaction rate of the secondary reaction between HF and alumino-silicates was found to

be very slow below 125°F, and then it became very fast and continued to completion very quickly at temperatures above 125°F (Gdanski 1999).

The tertiary reaction, for example for kaolinite shown in **Eq. 11** occurred when aluminum fluoride complexes continue to react with kaolinite further, which resulted in more silica gel precipitate.

$$2AlF_2^+ + Al_2Si_2O_5(OH)_4 + 4H^+ \rightarrow 4AlF^{2+} + 2SiO_2 \cdot 2H_2O \quad \text{.....(11)}$$

The reaction rate of the tertiary reaction was found to be very slow below 200°F (Gdanski 1998). With the occurrence of the tertiary reaction, aluminum fluoride precipitate can be formed as the HCl is consumed or the pH elevated, which can cause formation damage.

NMR Analysis

Several analytical techniques, including inductively coupled plasma, atomic absorption spectroscopies, scanning electron microscopy, X-ray diffraction, and X-ray fluorescence, have been utilized to interpret the chemical reactions involved in HCl-HF acids treatment. NMR analysis is the main research technique used in this study. This technique exploits the magnetic properties of certain atomic nuclei in the magnetic field which absorb and re-emit electromagnetic radiation that resonates with the intramolecular magnetic fields around an atom. The spectrum obtained can then provide detailed information about the

structure, dynamics, reaction state, and chemical environment of molecules, which can be used to confirm the identity of a substance.

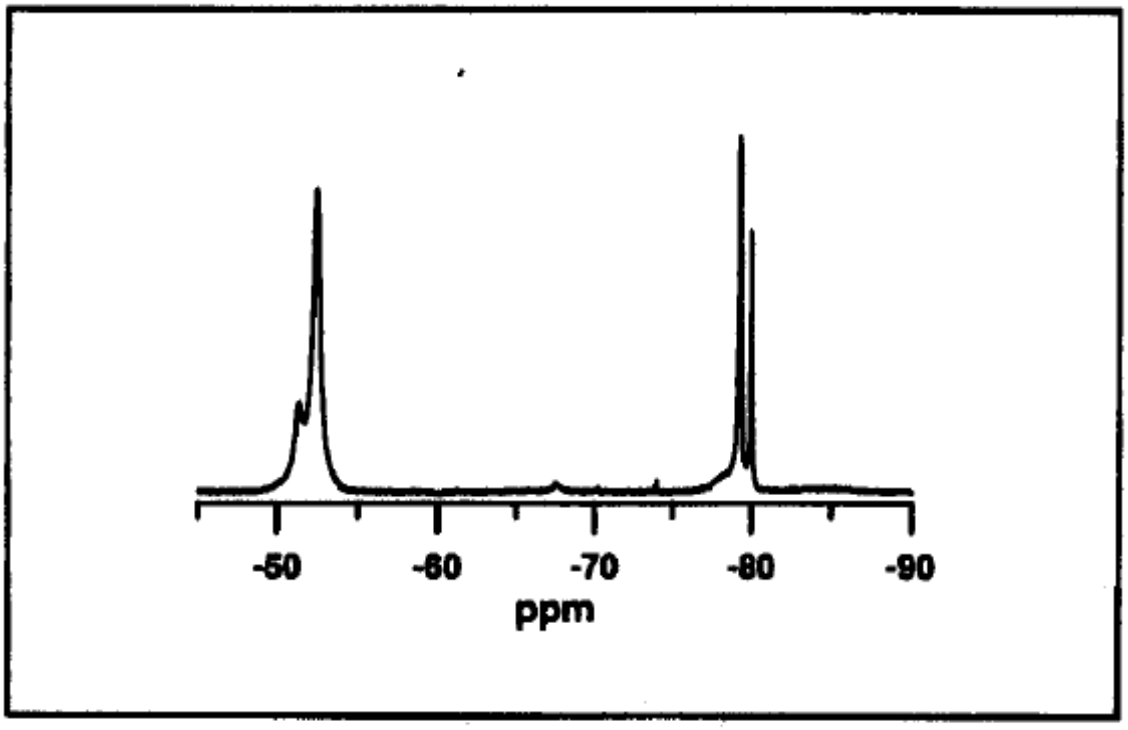

Fig. 10—^{19}F NMR spectrum of 13.5% HCl– 1.5 wt% HF reacted with kaolinite at room temperature (Shuchart and Gdanski 1996).

^{19}F nuclear magnetic resonance (NMR) was first employed by Shuchart (1995) to investigate the reactions between clay minerals and HCl/HF fluid systems, which can detect the chemical species in a spent solution and the distribution of fluoride ions among those species. Schuchart and Buster (1995) first analyzed a sample of 13.5 wt% HCl-1.5 wt% HF after reacting with kaolinite. Two groups of signals in the ^{19}F NMR

spectrum were observed at nearly – 50 ppm and – 80 ppm respectively when using CF_3COOH as reference (**Fig. 10**). The signals around – 80 ppm were assigned to aluminum fluorides, while the ones around – 50 ppm belong to silicon fluorides.

Shuchart and Gdanski (1996) utilized ^{19}F NMR for the first time to follow the reaction kinetics and products in organic HF acid systems. They concluded that the fluoride distribution strongly depends on the acid concentration. Yang et al. (2012) used ^{19}F NMR to determine reaction products in formic-HF acid systems, both silicon and aluminum species were observed in their studies, the fluoride distribution has a direct relationship to the clay mineral structures. Reyes et al. (2013) used ^{19}F NMR spectroscopic analysis to determine aluminum fluoride species in the chelant-based HF acid. The chemical kinetics of fluoroaluminate speciation shows that the fluoride ligand was able to bind to aluminum strongly.

Theoretically, aluminum can coordinate with up to 6 fluoride ions to complete the octahedral coordination. Therefore, aluminum and fluoride can form several different complexes including AlF^{2+}, AlF_2^{+}, AlF_3, AlF_4^{-}, AlF_5^{2-}, and AlF_6^{3-}. However, the distribution of different aluminum fluoride complexes depends on a lot of factors, such as the concentrations of ions, ionic strength, and pH, etc.

Shuchart and Buster (1995) showed that only AlF^{2+}, AlF_2^{+} were detected when F/Al ratio varies from 0.2 to 6.26 (**Fig. 11**) no higher aluminum fluorides, such as AlF_4^{-}, AlF_5^{2-}, and AlF_6^{3-} were identified, probably because of the instability of the higher aluminum fluoride species in acidic solutions. In solutions with lower HCl concentrations, AlF_3 appears to be more stable.

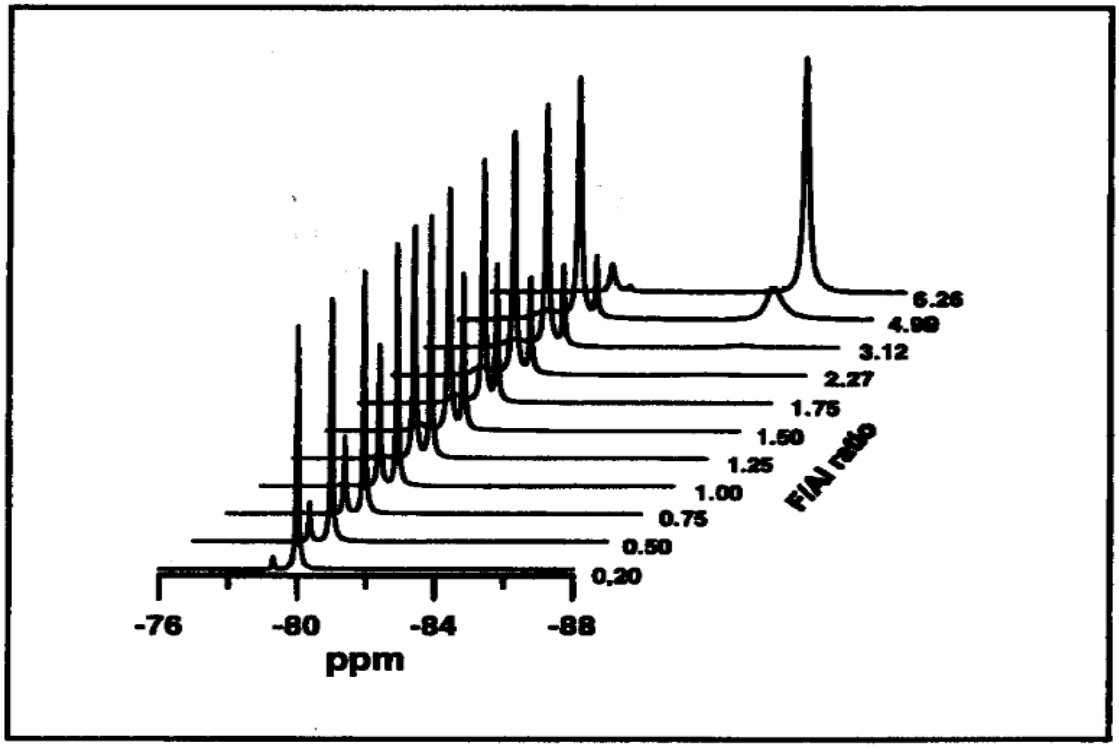

Fig. 11—^{19}F NMR spectra of aluminum solutions containing varying F/Al ratio (0.2 to 6.26)

The study of Shuchart and Gdanski (1996) showed one single peak was observed by ^{19}F NMR after 15 wt% HCl- 3 wt% HF reacting with $Si(OH)_4$, more peaks started to appear when temperature lowered (**Fig. 12**). And a total of five peaks were observed at –45°C, which were assigned as $SiF_3(H_2O)_3^+$, $SiF_5(H_2O)$-, SiF_6^{2-}, and $SiF_4(H_2O)_2$, respectively. The broad peak observed on ^{19}F NMR spectrum under room temperature was caused by fast exchange of different silicon fluoride species.

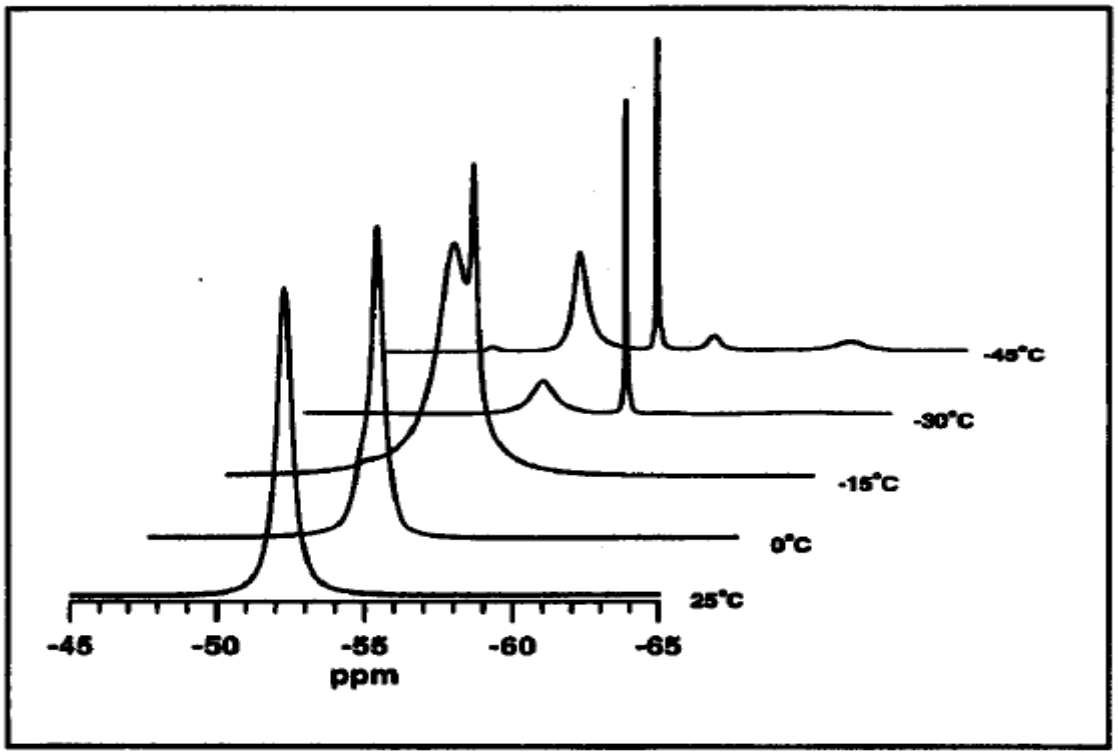

Fig. 12—^{19}F NMR spectra of HF acid reacted with $Si(OH)_4$ at variable temperature (Shuchart and Gdanski 1996).

Objectives

Phosphonic-based HF acid has been used in the field over the last few years to overcome the severe problem caused by regular mud acid. Reactions of this acid with clays and its propagation in sandstone cores have not been examined previously. Therefore, the main objectives of this study are to:

(1) Investigate the interaction of the phosphonic-based HF acid with different clay minerals;

(2) Evaluate the effect of acid concentration, temperature, and reaction time on the acid performance;

(3) Determine the nature of precipitate that might form during the reaction of this acid system with various clay minerals;

(4) Conduct coreflood tests to determine the impact of this acid system on core permeability.

CHAPTER III

INTERACTIONS BETWEEN A PHOSPHONIC-BASED HF ACID AND CLAY MINERALS: SOLUBILITY TESTS

Introduction

The phosphonic-based HF acid has been used as effective sandstone stimulation fluids over the last few years, very limited research, however, has been performed to investigate the interactions of this phosphonic-based HF acid with clay minerals in sandstone reservoirs. A deep understanding of the chemistry between sandstone minerals and acid formulation is essential for its field application.

In this part of the study, a phosphonic-based HF acid system with two HF concentrations (1.5 and 3 wt %) was used to evaluate the solubility of various clay minerals (kaolinite, bentonite, chlorite, and illite) as a function of time and temperature. Scanning Electron Microscopy (SEM) and Energy-dispersive X-ray Spectroscopy (EDS) were used to identify the reaction products. The concentrations of key cations in the supernatant were analyzed using inductively coupled plasma optical emission spectrometry (ICP-OES). ^{19}F, ^{31}P, and ^{27}Al liquid nuclear magnetic resonance (NMR) spectroscopy were used for the first time to evaluate the reaction of this phosphonic-based HF acid system with clay minerals.

Experiment Studies

Materials

Full and half strength phosphonic-based HF acids were obtained from a local services company, **Table 7** gives the compositions of the two concentration phosphonic-based

acids that were used in solubility tests. They contain 0.2 vol% corrosion inhibitor, 0.2 vol% clay stabilizer, and 1 vol% iron control agent. The corrosion inhibitor is a blend of quaternary salts, alcohols, formamide, and ethoxylatednonylphenol. The clay stabilizer is a complex polyamine salt, used for controlling clay. The iron control agent is citric acid.

TABLE 7—Formula of full and half strength phosphonic-based HF acids / 1000 gallons solutions

Component	**Full Strength Acid**	**Half Strength Acid**
Water	846 gal	915 gal
Ammonium Bifluoride	400 lbs	200 lbs
Phosphonic-based Acid	60 gpt	30 gpt
22° Baume HCl	80 gpt	40 gpt
Corrosion Inhibitor	2 gpt	2 gpt
Clay Stabilizer	2 gpt	2 gpt
Iron Control Agent	10 gpt	10 gpt

All clay minerals (kaolinite, bentonite, chlorite, and illite) were obtained from Ward's Natural Science Company, Florida, USA. A crushing process was done and a

sieve analysis was carried out to obtain the fine fraction with sizes between 45 to 75 μm. The element composition of these clay minerals is shown in **Table 8**.

TABLE 8—Elemental analysis of clay minerals using SEM/EDS

Element, wt%	Kaolinite	Bentonite	Chlorite	Illite
O	60.24	42.26	51.92	54.09
Si	19.81	33.45	11.46	24.82
Al	19.95	13.75	12.28	11.03
Ca	–	1.23	–	–
Fe	–	4.72	10.84	3.85
Mg	–	2.32	13.51	2.16
K	–	–	–	4.06
Na	–	2.23	–	–

Clay Particle Size Selection

A sonic sifter with a series of sieves complying with ASTM E 11 standard, from top to bottom: 212 μm, 150 μm, 106 μm, 90 μm, 75 μm, and 45 μm were used to separate dry

powdered clay as received from Ward's Science. Kaolinite and bentonite have a non-normal distribution for available sieve size ranges (**Figs. 13** and **14**). Although particles with diameters less than 45 μm, in order to compare with chlorite and illite tests, particles with diameters between 45-75 μm were selected to represent kaolinite and bentonite samples in this study, as this range is likely the mode of the size variation.

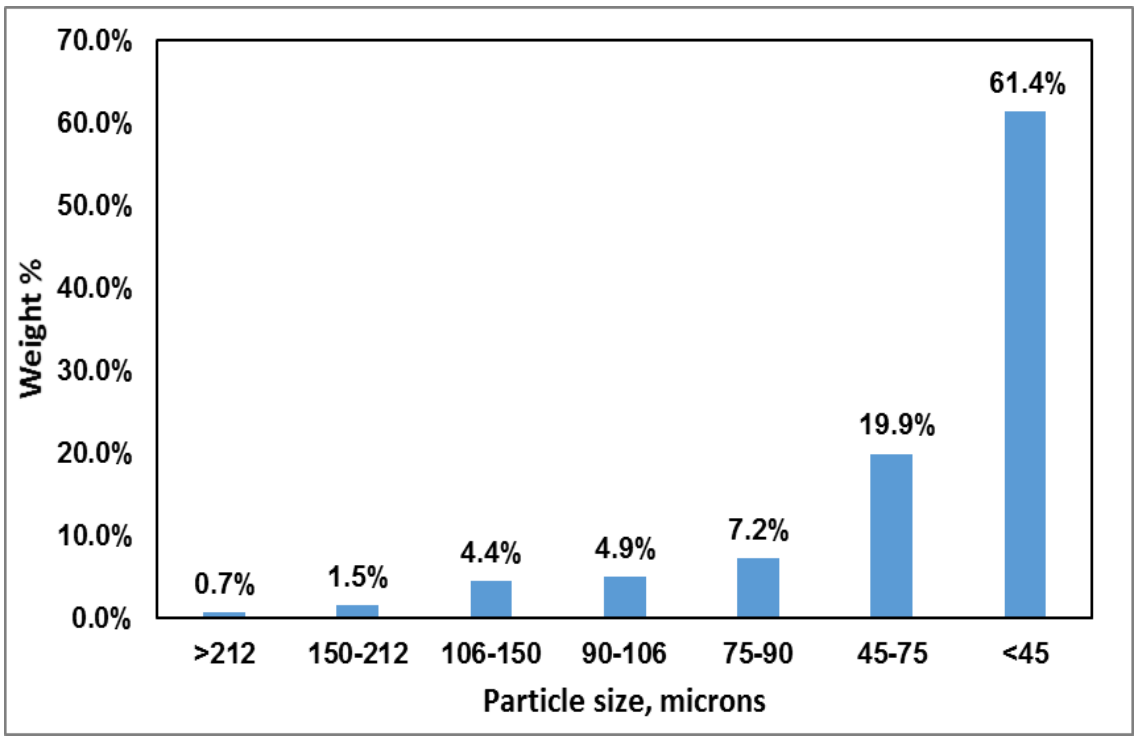

Fig. 13—Kaolinite particle size distribution histogram.

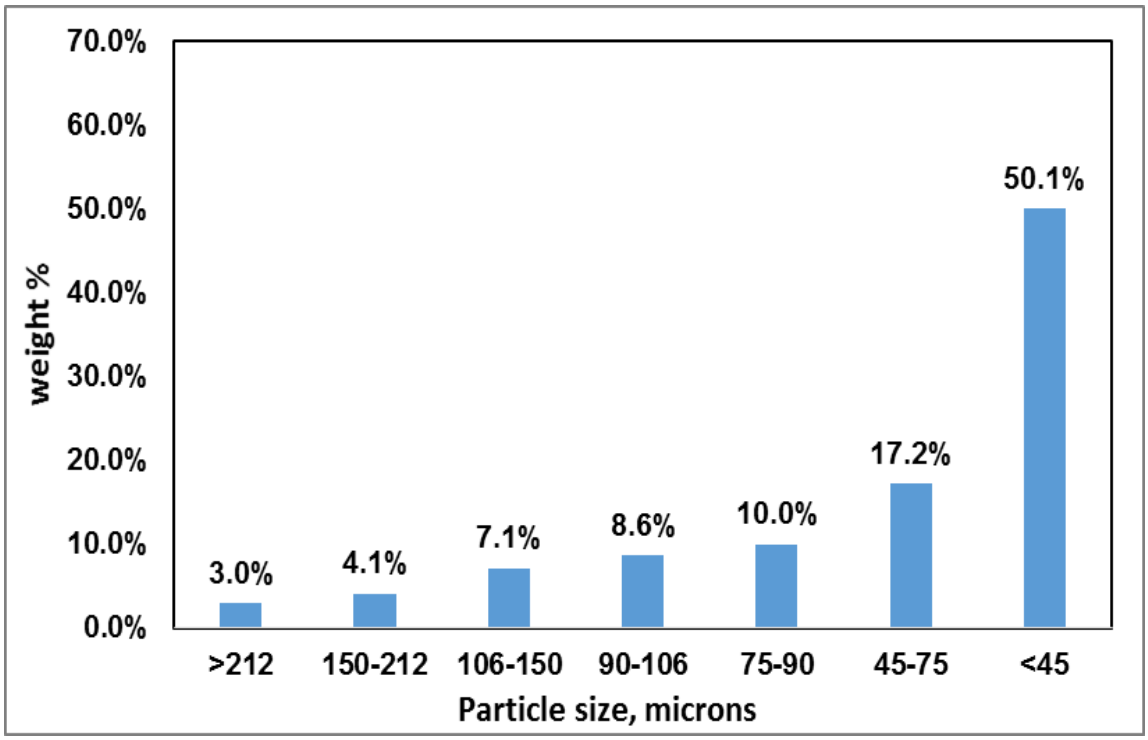

Fig. 14—Bentonite particle size distribution histogram.

Chlorite and Illite samples were received in cobble sizes. They were broken down to final sizes using a rock grinder and a shatter box. Its particle distribution histogram appeared to be a normal-right skewed pattern, and is shown in **Figs. 15 and 16**. The particle diameters ranging from 45-75 μm were selected to represent chlorite and illite samples.

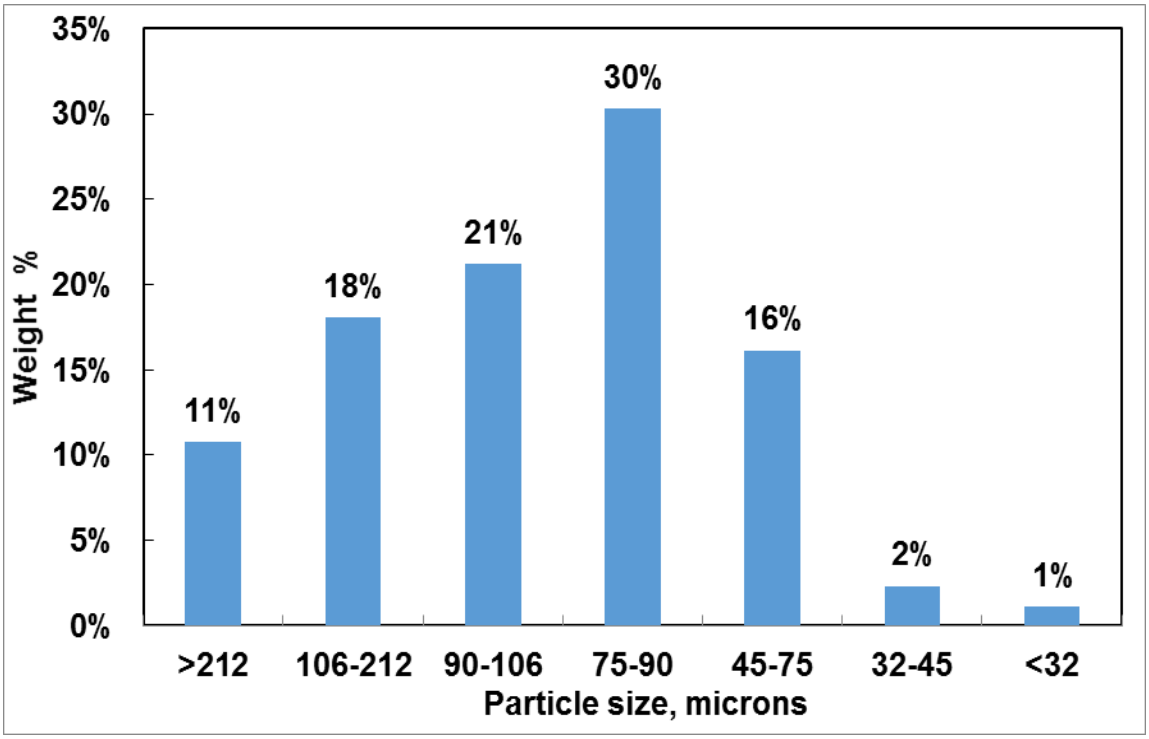

Fig. 15—Chlorite particle size distribution histogram.

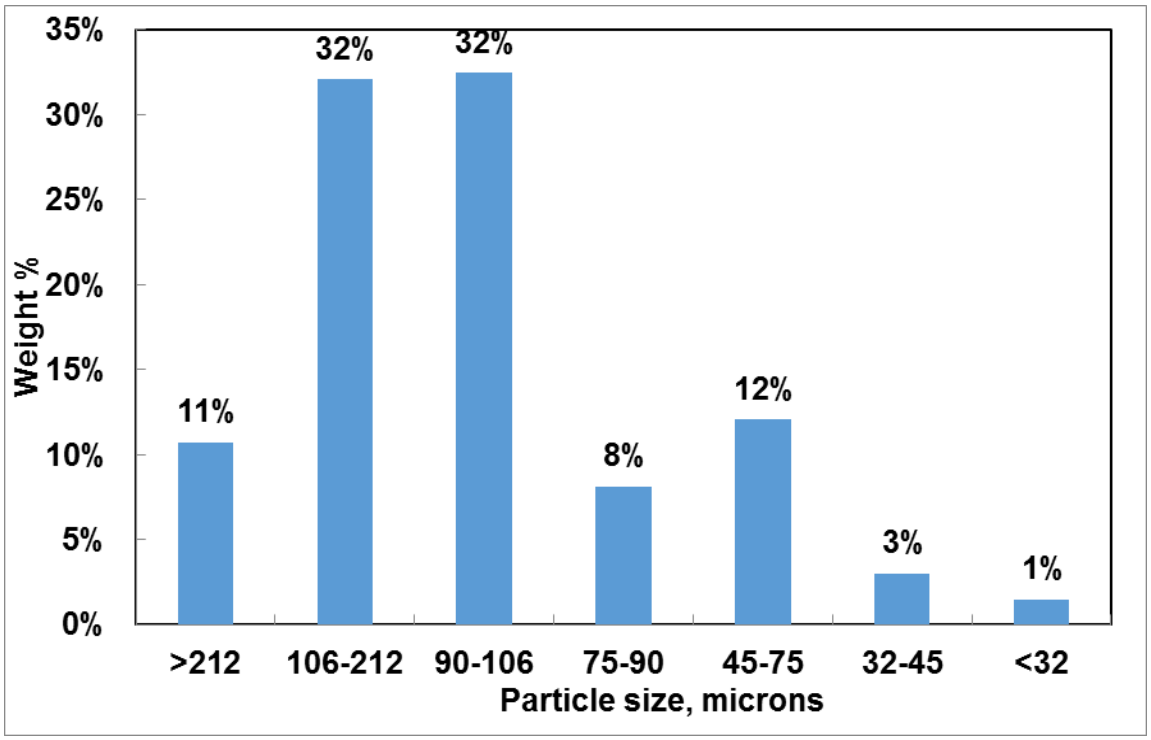

Fig. 16—Illite particle size distribution histogram.

Clay Solubility Tests

Four types of clay minerals (kaolinite, bentonite, chlorite, and illite) were reacted with phosphonic-based HF acid at the weight ratio of 1 to 10. Two grams of clay minerals were weighed into 50 cm^3 plastic tubes, and 20 cm^3 of acid with different concentrations of HF were added to each sample and left to react at different temperatures. Reaction times ranged from 0.5 to 24 hours at 77°F. After the reaction, the suspension was filtered using 2 μm filter paper. The concentration of aluminum (Al), silicon (Si), magnesium (Mg), calcium (Ca), iron (Fe), sodium (Na), and potassium (K) ions in the filtrate were analyzed by Inductivity Coupled Plasma using an Optima 7000DV ICP-OES system and

WinLab 32^{TM} software (**Fig. 17**), a type of mass spectrometry which is capable of detecting metals and several non-metals at concentrations as low as one part in 10^{12} (part per trillion). The filtered solids were washed with DI water, dried, and then analyzed with Evex Mini-SEM/EDS NanoAnalysis to obtain their composition.

Fig. 17— Optima 7000 DV Inductively Coupled Plasma (ICP).

For the solubility tests at high temperatures, for example, 302°F, the oven was preheated to 302°F, then 4 grams of clay minerals and 40 grams of acids were mixed and put into a Teflon liner, the Teflon liner was then pressurized into an aging cell (**Fig. 18**)

using nitrogen source, and rotated in the oven for different times. The supernatants and solids were analyzed through the same procedures as at the room temperature condition.

Fig. 18—OFITE Aging Cell

NMR Analysis

Nuclear Magnetic Resonance (NMR) analysis is the main research technique used in this study. This technique exploits the magnetic properties of certain atomic nuclei in a magnetic field which absorb and re-emit electromagnetic radiation that resonates with intramolecular magnetic field around an atom. The obtained spectrum can provide

detailed information about the structure, dynamics, reaction state, and chemical environment of molecules, which can be used to identify a substance.

Reacted fluoride complexes in the spent acids were analyzed by ^{19}F NMR spectroscopy using a 400 MHz Oxford NMR spectrometer (**Fig. 19**). Samples were prepared in 7 cm NMR tubes with deuterated water (D_2O) added to provide a reference lock. ^{19}F chemical shifts was externally referenced to boron trifluorideetherate ($BF_3 \cdot Et_2O$). Together with the standard NMR sample tubes, 5 mm PTFE-FEP (polytetrafluoroethylene/fluorinated ethylene polypropylene copolymer) tube liners were used to avoid HF reactions with glass. More details regarding the procedure using ^{19}F spectroscopy to determine the chemistry of HF acidizing are given by Schuchart and Buster (1995). They used trifluoro acetic acid (CF_3COOH) as a reference, and did not use an internal lock signal for the reference.

^{31}P NMR measurements were performed on a Varian Unity Inova-400 MHz spectrometer at ambient temperature. Spectra were recorded using a 45° observe pulse, an acquisition time of 1.6 s, and a relaxation delay of 1.0 s. Chemical shifts were reported relative to an external 85% H_3PO_4 standard ($\delta = 0$, that is chemical shift is 0). Signals were assigned to the P species based on literature (Cade-Menun 2005). Similar to the ^{19}F NMR tests, samples were prepared in 7 cm NMR tubes with deuterated water (D_2O). All NMR experiments were carried out at 75°F. ^{19}F and ^{31}P NMR acquisition parameters are shown as **Table 9**.

TABLE 9—NMR acquisition parameters	
^{19}F NMR Acquisition Parameters	^{31}P NMR Acquisition Parameters
○ Inova400, tuned to 375.9MHz ○ Run sample w/o internal lock signal in 5 mm OD tubes ○ Acquisition parameters ▪ 45° pulse angle ▪ 2.000 sec relax. delay ▪ Spectral width of 50000.0 Hz ▪ 1.000 sec acquisition time	○ Inova400, tuned to 128.2 MHz ○ Run sample w/o internal lock signal in 5 mm OD tubes ○ Acquisition parameters ▪ 45° pulse angel ▪ 1.000 sec relax. delay ▪ Spectral width of 21025.0 Hz ▪ 1.600 sec acquisition time

Fig. 19—NMR Spectrometer

SEM/EDS Analysis

The composition of different clay minerals before and after a chemical reaction was analyzed using Evex Mini Scanning Electron Microscope (SEM) with MSC-1000 Mini-Sputter Coater and energy-dispersive X-ray spectroscopy (EDS) (**Fig. 20**). SEM is a type of electron microscope that produces images of a sample by scanning it with a focused beam of electrons. MSC-1000 Mini-Sputter Coater is used to coat the gold to the samples for SEM.

Fig. 20—Evex Mini- Scanning Electron Microscope (SEM) with MSC-1000 Mini-Sputter Coater and energy-dispersive X-ray spectroscopy (EDS).

Results and Discussion

Solubility tests were carried out over the temperature range of 77 to 302°F for various time intervals. The progress of the dissolution reactions of different clay minerals was mainly followed in terms of the release of key ions from the minerals to the spent acids.

Effect of Reaction Time

The ion concentrations in the full strength phosphonic-based HF acid after reaction with clay minerals at 77°F were measured as a function of the reaction time (**Figs. 21 to 24**).

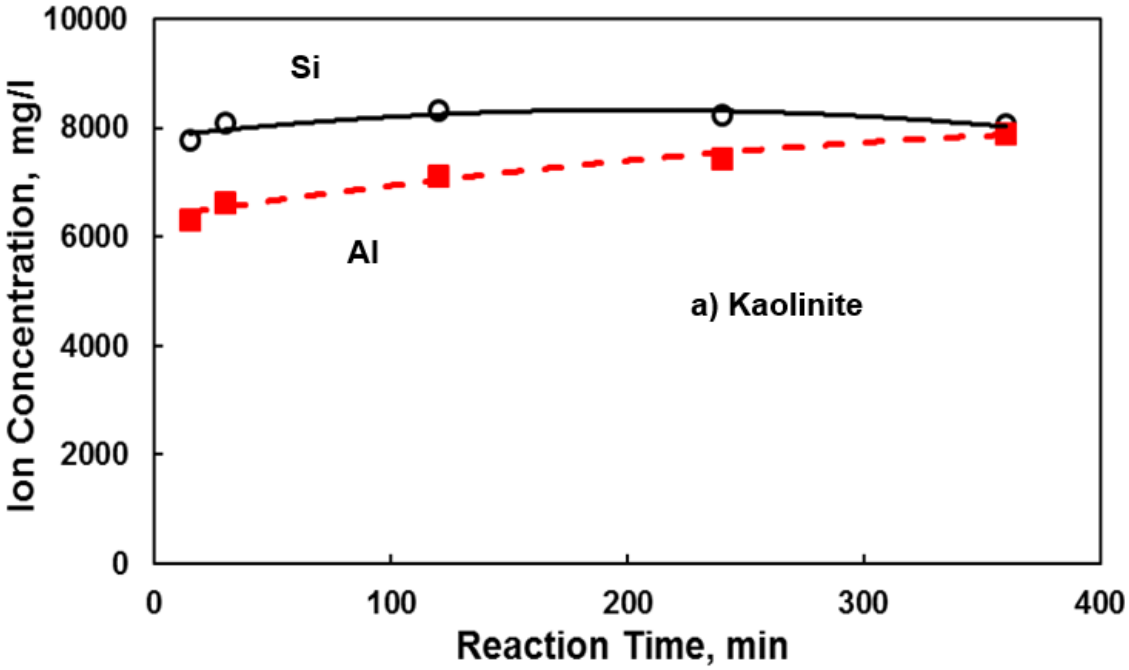

Fig. 21— Ion concentrations in the spent acids after full strength phosphonic-based HF acid reacted with kaolinite at 77°F.

After reaction with kaolinite (**Fig. 21**), only Si and Al were detected in the spent acid solution. Kaolinite is composed of Al, Si, and O (Table 8), and it contains equal amounts of aluminum and silicon. It has a 1:1 layer structure, with one tetrahedral silica sheet stacked to one octahedral alumina layer. The two layers are equally exposed in the solution. Therefore, the silicon and aluminum concentrations should be approximately the same when reacted with the phosphonic-based HF acid, as long as no secondary reaction takes place. The results showed that the concentration of Al was less than that of Si during the first 4 hours. However, more Al was dissolved than Si when

phosphonic-based HF acid reacted with kaolinite for 24 hours (**Tables 10**). This indicated that increasing soaking time might have caused Si precipitation in the phosphonic-based HF acid solution.

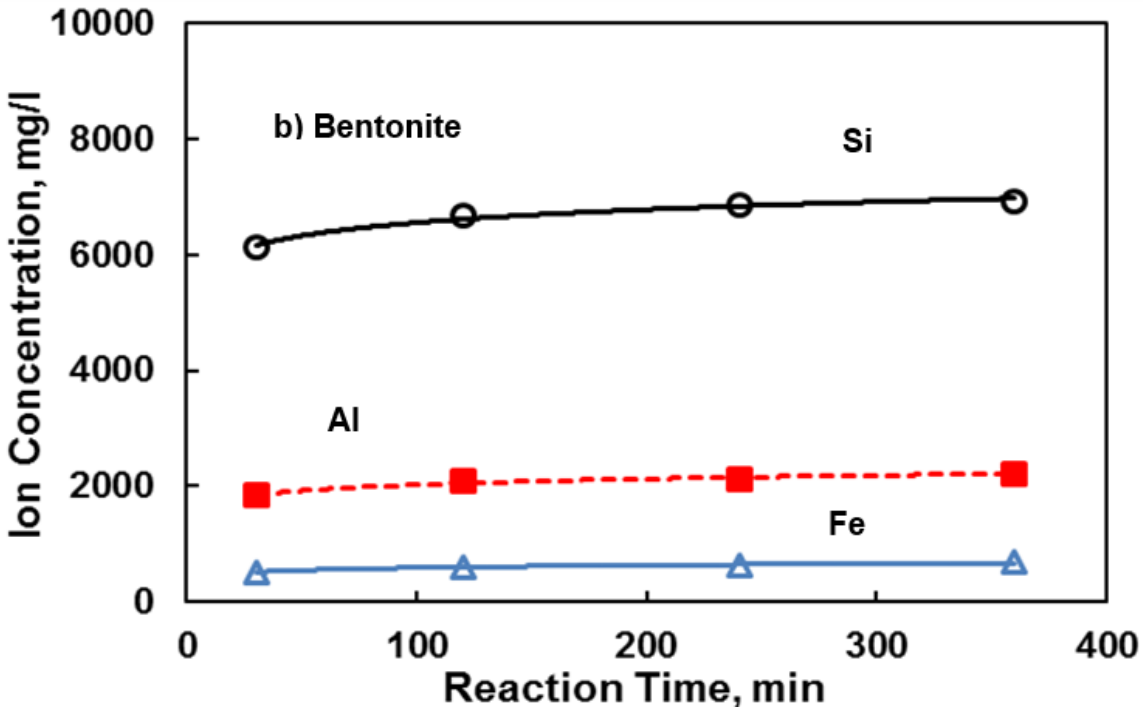

Fig. 22— Ion concentrations in the spent acids after full strength phosphonic-based HF acid reacted with bentonite at 77°F.

After the phosphonic-based HF acid reacted with bentonite (**Fig. 22**), Si and Al were the major ions in the spent acid. The Si/Al molar ratio was close to the molar ratio of both elements in the clay mineral, indicating that phosphonic-based HF acid could dissolve aluminum and silicon equally. While for the cases of chlorite and illite (**Figs. 23**

and 24), Si and Fe were the major ions in the spent acid solutions, the concentration of aluminum was relatively low, although the element compositions of aluminum in chlorite and illite are 12.28 and 11.03 wt%, respectively (Table 8). The low concentration of aluminum in spent acid might be caused by the structures of these two minerals, which contains one alumina layer sandwiched between two silica layers. This structure makes the Al not very accessible to the acid.

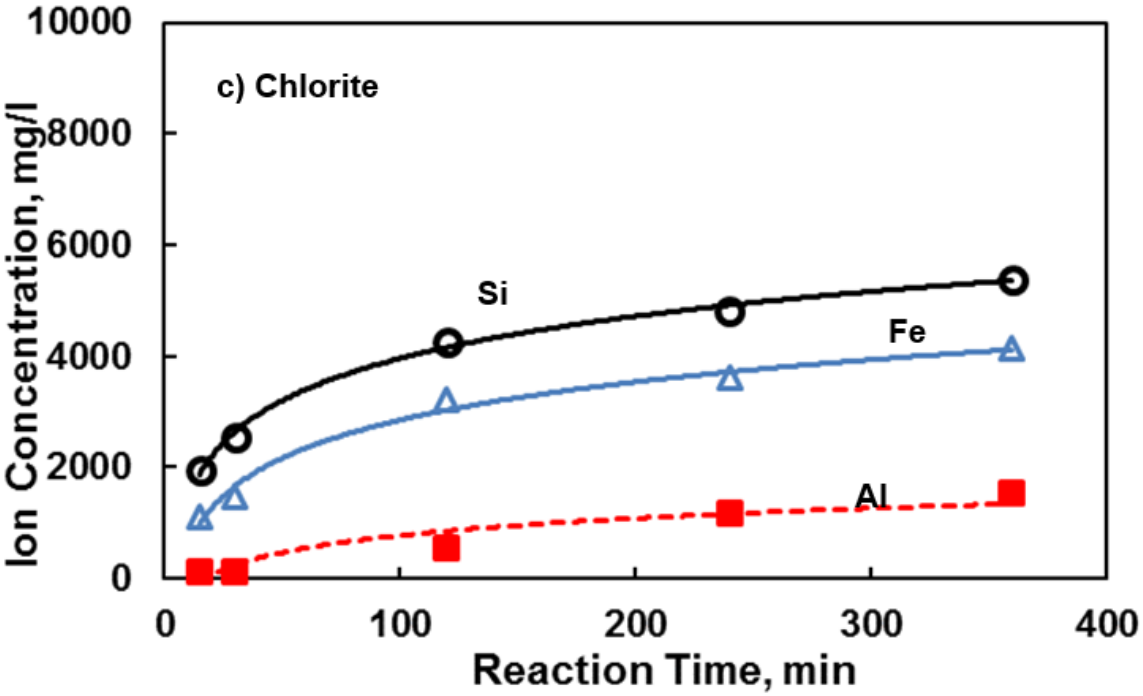

Fig. 23— Ion concentrations in the spent acids after full strength phosphonic-based HF acid reacted with chlorite at 77°F.

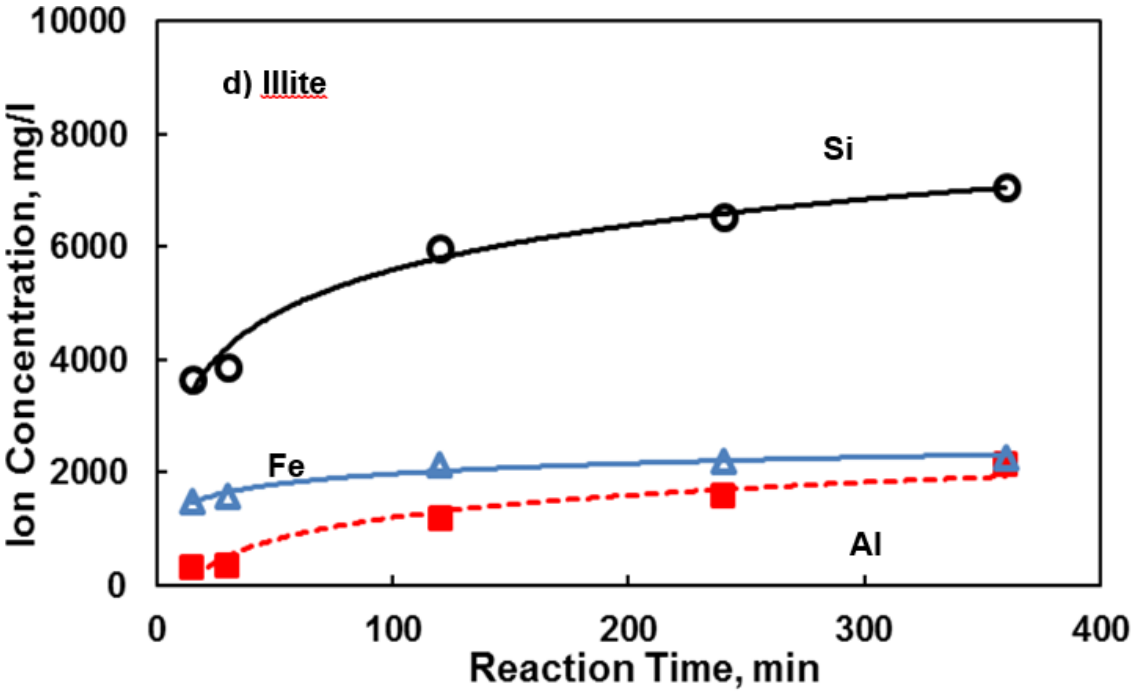

Fig. 24— Ion concentrations in the spent acids after full strength phosphonic-based HF acid reacted with illite at 77°F.

The dissolution of clay minerals was also investigated as a function of reaction time at 302°F to better understand the effect of the treatment time at high temperatures. **Fig. 25** illustrates the ion concentrations in the spent acid solution after a full strength phosphonic-based HF acid reacted with kaolinite at 302°F, where the Al concentration increased with increasing reaction time and reached 16,868 mg/l after 6 hours. In contrast to the Al concentration trend, the Si concentration decreased with an increase in time. The concentration of Al was greater than that of Si even during the initial 30 minutes of reaction, demonstrating secondary reactions did occur in the first 30 minutes of the reaction at 302°F.

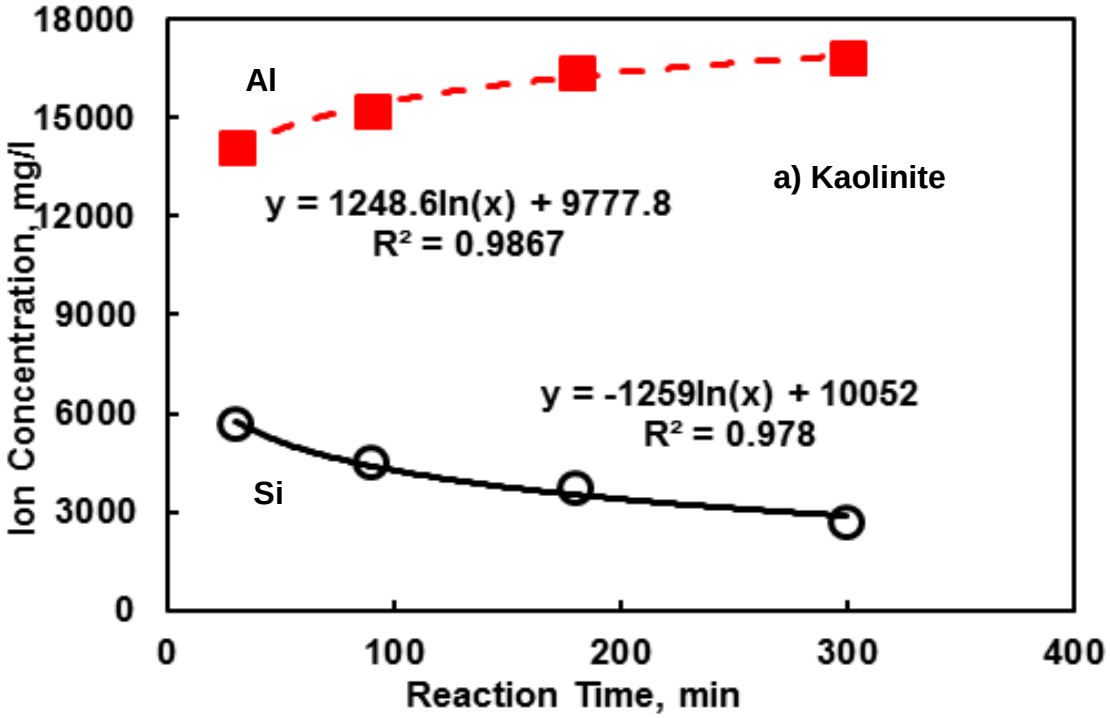

Fig. 25—Ion concentrations in the spent acids after full strength phosphonic-based HF acid reacted with kaolinite at 302°F.

The dissolution trend of bentonite at 302°F was similar to the results of kaolinite (**Fig. 26**); nearly 2 times the amount of silicon was dissolved than aluminum in the initial 30 minutes of the reaction. With the increase in reaction time, more aluminum was extracted while the detected silicon concentration decreased. This observation also indicated that secondary reactions occurred at 302°F.

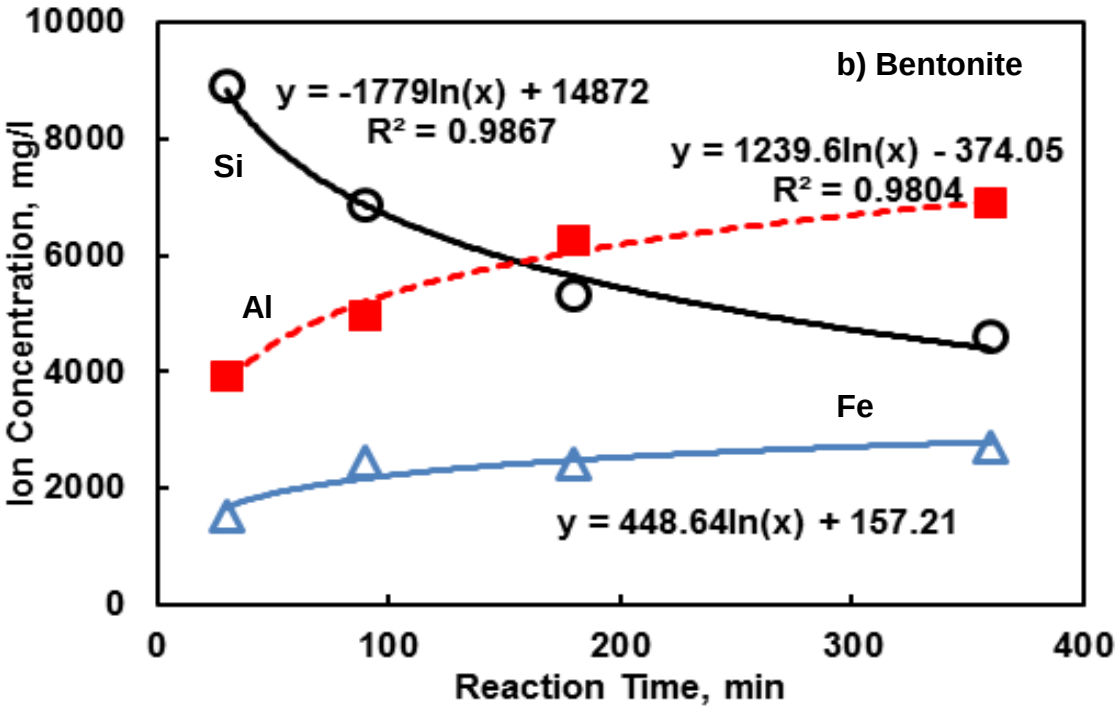

Fig. 26—Ion concentrations in the spent acids after full strength phosphonic-based HF acid reacted with bentonite at 302°F.

Fig. 27 shows the ion concentrations in the reaction solution of a full strength phosphonic-based HF acid after reaction with chlorite at 302°F for different intervals. The decrease in the Si concentration indicated Si precipitation. The concentration of Al was much lower than that of Si, although the element composition of Al in chlorite was almost the same as Si, which were 12.28 and 11.46 wt%, respectively (**Table 8**). This may be attributed to either the reduced efficiency of the full strength phosphonic-based HF acid in dissolving Al or the precipitation of dissolved Al. Chlorites are 2:1:1 phyllosilicates minerals, the 2:1 layers are formed by the stacking of two tetrahedral silica sheets and one octahedral alumina sheet. They have an additional layer that is

octahedrally coordinated. The elemental composition in the present study indicates a Si/Al ratio of 1, which is due to the substitution of Si by Al in the tetrahedral layer. As a result, the structure of the chlorite, used in this study, makes it more reactive in the full strength phosphonic-based HF acid. Therefore, more Al should be detected. The low Al concentration in spent acid solutions is an indication of aluminum fluoride precipitation.

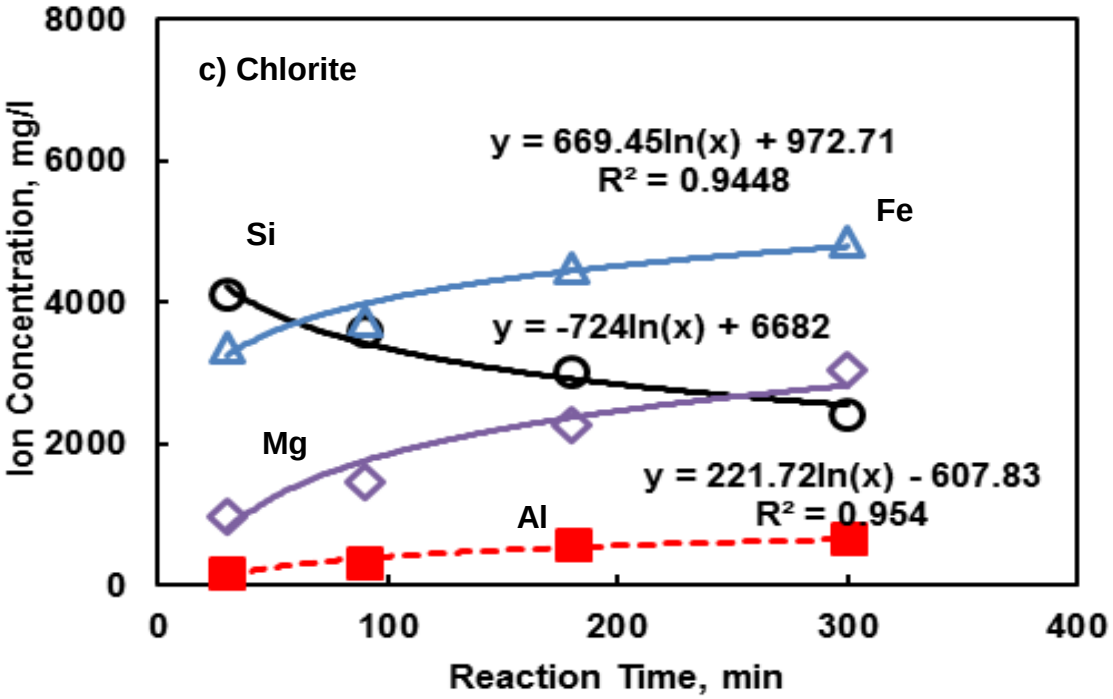

Fig. 27—Ion concentrations in the spent acids after full strength phosphonic-based HF acid reacted with chlorite at 302°F.

The dissolution trend of chlorite in the present study was different from that in the 9:1 mud acid reported by Hartman et al. (2006). They reported that 9:1 mud acid was able to extract approximately 8,100 mg/l of Al when reacted with chlorite for 3 hours at

212°F. This is significantly higher than the Al concentration detected in the full strength phosphonic-based HF acid after it reacted with chlorite for 4 hours at 302°F. Moreover, more Mg was detected in the reaction solution after the 9:1 mud acid reacted with chlorite than that detected in the full strength phosphonic-based HF acid reaction solution. The full strength phosphonic-based HF acid, however, have a higher HF concentration (3 wt%) than the 9:1 mud acid. The difference in reactivity is mainly due to the different compositions and structures of the chlorite samples used in their study. The elemental composition in their study indicates a Si/Al ratio of 2, whereas the ratio in the present study was near 1. As a result, the structure of the chlorite used in this study was less stable in the acids. Also, chlorite samples used in the present study contained 10.84 wt% Fe and 13.51 wt% Mg, whereas Hartman et al. used samples containing approximately 1.6 wt% Fe and 31 wt% Mg. This difference in Fe and Mg content may have led to a higher reactivity of the chlorite, and the dissolution rate of the chlorite increased with an increase in Fe and decrease in Mg content (Ross 1969). Also, large amounts of Fe and Mg were leached from the chlorite during dissolution at 302°F, and both concentrations increased with reaction time.

Analysis of the reaction solution for the dissolution of illite in the full strength phosphonic-based HF acid showed that the concentration of Si also decreased at 302°F indicating Si precipitation (**Fig. 28**). The Al concentration increased slightly with reaction time to reach 4,136 mg/l within 5 hours. Compared to 9:1 mud acid, the present studied acid system was able to dissolve high Si contents and lower Al concentrations. According to Hartman et al. (2006), 9:1 mud acid extracted approximately 8,000 mg/l of

the Al when reacted with illite at 212°F for 4 hours. This amount was greater than the amount detected in the spent full strength phosphonic-based HF acid solutions.

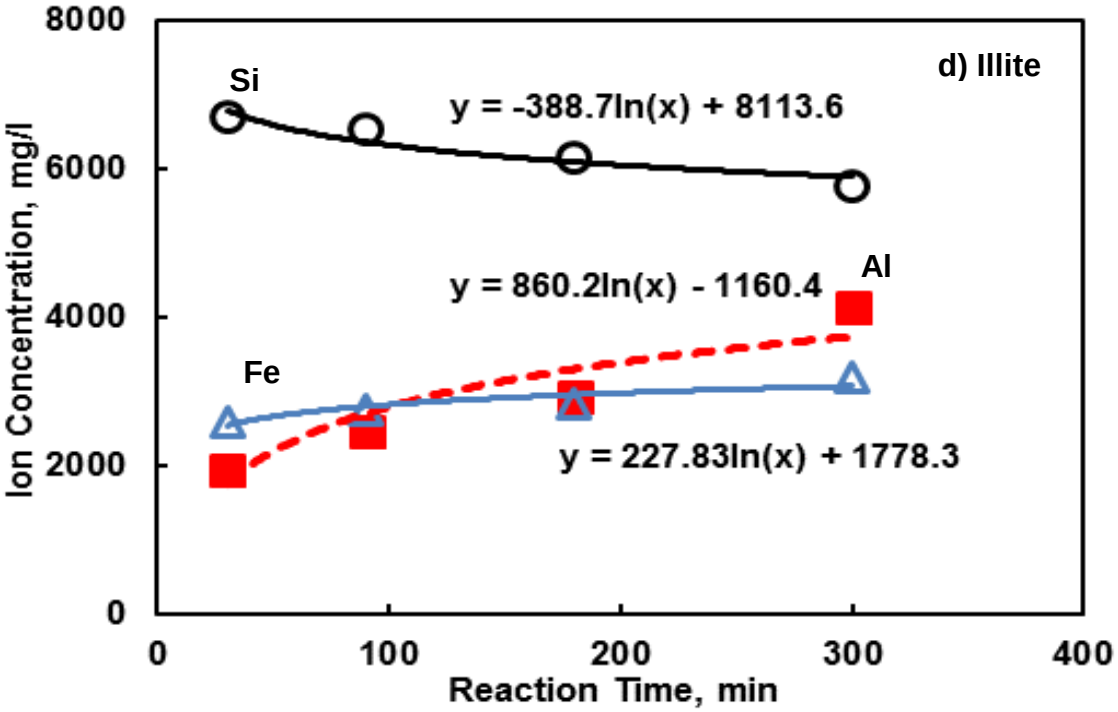

Fig. 28—Ion concentrations in the spent acids after full strength phosphonic-based HF acid reacted with illite at 302°F.

Effect of Temperature

To better understand the reactivity and potential precipitation of the phosphonic-based HF acid with clay minerals, solubility tests were conducted as a function of temperature. After four types of clay minerals reacting with full strength phosphonic-based HF acid, the ion concentrations in the spent acid solutions were analyzed (**Figs. 29 to 32)**.

The ion types, corresponding concentrations, and general trends are quite different for these clay minerals. After the reaction with kaolinite (**Fig. 29**), only Si and Al were detected in the spent acid solution. Approximately equal amounts of aluminum and silicon were dissolved at 77°F. The silicon concentration decreased from 9,297 at 77°F to 5,661 mg/l at 302°F, while the aluminum concentration increased from 6,473 to 14,087 mg/l with the increase of reaction temperature.

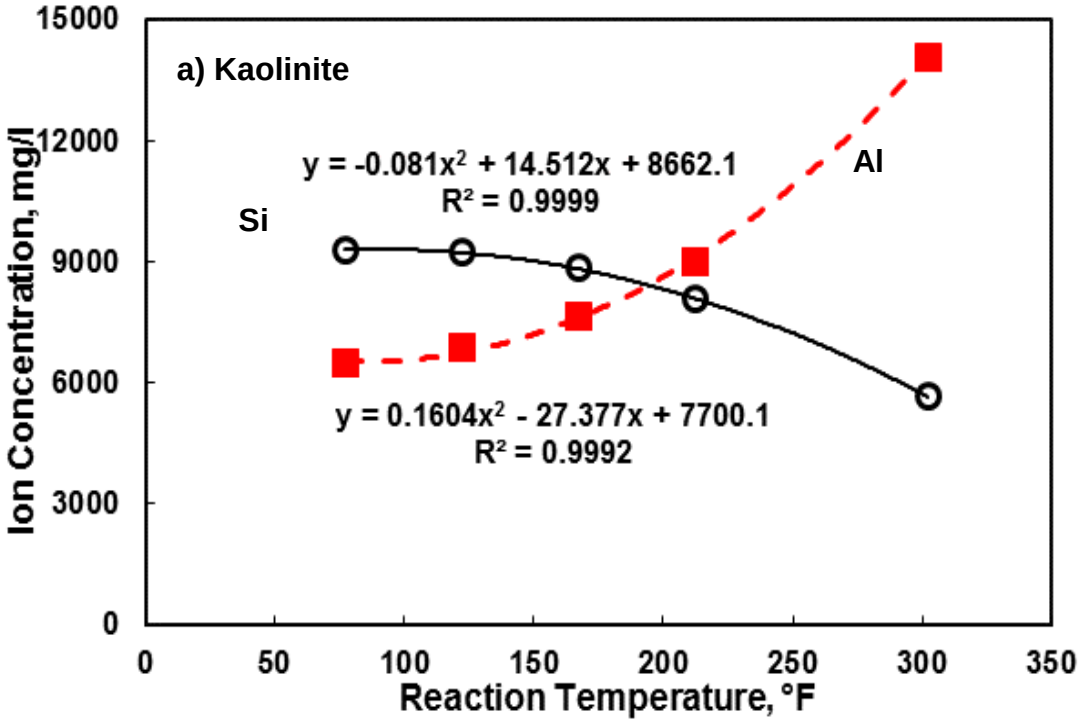

Fig. 29—Concentrations of key cations in the spent acids after full strength phosphonic-based HF acid reacted with kaolinite at different temperatures for 30 minutes.

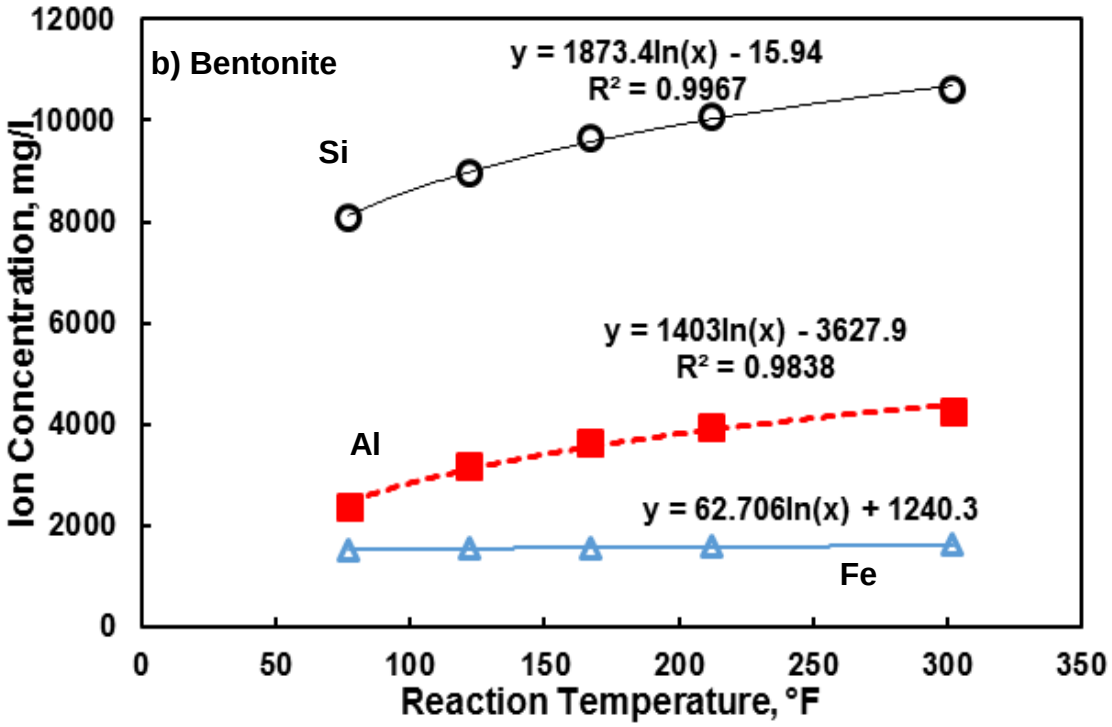

Fig. 30—Concentrations of key cations in the spent acids after full strength phosphonic-based HF acid reacted with bentonite at different temperatures for 30 minutes.

A similar trend was found for bentonite (**Fig. 30**), except that more than two times the amount of silicon than aluminum was dissolved by the acids. This indicated that the secondary reaction between clay minerals and HF acid was very slow at low temperatures and became faster at higher temperatures. For chlorite and illite (**Fig. 31 and Fig. 32**), nearly no Al was detected at low temperatures. Both silicon and aluminum concentrations increased with the increased reaction temperature.

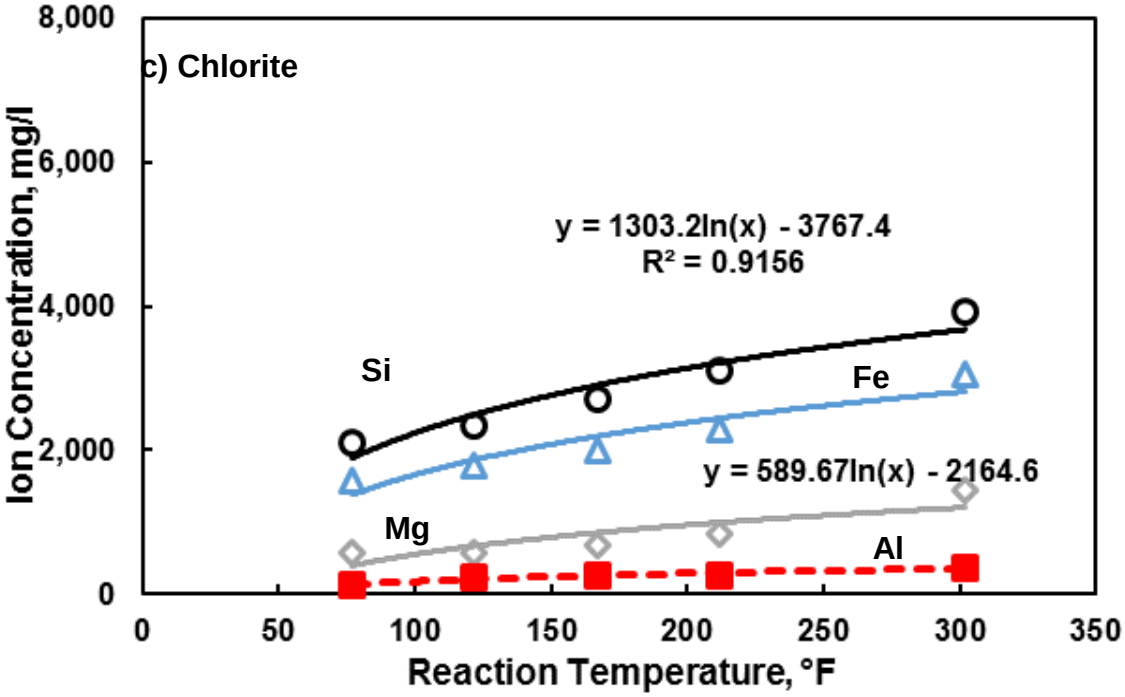

Fig. 31—Concentrations of key cations in the spent acids after full strength phosphonic-based HF acid reacted with chlorite illite at different temperatures for 30 minutes.

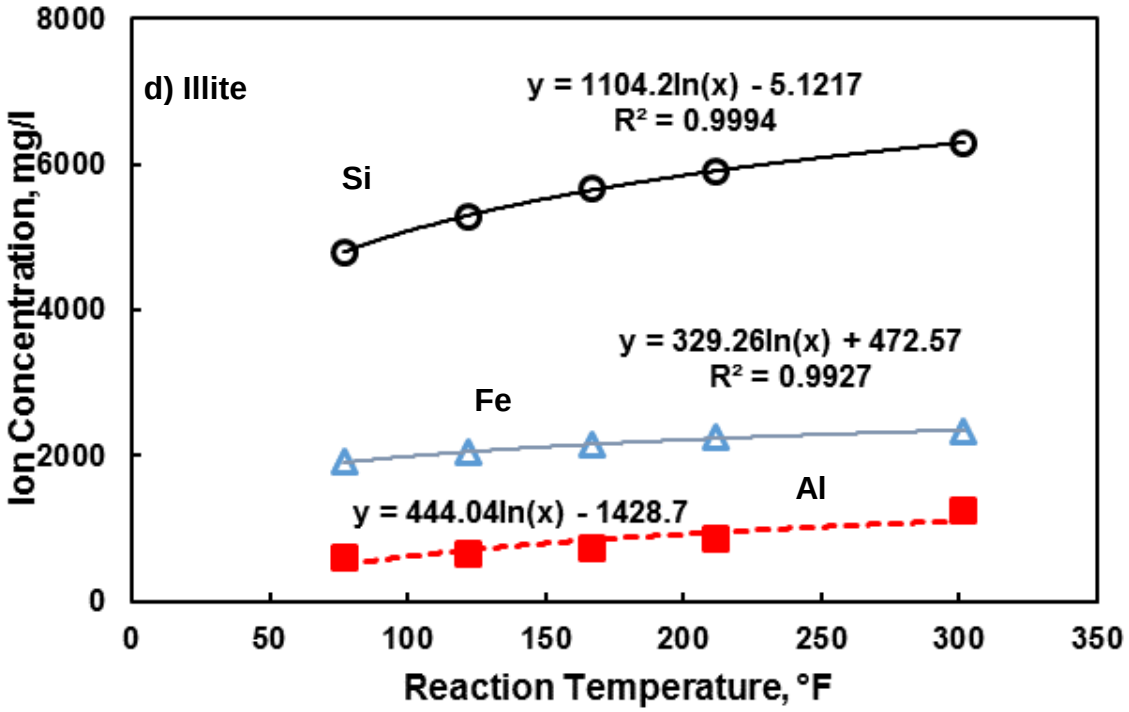

Fig. 32—Concentrations of key cations in the spent acids after full strength phosphonic-based HF acid reacted with illite at different temperatures for 30 minutes.

Since the secondary and tertiary reactions could have altered the Si/Al ratio significantly, the ratio of Si/Al was investigated to further confirm that the secondary reaction occurred for the chlorite and illite. The results are shown in **Fig. 33**. For all four types of clays, the Si/Al ratio decreased when the temperature increased. This can be explained by the secondary reaction of aluminosilicates with HF. In the secondary reaction, fluosilicic acid produced from the primary reaction continued to reacts with aluminosilicates to generate more aluminum fluoride species. During this process, Si transferred from fluosilic acid to silica gel, thus, the concentration of Al in the spent acid

solution increased, while the concentration of Si decreased. As a result, the ratio of Si/Al decreased.

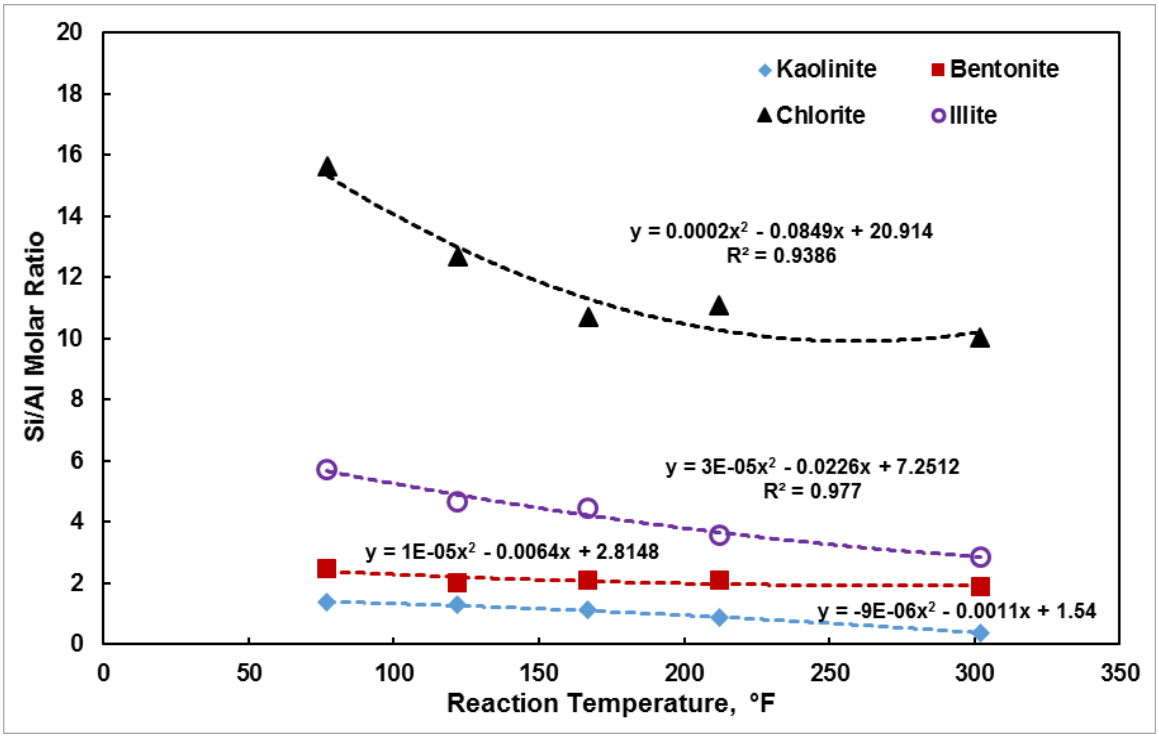

Fig. 33— Si/Al molar ratio in spent acid solutions after full strength phosphonic-based HF acid reacted with clay minerals at different temperatures for 30 minutes.

Effect of HF Acid Concentration

The effect of the HF concentration of phosphonic-based HF acid was also evaluated by using a full and a half strength phosphonic-based HF acid, which has 3 and 1.5 wt% HF acid, respectively. The results are shown in **Table 10**.

TABLE 10— Ion concentrations in spent acid after clays reacted with full and half strength phosphonic-based HF acids for 24 hours at 77°F[a]

Concentration, mg/l	Kaolinite		Bentonite		Chlorite		Illite	
	Full	Half	Full	Half	Full	Half	Full	Half
Al	12100	6420	3278	1837	537	189	3407	2014
Si	7610	4060	8225	4370	5135	2878	6595	3810
Fe	–	–	1228	885	4193	2370	2415	1939
Mg	–	–	551	392	2435	1333	956	578
Ca	–	–	893	458	–	–	–	–
Na	–	–	761	595	–	–	–	–
K	–	–	–	–	–	–	581	393
P	16012	8140	1578	8080	15950	8035	16045	8090
pH	0.561	0.988	0.53	0.842	0.523	0.834	0.541	0.855

a. **pH values of fresh full and half strength phosphonic-based HF acid are 2.106 and 2.236; respectively, and P concentrations in full and half strength phosphonic-based HF acid are 16120 and 8095 g/ml; respectively.**

After reaction with clay minerals for 24 hours at 77°F, the full strength phosphonic-based HF acid dissolved more aluminum and silicon from four types of clay minerals than the half strength phosphonic-based HF acid. For example, in the spent acid solution

after reacting with illite, the aluminum concentration decreased from 3,407 mg/l in full strength phosphonic-based HF acid to 2014 mg/l in half strength phosphonic-based HF acid. It also can be seen that spent acid, after reacting with kaolinite, had a much higher aluminum concentration than the other three clays. This was caused by the high weight percentage of aluminum in kaolinite (Table 8). A similar trend was found for the silicon concentration, except that more silicon was dissolved from bentonite than from the other three clay minerals.

The results also showed that the silicon and aluminum concentrations in spent acid of 3 wt% HF after reacting with clay minerals were almost double the concentrations in the spent acid solution of 1.5 wt% HF after reaction for the same clay minerals. For example, for the kaolinite case, the Si concentration is 7,610 mg/l in 3 wt% HF while it is 4,060 mg/l in 1.5 wt% HF. This result showed that the high concentration of HF is more effective in dissolving the aluminosilicates and Si and Al concentrations are almost proportion to the HF concentration. While for the other ions such as iron, magnesium, sodium and potassium, especially for calcium, the concentration in 3 wt% HF is very close to that in 1.5 wt% HF, this result indicated that the 1.5 wt% HF acid already has enough HCl to dissolve these elements in clay minerals when it reacted with clay minerals at a weight ratio of 10:1. The 3 wt% HF acid has extra HCl after reacting with clay minerals at the same weight ratio, which can dissolve more minerals except clay minerals in sandstone formations during acidizing treatment.

The ratio of Si/Al was also investigated for phosphonic-based HF acid with different HF acid concentrations after reaction with clay minerals (**Fig. 34**). When

compared with the other three clays, the highest Si/Al ratio was found in chlorite for both strengths of phosphonic-based HF acid. While for the same clay mineral, the strength difference between two phosphonic-based HF acid does not make a significant difference in the ratio. This trend can be explained by the structures of clay minerals as discussed previously.

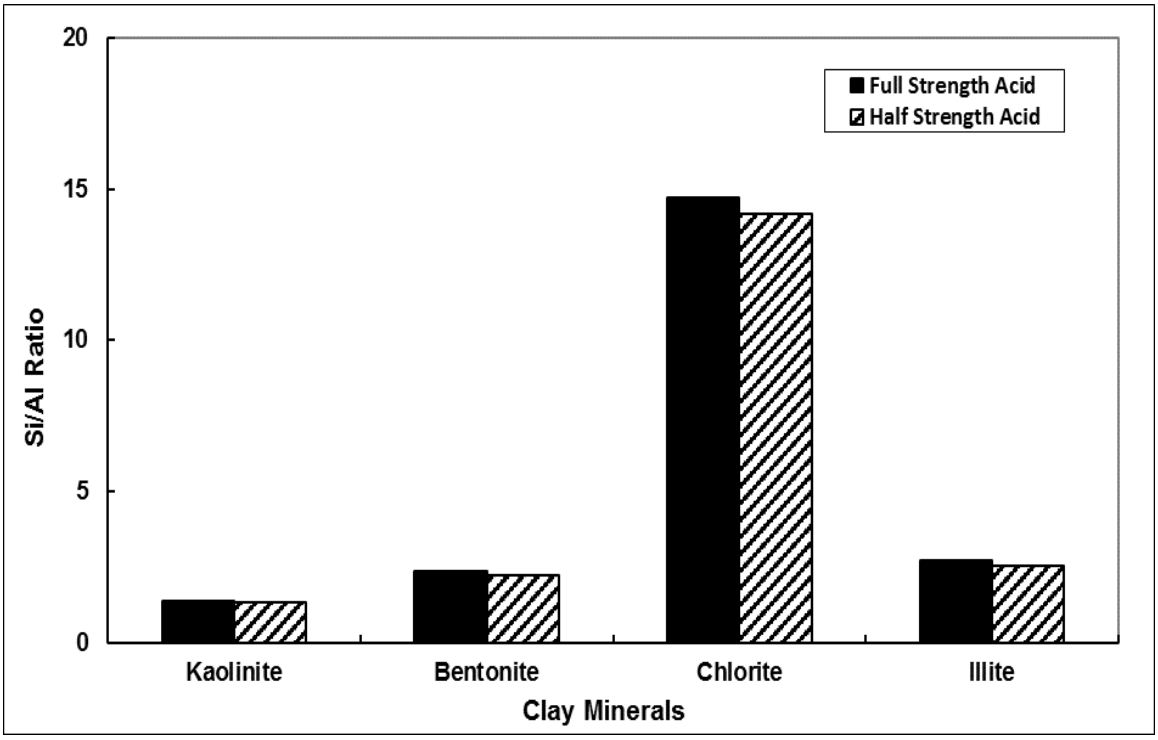

Fig. 34—Si/Al molar ratio in the spent acids after full and half strength phosphonic-based HF acid reacted with clay minerals at 77°F for 30 minutes.

Effect of Acid to Clay Weight Ratio on Solubility

To better understand the reactivity and potential precipitation of the phosphonic-based HF acid system, the solubility tests were conducted as a function of reaction ratio. Clay

minerals tested were reacted with full strength the full strength phosphonic-based HF acid at three weight ratios of 1:10, 1:20, and 1:30. The solubility of clays in bulk was showed in **Fig. 35**. It can be seen that kaolinite has higher solubility than the other two clays, which increase from 25% at weight ratio of 1:10 to 65% at weight ratio 1:30. For the cases of chlorite and illite, however, the different weight ratio between the full strength phosphonic-based HF acid and clay minerals does not make significant difference in the solubility.

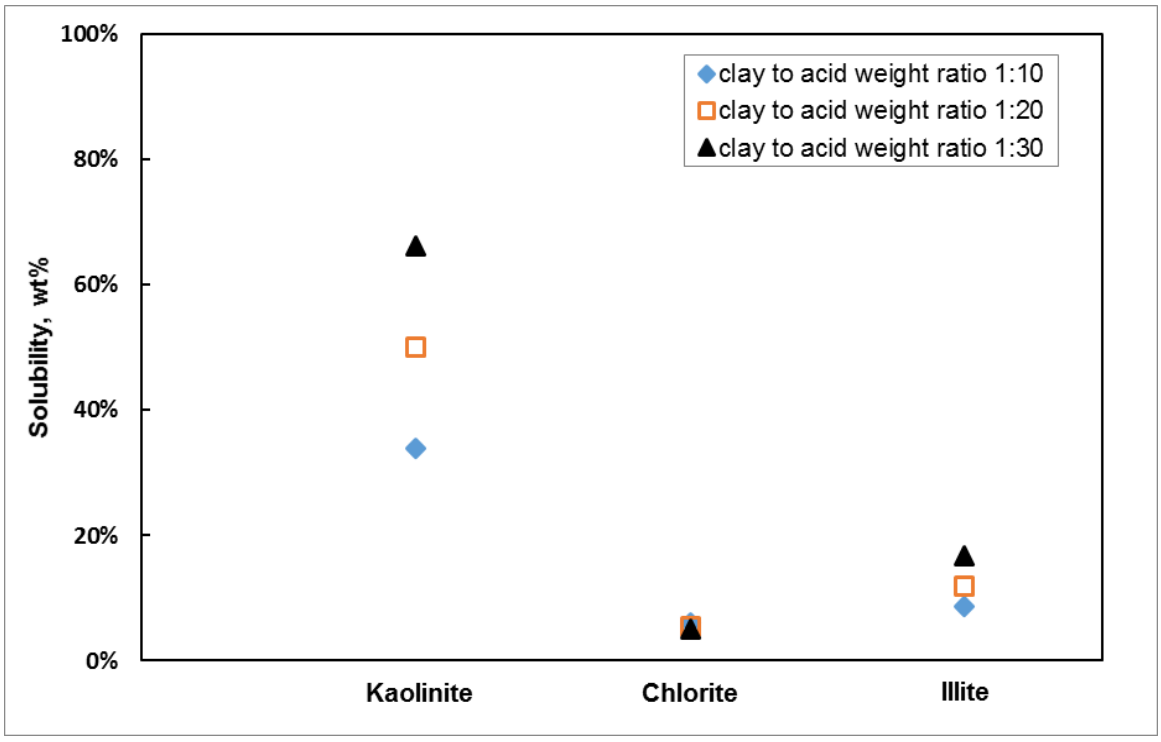

Fig. 35–Solubility of clays treated with full strength phosphonic-based HF acid system for 30 minutes at room temperature at different weight ratio.

The molar ratio of Si to Al in solid samples after reaction with the full strength phosphonic-based HF acid were also investigated, since the Si/Al ratio, just as that in the spent acid, can show the reaction extent. The stoichiometry of the dissolution reaction can be followed by comparing the Si/Al ratios of the reacted minerals with those of the untreated minerals (Table 8). **Fig. 36** showed that different weight ratio does not alter the Si/Al ratio significantly. It can be concluded that the dissolution at room temperature with different weight ratio was stoichiometric. For kaolinite, increasing weight ratio can increase the solubility, while for chlorite and illite, the optimum weight ratio was 1:10.

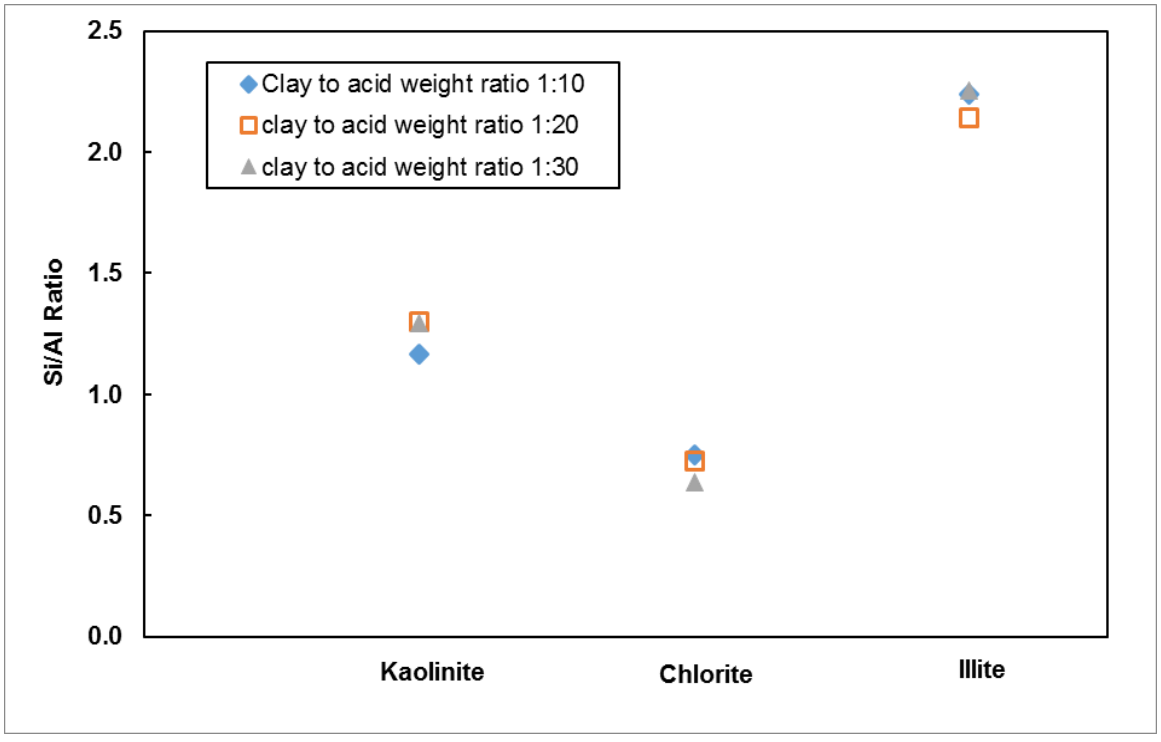

Fig. 36–Si/Al molar ratio in the reaction precipitates when full strength phosphonic-based HF acid reacted with clay minerals at room temperature at different weight ratio, reaction time is 30 minutes.

NMR Results

The ^{19}F NMR spectra of a full strength phosphonic-based HF acid after the reactions with kaolinite, bentonite, chlorite, and illite are shown in **Figs. 37 through 40**. All ^{19}F chemical shifts are reported relative to $\delta = 0$ ppm for $CFCl_3$, via an external reference of boron trifluorideetherate ($BF_3.Et_2O$) that was referenced at $\delta = -153$ ppm. Chemical shifts of the fluoride complex were first reported by Shuchart and Buster (1995) relative to trifluoro acetic acid (CF_3COOH), in their paper, they assigned the group of peaks near –50 ppm as silicon fluoride species, while those near –80 ppm as aluminum fluoride species. The chemical shift of HF was also found at –85.5 ppm in their study. To compare our results with literature reported values, their chemical shifts were converted using $CFCl_3$ as a reference first. CF_3COOH has a chemical shift of –76.55 ppm relative to $CFCl_3$ (Dungan and Van Wazer 1970). Therefore, the chemical shifts in their study can be converted to chemical shifts relative to $CFCl_3$ by –76.55 ppm. That is, the chemical shifts of silicon fluoride species were around –126.55 ppm, the signals of aluminum fluoride species were around –156.55 ppm, and HF has signal around –162 ppm relative to $CFCl_3$. The values were very similar to those reported by Yang et al. (2012).

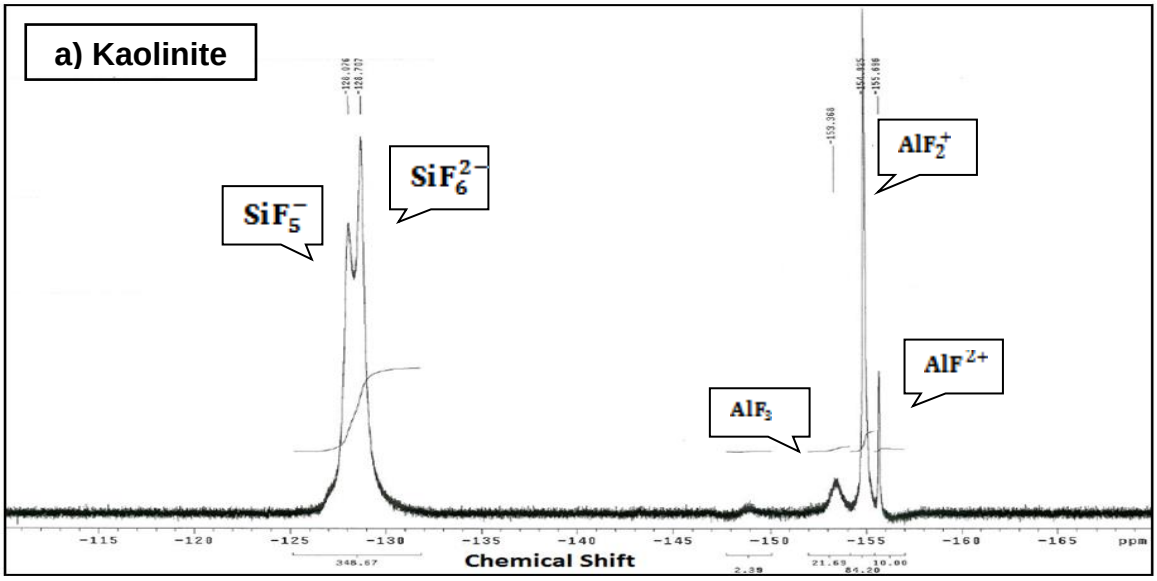

Fig. 37—^{19}F NMR spectra after full strength phosphonic-based HF acid reacted with kaolinite for 24 hours at 77°F.

In the ^{19}F NMR spectrum of full strength phosphonic-based HF acid after the reaction with kaolinite for 24 hours (**Fig. 37**), there are two groups of signals, one is around –128.08 and –128.77 ppm and the other at –154.01~ –155.08 ppm. These values are very close to the values reported by Shuchart and Buster (1995), which are silicon fluoride species and an aluminum fluoride complex, respectively. However, there is no peak at –162.05 ppm in the spectrum, which means no HF signal was observed. The results indicated that when the weight ratio between kaolinite and full strength phosphonic-based HF acid was 1:10, HF acid was completely consumed, and both silicon fluoride and aluminum fluoride species were formed. These results match the ICP analysis that showed the spent acid solution after reaction contained high concentrations of Si and Al (Table 9).

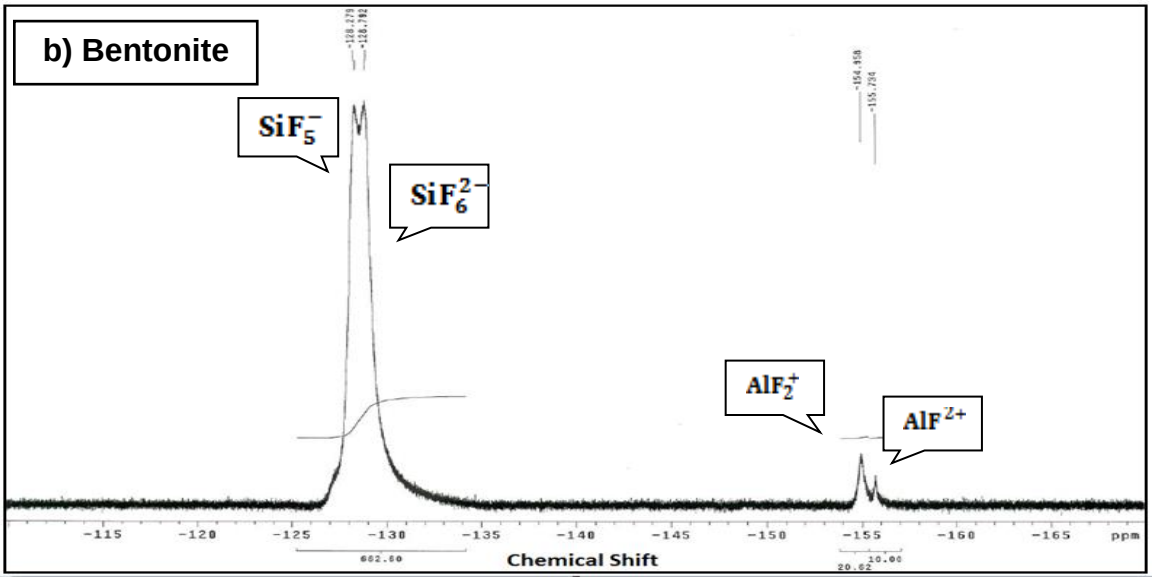

Fig. 38—^{19}F NMR spectra after full strength phosphonic-based HF acid reacted with bentonite for 24 hours at 77°F.

Figs. 37 and **38** both show two chemical shifts at –128.01 ~ –128.81 ppm. Based on the results reported by Finney et al. (2006), these two shifts belong to SiF_6^{2-} and SiF_5^-, the dominant species produced from the primary reaction. Based on the study of Sur and Bryant (1996) and Bodor et al. (2003) the main aluminum fluoride complexes in Fig. 37 can be assigned as being species AlF^{2+}, AlF_2^+ and AlF_3 This assignment is consistant with the statement of Shuchart and Buster (1995) that no higher aluminum fluoride species, such as AlF_4^-, AlF_5^{2-} and AlF_6^{3-}, were identified in acidic solutions. This was due to the solutions containing phosphonate ligands, which compete with fluoride for Al coordination, thereby leading to the formation of low aluminum fluoride species. Bodor et al. (2000) and Martinez et al. (1996) suggested that the chemical shifts of various aluminum fluoride complexes in the ^{19}F NMR move downfield as more F^- combines

with Al. For the bentonite case, only AlF^{2+} and AlF_2^+ were detected at –154.01~ –155.08 ppm. This is caused by the relatively low concentration of Al in the spent acid after the reaction with bentonite.

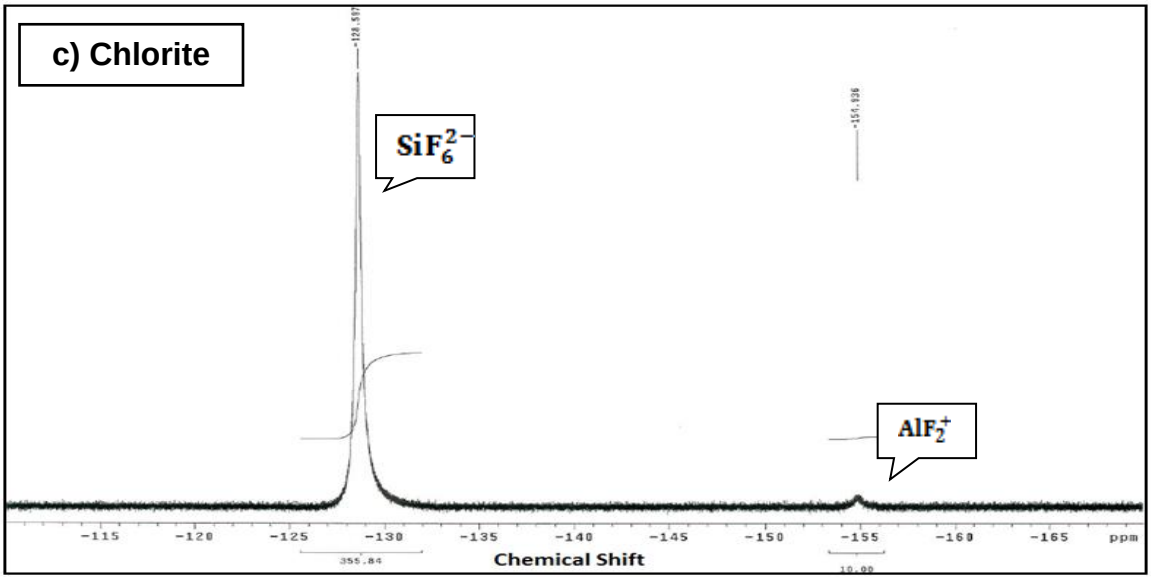

Fig. 39—^{19}F NMR spectra after full strength phosphonic-based HF acid reacted with chlorite for 24 hours at 77°F.

In the ^{19}F NMR spectra of full strength phosphonic-based acid after the reaction with chlorite and illite for 24 hours (**Figs. 39 and 40**), the major peaks are around –128 ppm. These are silicon fluoride species, and the signals around –156 ppm are very minor. Also, no HF peak is observed for this spectrum. These results indicate that HF was completely consumed and most of the fluoride ions in the spent acid were coordinated with silicon. This result agreed with the ICP analysis that showed a large amount of Si and a low concentration of Al in the spent acid solution (Table 9). This

trend is different from that of kaolinite, where a significant amount of aluminum fluoride was noted. This difference in aluminum concentration comes from the different structures of these minerals. Kaolinite has a 1:1 layered structure, so more acid can contact with the alumina sheet. While chlorite is a 2:1 layered mineral that consists of an octahedral sheet between two silica tetrahedral sheets, there is one octahedral interlayer between 2:1 layer structures. The chlorites have a wide range of compositions, since substitution can occur both in the 2:1 layers and in the interlayers. One of the most common substitutions in chlorites is the substitution of silicon by aluminum or iron (Worden and Morad 2003). The chlorite used in this study has a Si/Al molar ratio of near 1:1 and a high proportion of iron (10.84 wt%) that might be due to the substitution of aluminum or iron for the silicon in tetrahedral layer. This structure makes it hard for more acid to dissolve alumina. Therefore, less Al was detected in the acid solutions.

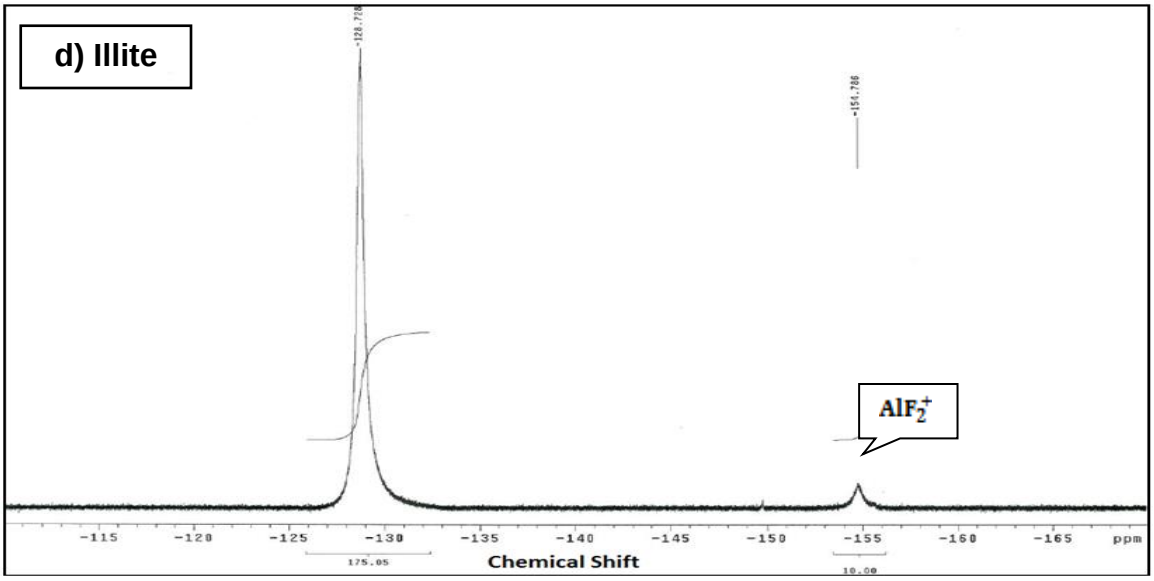

Fig. 40—^{19}F NMR spectra after full strength phosphonic-based HF acid reacted with illite for 24 hours at 77°F.

TABLE 11—Fluorine chemical shifts assignment in ^{19}F NMR spectra[a]				
Chemical shift, δ	**–128 ppm**	**–153 ppm**	**–155 ppm**	**–155.8 ppm**
Assigned as	SiF_6^{2-}, SiF_5^-	AlF_3	AlF_2^+	AlF^{2+}

a. Sur and Byrant (1996)

^{19}F NMR analysis was also conducted to investigate the effect of temperature on the reaction of the full strength phosphonic-based acid systems on kaolinite. **Table 11** shows the chemical assignment in the ^{19}F NMR spectra.

TABLE 12—Relative intensities of the ^{19}F NMR peaks in the spent acid as a function of reaction temperature [b]

Reaction Temperature, ºC	–128 ppm, SiF_6^{2-}, SiF_5^-	–153 ppm, AlF_3	–155 ppm, AlF_2^+	–155.8 ppm, AlF^{2+}
50	90.58	–	8.71	0.71
75	89.46	–	9.57	0.96
100	88.01	–	10.42	1.57
150	76.68	3.41	17.51	2.41

b. Relative intensities were determined by integrating the SiF_6^{2-}, SiF_5^-, AlF_3, AlF_2^+ and AlF^{2+} ^{19}F NMR peak areas for each sample.

The relative intensities of the different ^{19}F NMR signals in the spent acid was shown in **Table 12** as a function of reaction temperature. With the increase of reaction temperature, the peaks around –128 ppm decreased while the signals around –156 ppm increased (**Fig. 41**). These results indicated that more aluminum was dissolved at high temperatures, which coordinated more fluoride; meanwhile, the silicon ions decreased due to silicon precipitation. This is consistent with the solubility test results of kaolinite at different temperatures (122, 167, 212, and 302ºF), and the concentrations of aluminum are 6,868; 7,627; 8,996; and 14,087 mg/l, respectively. The continual leaching of aluminum and precipitation of silicon may be due to the secondary reaction of fluosilicic acid with kaolinite, which becomes fast at high temperatures.

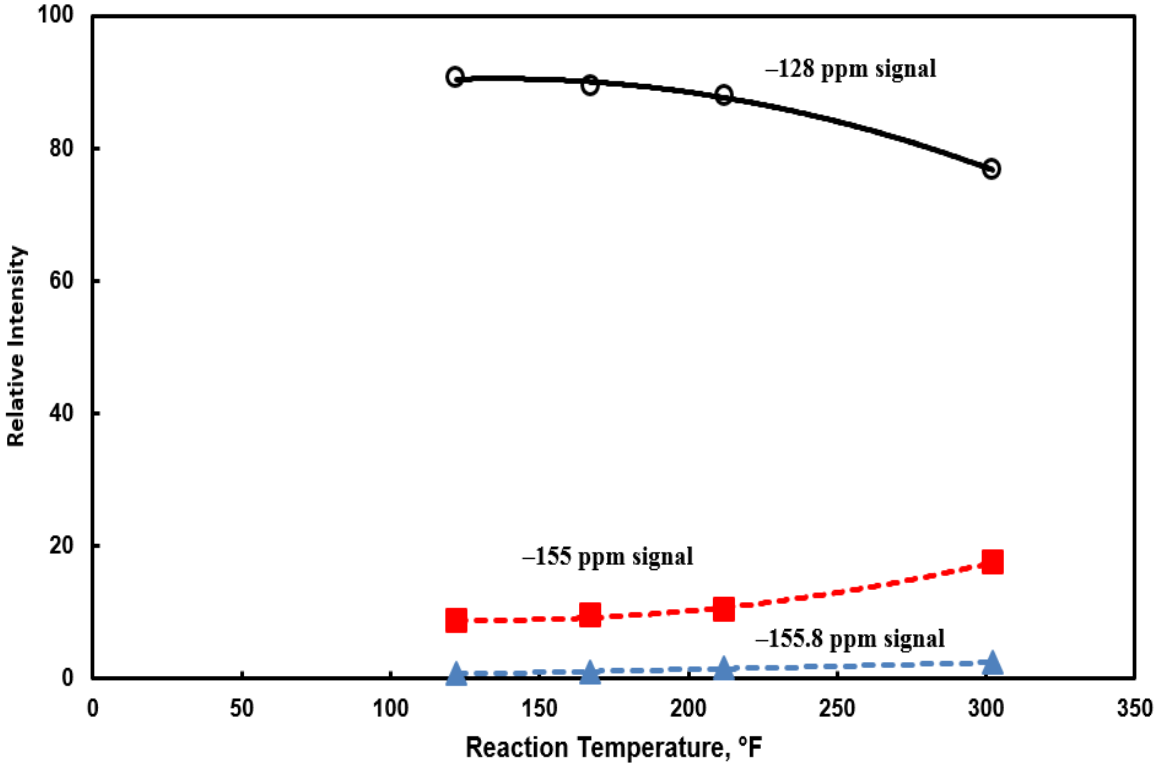

Fig. 41—Relative intensities of the ^{19}F NMR signals in the spent acid after full strength phosphonic-based HF acid reacted with kaolinite for 30 minutes as a function of temperature. Relative intensities were determined by integrating the SiF_6^{2-}, SiF_5^-, AlF_3, AlF_2^+, and AlF^{2+} ^{19}F NMR peaks for each sample using $CFCl_3$ as internal reference.

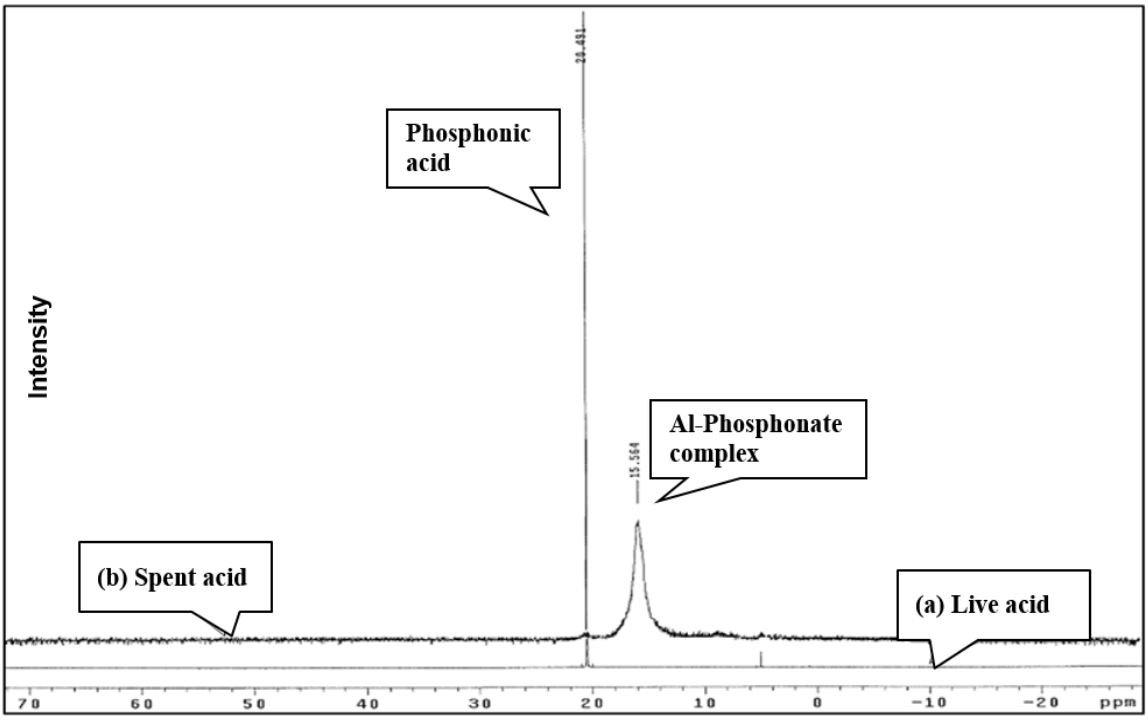

Fig. 42—Liquid ^{31}P NMR spectra of (a) full strength phosphonic-based HF acid and (b) spent acid after the full strength phosphonic-based HF acid reacted with kaolinite for 24 hours.

To evaluate the function of the phosphonic acids in the phosphonic-based HF acid, ^{31}P NMR was introduced to detect and identify phosphorus species present in the solution. The ^{31}P NMR spectra of the full strength phosphonic-based HF acid before and after reacting with kaolinite for 24 hours were showed in **Fig. 42**. The chemical shift at 20 ppm in the spectrum is assigned to the phosphonic acids (Moedritzer et al. 1962), and changes in the chemical shifts of the phosphorus signals of the live and spent acids were observed. These changes may be due to the decomposition products of phosphonic acid, chelating of phosphonic acid with the metal ions dissolved from kaolinite or the

deprotonation of phosphonic acid. Cade-Menun (2005) reported that the C–P bond is highly resistant to chemical hydrolysis, thermal decomposition, and photolysis, which allow phosphonates to persist relative to other P forms.

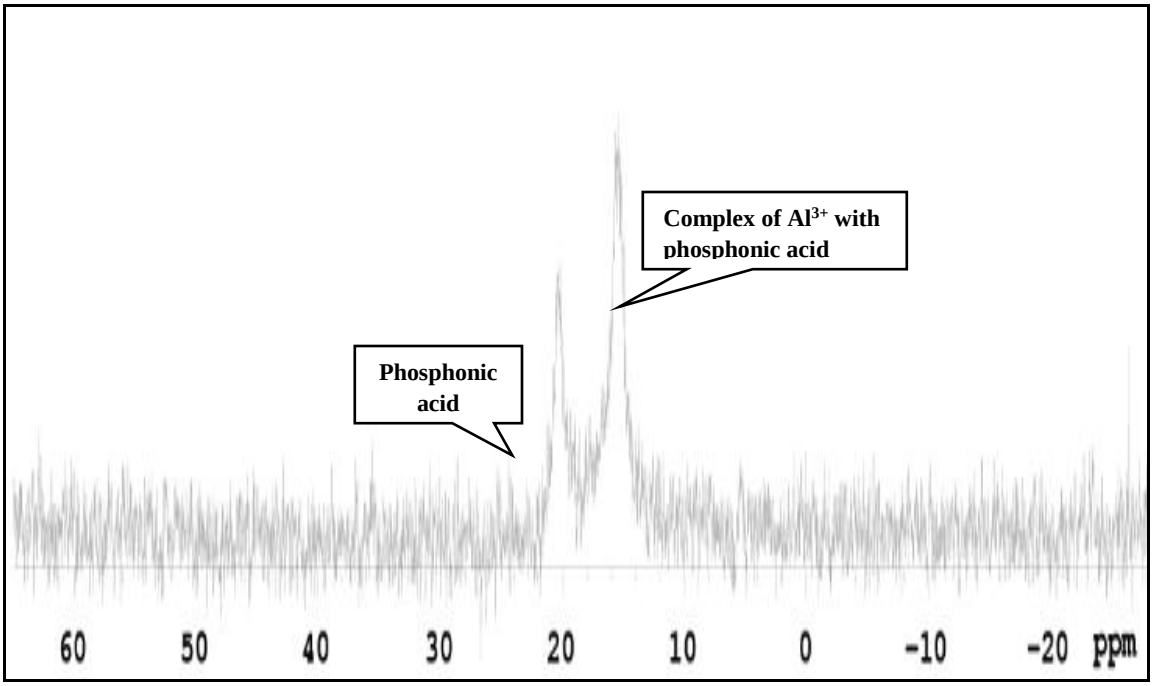

Fig. 43—^{31}P NMR spectrum of full strength phosphonic-based HF acid mixed with 8,000 ppm $AlCl_3$.

The complexation of Al^{3+} with phosphonic acid groups was reported by Lacour et al. (1998). The phosphonate anion can form relative stable complexes with Al^{3+}, which prevent further aluminum precipitation during the acidizing treatment stage. The interactions of Al^{3+} with phosphonates has been studied extensively (Gumienna-Kontecka et al. 2002), they reported that bisphosphonate ligands were found to be very

efficient chelating agents for Al^{3+} and Fe^{3+}. In order to investigate the chelating effect of Al^{3+} and Fe^{3+} on phosphonates, 8000 ppm Al^{3+} and 5000 ppm Fe^{3+} were added into the live acid separately. The mixtures were analyzed using ^{31}P NMR, as shown in **Fig. 43**, upfield shifts of chemical shift was observed after mixing live acid with 8000 ppm Al^{3+}, and no obvious signal was observed for the mixture of 5000 ppm Fe^{3+} and live acid. Also no obvious precipitation was observed for this mixture, and no signal was detected at 20 ppm, the possible reason for this observation was the paramagnetic effects of Fe^{3+} on ^{31}P NMR measurement. The pH value of the live full strength phosphonic-based HF acid was 2.106, which corresponded to the release of one proton from the phosphonic acid. In the case of the spent acid after full strength phosphonic-based acid system reaction with kaolinite, there is no Fe^{3+}, so the upfield shifts of the ^{31}P NMR signals was attributed to the complexation of bisphosphonate ligands with Al^{3+} in the spent acid. Therefore the chemical shift at 15 ppm in the spectrum shown in Fig. 42(b) should be a complex of Al-phosphonate. The coordination of Al^{3+} with phosphonic acid groups also broadened the ^{31}P NMR signals, which can be observed in the spectra. Therefore, it can be concluded that the 15 ppm peak observed in the NMR spectrum of spent acid was most likely due to the complexation of phosphonic acid groups with Al^{3+} in the spent acid.

SEM/EDS and XRD Analyses

The composition of different clay minerals before a chemical reaction was obtained by SEM/EDS and the results are given in Table 8. The molar ratio of Si/Al was close to 1:1

for kaolinite and chlorite, and it was 2:1 for bentonite and illite. It has been reported that AlF_3 was more likely to precipitate when a higher concentration of HF was used (Shuchart and Gdanski 1996).

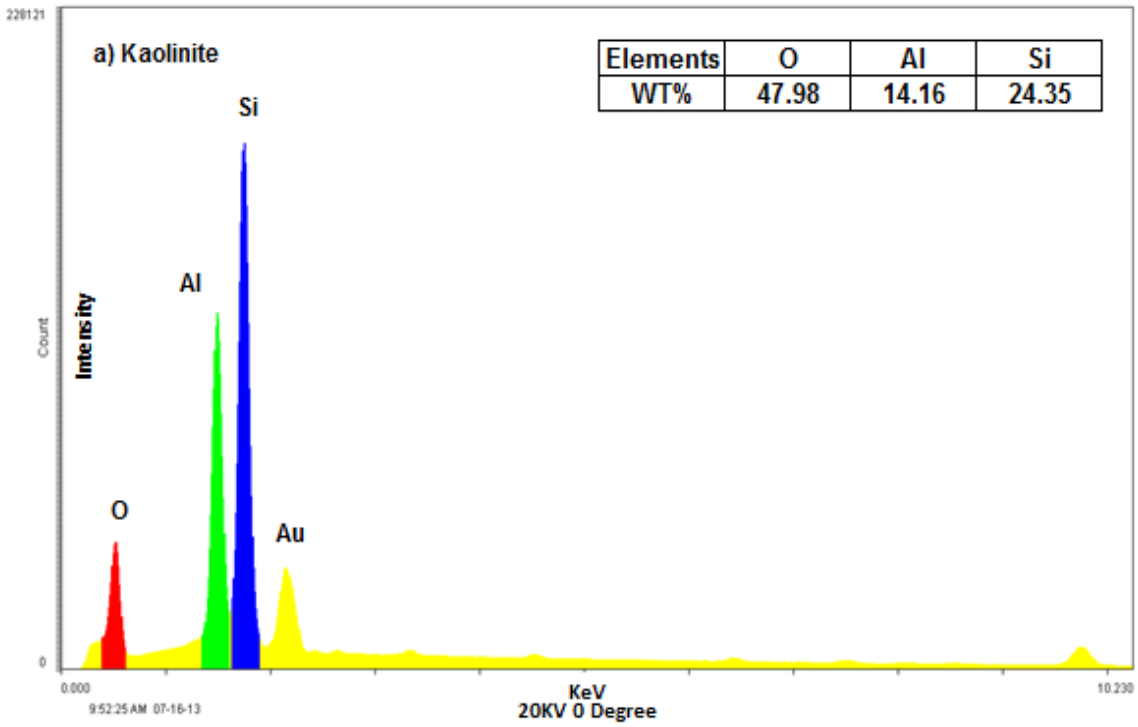

Fig. 44— Elemental analysis of kaolinite after treated with full strength phosphonic-based HF acid at 77°F for 24 hours.

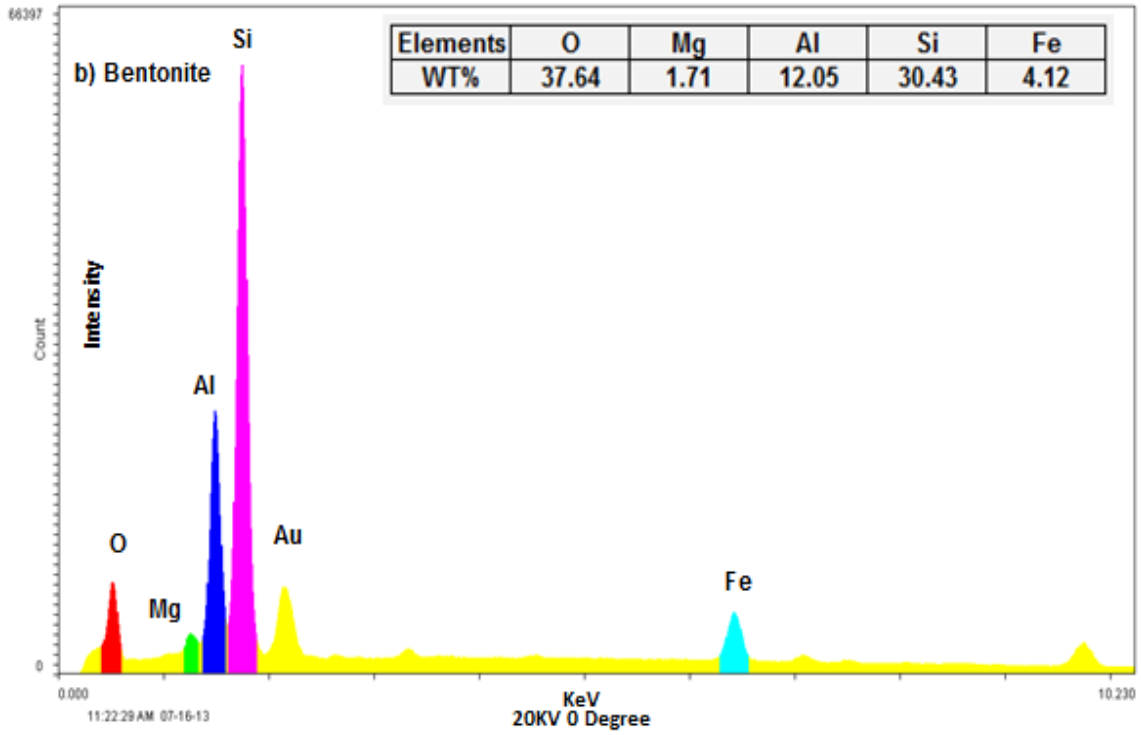

Fig. 45— Elemental analysis of bentonite after treated with full strength phosphonic-based HF acid at 77°F for 24 hours.

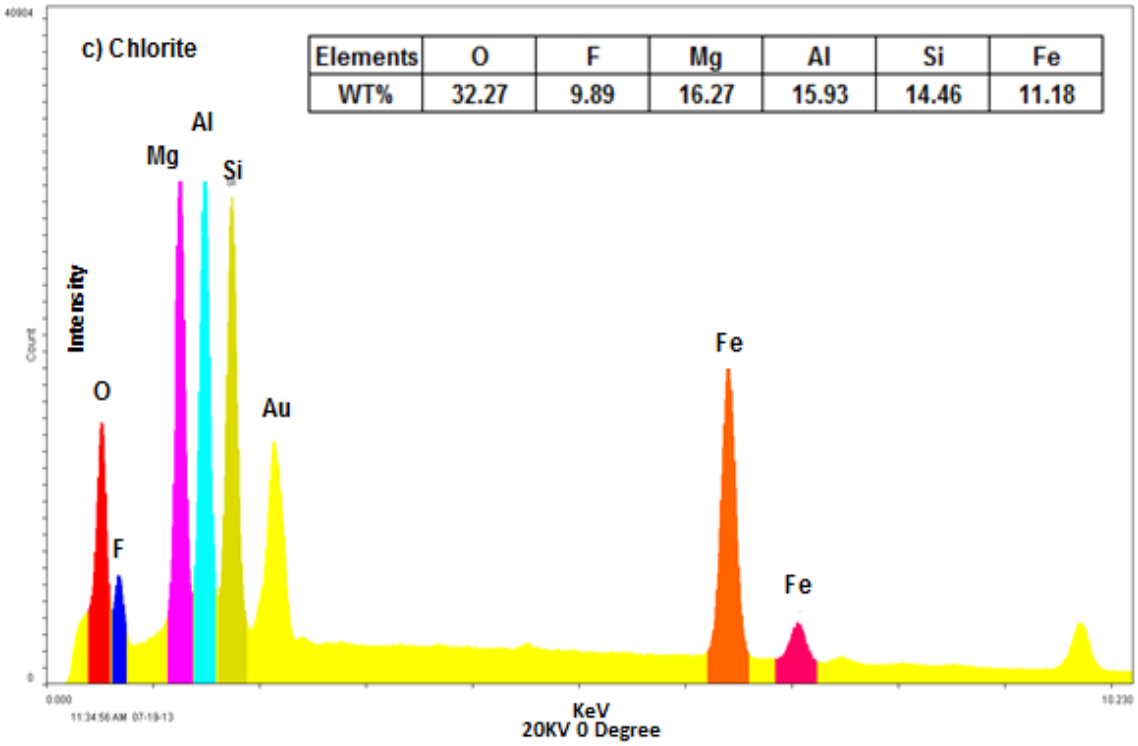

Fig. 46— Elemental analysis of chlorite after treated with full strength phosphonic-based HF acid at 77°F for 24 hours.

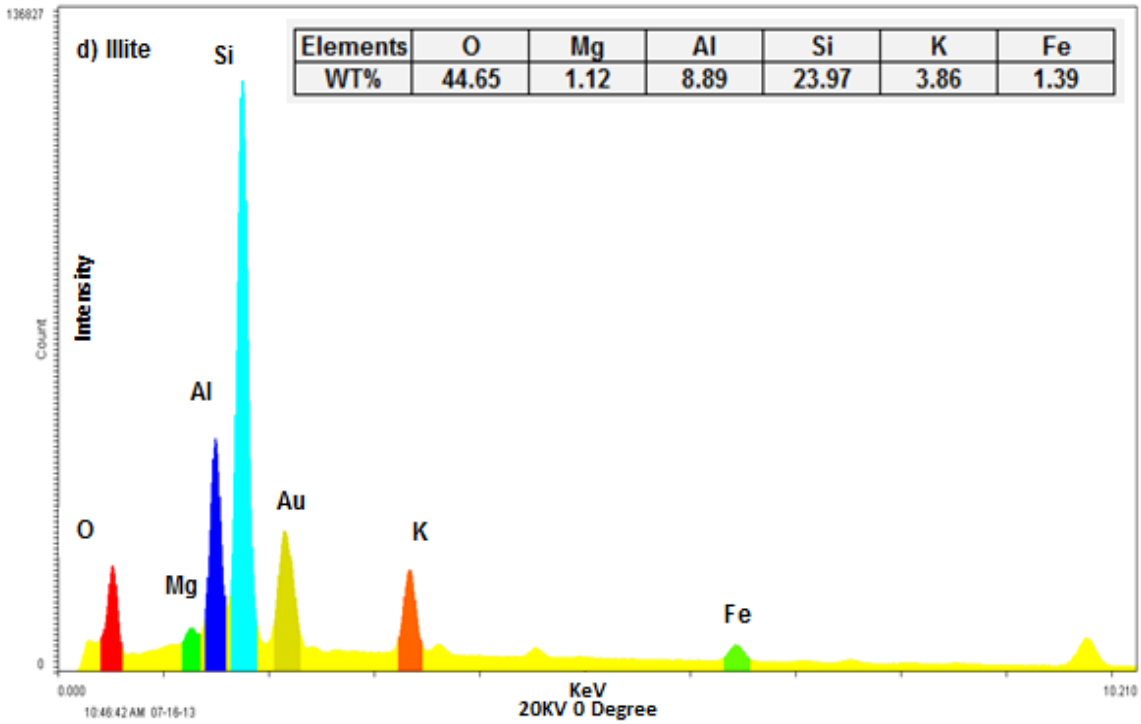

Fig. 47— Elemental analysis of illite after treated with full strength phosphonic-based HF acid at 77°F for 24 hours.

To investigate whether AlF_3 precipitated under our experimental conditions, SEM/EDS analyses were utilized to analyze all the clay samples after being treated by the full strength phosphonic-based acid system at room temperature for 24 hours. The results are shown in **Figs. 44 to 47**. The elemental analysis of kaolinite, bentonite, and illite samples did not indicate the existence of an F peak in these spectra. Therefore, there was no AlF_3 in the reaction products at all. However, the results of chlorite were

different where a significant F peak was observed in the spectrum. This was confirmed by comparison with the spectrum of chlorite before treatment (**Fig. 48**).

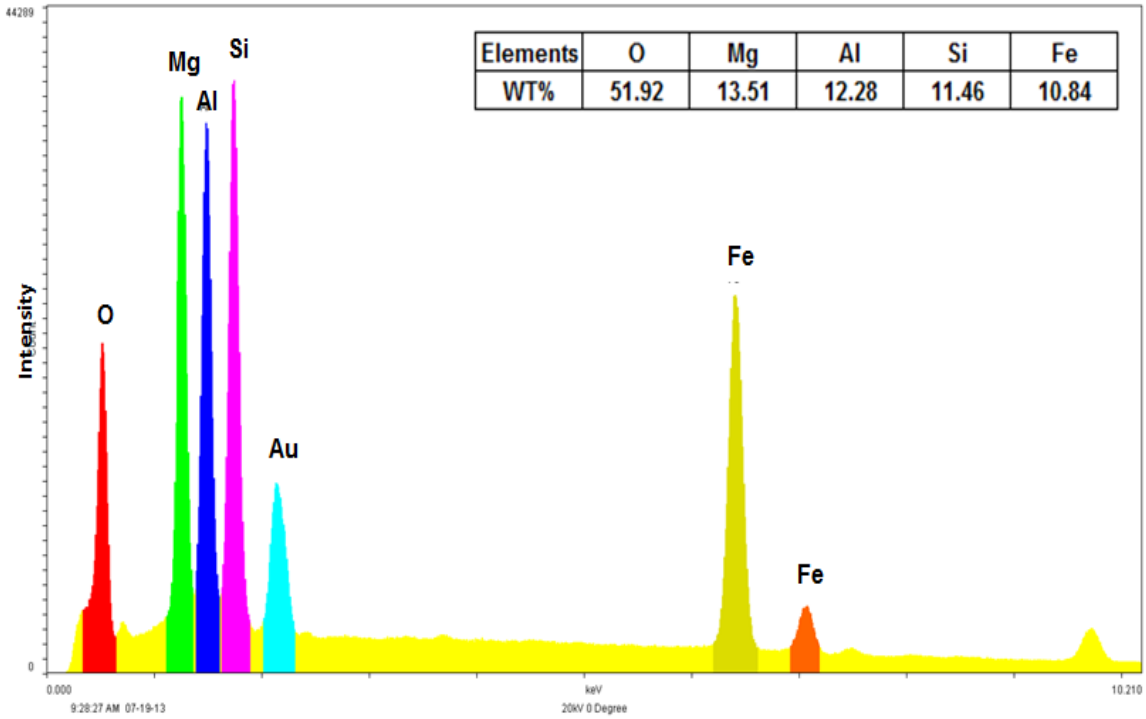

Fig. 48—Elemental analysis of chlorite before treated with full strength phosphonic-based HF acid.

In the X-ray powder diffraction patterns shown in **Fig. 49**, an additional peak appeared at 2θ =15.8º after being treated with full strength phosphonic-based acid, which indicated new mineral formation or mineral transformation. This peak can be assigned to β-$AlF_3 \cdot 3H_2O$, one phase of aluminum trifluoride, which can be formed by AlF_3 in presence of humidity (Alonso *et al*. 2000). This result further supported the SEM/EDS

measurement that AlF_3 precipitate occurred in the chlorite samples after being treated with full strength phosphonic-based acid. All of these results explained the low Al concentrations in the spent acid solution.

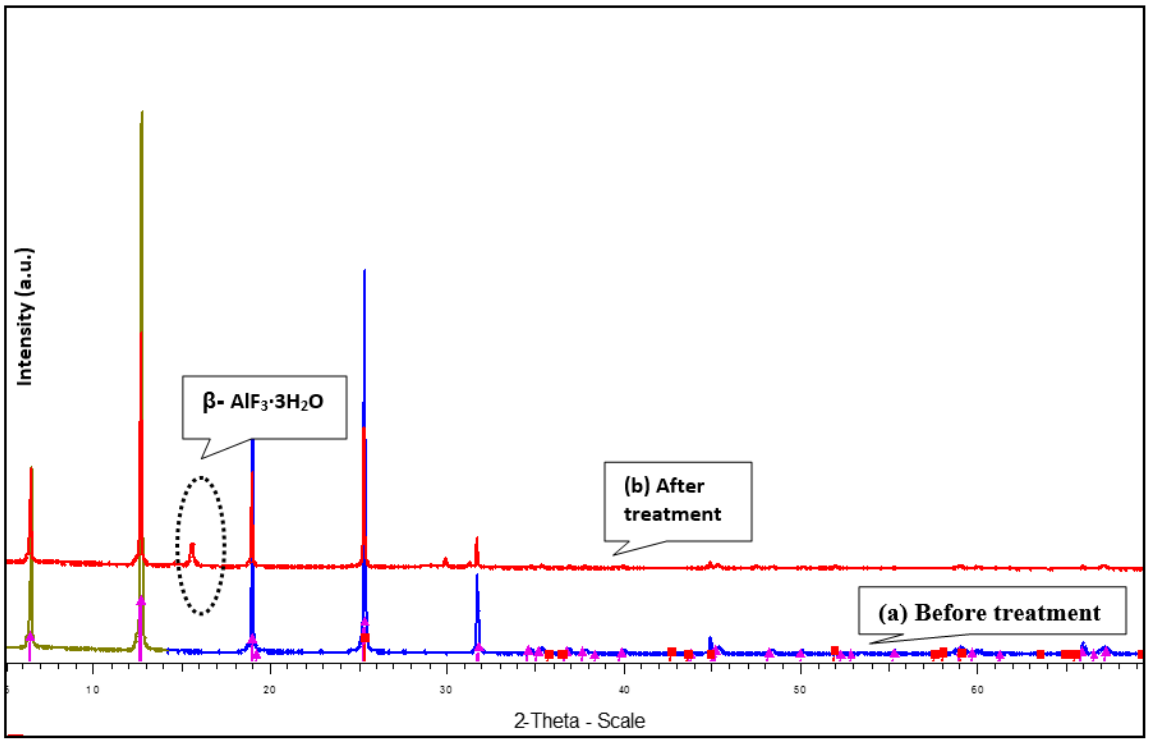

Fig. 49—X-ray powder diffraction pattern of chlorite (a) before treated with full strength phosphonic-based HF acid and (b) after treated with full strength phosphonic-based HF acid.

The ratio of Si/Al was also investigated. For kaolinite, the molar ratio of Si/Al increased from 1.0 before reaction to 1.4 after reaction with full strength phosphonic-

based acid. The results revealed that more aluminum was extracted from kaolinite. For chlorite, the molar ratio of Si/Al was 1.0 before the reaction, which indicated some Si in the chlorite was displaced by Al, Fe, and Mg. This ratio decreased to 0.5 after 24 hours of reaction with the full strength phosphonic-based acid systems. This indicated the precipitation of aluminum.

Conclusions

1. The concentration of Si decreased in the spent acid after full strength phosphonic-based HF acid reacted with clay minerals at 302ºF. This indicated that secondary precipitation had occurred. The ^{19}F NMR results at high temperature also demonstrated the occurrence of a secondary reaction, which became fast at high temperatures.
2. ^{19}F NMR results indicated that each fluoro complex had distinct ^{19}F chemical shifts. AlF_3, AlF_2^+ and AlF_2^+ were detected in the spent acid due to the low acid (H^+) concentration. AlF_3 precipitated in the phosphonic-based acid when it reacted with the chlorite mineral at room temperature and 302°F. No AlF_3 precipitate was identified by SEM and EDS after kaolinite, bentonite, and illite reacted with phosphonic-based acid under similar conditions.
3. ^{31}P NMR was able to determine the phosphorus species present in the live and spent acid solutions. The results showed that the phosphonic acid in the phosphonic-based HF acid mixtures was effective in preventing fluoride precipitation.

4. ^{27}Al NMR was not an effective tool to characterize the aluminum complexes in the spent acid. All ^{27}Al chemical shifts of all of the Al complexes were approximately the same.

CHAPTER IV

EVALUATION OF SANDSTONE ACIDIZING USING PHOSPHONIC-BASED HF ACID: COREFLOOD STUDIES

Introduction

To evaluate the performance of the phosphonic-based HF acid on the sandstone acidizing treatment, coreflood experiments were conducted beside the clay solubility tests. Coreflood studies were conducted to investigate and understand the permeability changes in the sandstone cores as the acid is injected at different conditions. The inductively coupled plasma (ICP) is used to measure the effluent samples from the coreflood analysis in order to understand this system properly.

As introduced previously, carbonate minerals present in sandstone formations will cause serious formation damages. To prevent the precipitation of calcium floride and calcium fluorosilicate, there is a need to remove these carbonate minerals to enhance the well performance, especially when the HF-based fluids are used. In one part of this study, Berea sandstone core is used since it is the most commonly used media in studying core flow test due to its homogeneity, which is favorable in control experiments. The samples used has permeability range from 100-200 md. In another part of the coreflood study, Bandera sandstone cores containing a considerable amount of HCl sensitive clays were used, which contain 14 wt% clay minerals, including significant amount of illite, kaolinite, chlorite and feldspar. Three different fluids were compared as a preflush fluid to remove carbonate minerals from Bandera sandstone cores, which are 9 wt% formic acid, GLDA (glutamicacid-N,N-diaceticacid), and HEDTA

(hydroxyethylenediaminetriacetic acid). The coreflood experiments were run at a flow rate of 2 cm^3/min and at a temperature of 300°F.

Experimental Studies

Materials

Ammonium chloride (NH_4Cl) used in the core flood was purchased from Macron Fine Chemicals. The corrosion inhibitor and intensifier were provided by a local service company. Formic and hydrochloric acids were obtained from Sigma-Aldrich with concentrations of 99.0 and 36.5 wt%, respectively. Ammonium bifluoride was supplied by Alfa Aesar, and the purity was 95 wt%. HF acid was prepared using ammonium bifluoride and HCl based on the following equation:

$$HCl + NH_4HF_2 \rightarrow NH_4Cl + 2HF \quad \text{.....(12)}$$

The chelating agents that were used in this study were GLDA (L-Glutamic acid N, N-diacetic acid), HEDTA (hydroxyethylethylenediaminetriacetic acid), which were obtained from AkzoNobel. The concentration of chelating agents used was 0.6M prepared from original solutions with different concentrations.

12 : 3 mud acid were prepared using 18.2 Mcm DI water, concentrated ACS grade HCl acid 36.5 wt% concentration, crystalized ammonium bifluoride. Acid component is show in **Table 13**.

TABLE 13— Formula of 12:3 mud acid				
	36.5 wt% HCl solution, g	**NH_4HF_2, g**	**H_2O, g**	**Total, g**
Weight	80.75	8.55	110.696	200

Core plugs were cut from Berea and Bandera sandstone blocks and the size of the cores was 1.5 in. × 6 in. The mineralogy of Berea and Bandera sandstone cores are given in **Table 14**. The Bandera sandstone cores contains 16 wt% dolomite, and 12 wt% Ca-feldspar, which are major sources of calcium, 10 wt% illite, which may cause fines migration, The porosity and permeability of each core were measured using a coreflood instrument shown in **Fig. 50**.

TABLE 14—Mineral composition for Berea and Bandera sandstone cores based on weight

Mineral, wt%	Berea	Bandera
Quartz	86	57
Dolomite	1	16
Calcite	2	—

TABLE 14 Continued

Mineral, wt%	Berea	Bandera
Feldspar	3	12
Kaolinite	5	3
Illite	1	10
Chlorite	2	1

Experimental Procedure

Coreflood experiment were performed using the setup shown in **Fig. 50**, the core was first loaded into a Hassler sleeve core holder at an overburden pressure of 2,000 psig. A backpressure of 1,100 psi was applied in the coreflood experiments to achieve good saturation and displacement of the fluid and to keep CO_2 in the solution. Pressure transducers were connected to a computer to monitor and record the pressure drop across the core during the experiments. A Teledyne ISCO D500 precision syringe pump, which has a maximum allowable working pressure of 2,000 psi, was used to inject the acid into the cores. Based on the maximum pump pressure and the backpressure, the maximum pressure drop across the cores was 900 psi. The pore volume of the core was determined after saturating the core by dividing the difference between the saturated core and dry core by the brine density (1.034 g/cm^3 at 22°C).

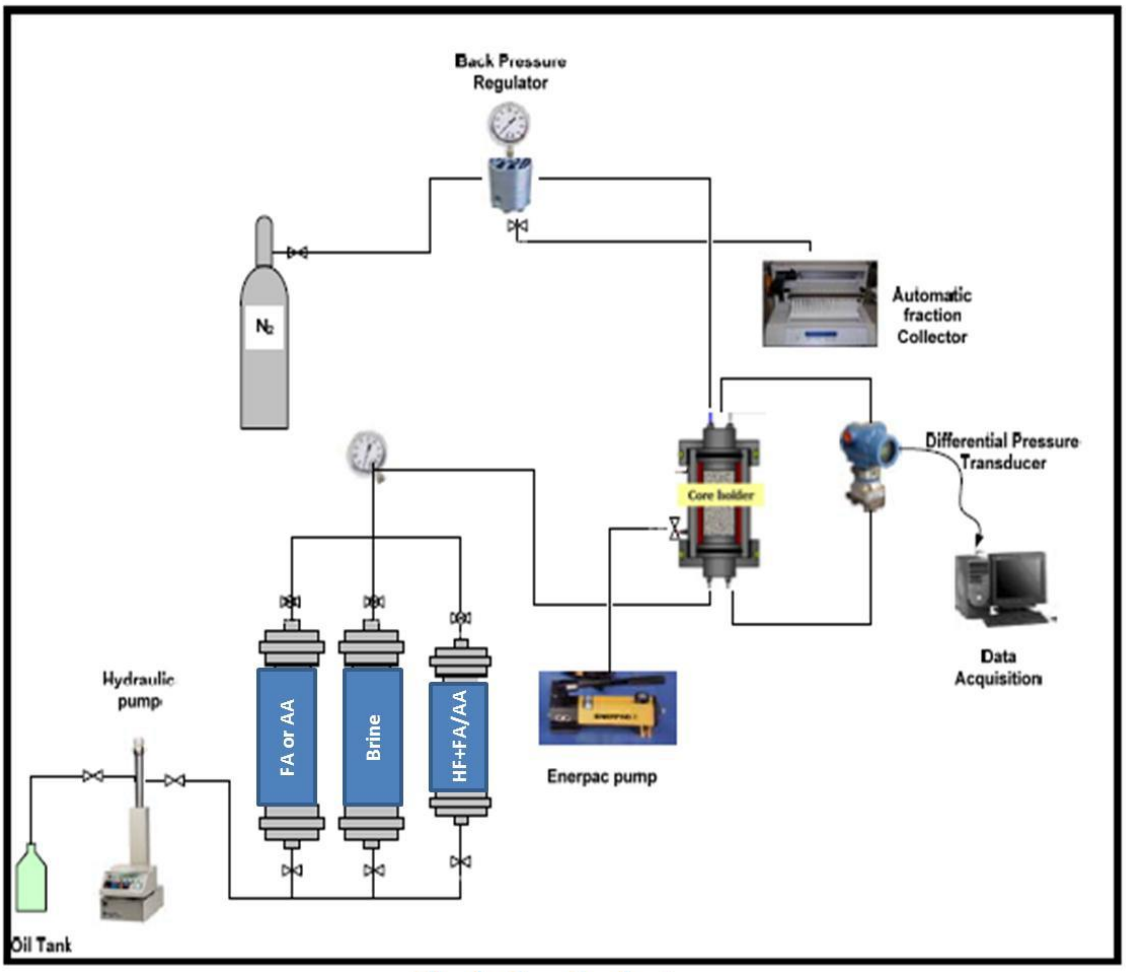

Fig. 50—Coreflood Experiment Setup.

Fig. 51—pH Meter and HF Resistant Submersible Electrode.

The core was scanned by X-ray Computed Tomography (CT) machine dry, saturated with 5 wt% NH_4Cl, and after the coreflood experiment, and the CT results were analyzed utilizing ImageJ software. The model of the CT is Toshiba Aquilion RXL and the resolution is 0.5 mm. The effluent samples in all the coreflood experiments were collected to analyze the ion concentrations of calcium, magnesium, iron, aluminum, and silicon using ICP shown in Fig. 17. A Cole-Parmer HF Resistant Submersible Electrode connected with Oakton PC700 meter, **Fig. 51**, was used to measure the pH values of the core effluent samples.

To compare the efficiency of the phosphonic-based HF acid with 12:3 mud acid, coreflood tests were also conducted using 12:3 mud acid under the same experiment

condition. In each coreflood experiment, the cores were first dried at 250°F for 5 hours and then saturated with 5 wt% NH_4Cl for 2 hours under vacuum. The pore volume of the core was determined by dividing the weight difference of the saturated core and the dry core by the density of the 5 wt% NH_4Cl brine. Coreflood tests were performed using Berea sandstone cores that were 1.5 in. diameter and 6 in. long. Tests were performed with a back pressure of 1100 psi and the overburden pressure was adjusted to 2000 psi. The injection flow rate was 2 cm^3/min. A differential pressure transducer was used to measure the pressure drop between the core inlet and outlet. Samples of the core effluent were collected in plastic test tubes and analyzed to determine acid reactions with various minerals present in the cores. A concentration of 5 wt% NH_4Cl brine was used to calculate the initial and final permeability of the core.

Tests were performed with back pressure of 1200 psi and the overburden pressure was adjusted to 2000 psi. The injection flow rate was 2cm^3/min in all experiments of this study. A differential pressure transducer was used to measure the pressure drop between core inlet and outlet. The core effluent samples were collected in all coreflood experiments and analyzed to determine the concentrations of Ca, Mg, Fe, Al, and Si by Inductively Coupled Plasma (ICP) analysis using Optima 7000 DV ICP-OES system and WinLab 32^{TM} software. Samples were diluted to make sure the concentrations of each ion were below 30 mg/L.

The pressure drop across the core during the treatment was monitored by the Lab view software and the core permeability was determined before and after the acidizing

treatment using Darcy's law, which is one of the most well-known theories that describe fluid flow in a porous media as shown below:

$$k = 122.812\ q*\mu*L_{core} / \Delta p*d^2_{core} \quad \text{.....(12)}$$

Where

k = the core permeability, md,

q = flow rate, cm^3/min

μ = fluid viscosity, cP

L_{core} = core length, in.

Δp = pressure drop across the core, psi

d_{core} = core diameter, in.

Results and Discussion

Stimulating Berea Sandstone Core Using Full Strength Phosphonic-based HF Acid without Preflush

To investigate the effect of the phosphonic-based HF acid on Berea sandstone cores, coreflood experiment was performed on Berea sandstone core at 300°F and 2 cm^3/min. The core was saturated with 5 wt% NH_4Cl, and then main acid was injected followed by the postflush of 5 wt% NH_4Cl. **Fig. 52** shows that the pressure drop across the core was steady when 2.5 PV acids were injected, while with the injection of more acids, the pressure drop across the core was variable. This means that less than 2.5 PV main acid

injections did not cause fine migration or particle movements, and more acid injection caused fines migration. Finally, the permeability of the core increased from 49.12 md to 75.56 md after treatment with 1.48 improvement factor ($k_{final}/k_{initial}$). Physical examination of the core after treatment indicated that the acid did not cause deconsolidation of the cores. No solid or precipitation was noted in the sample collected from the core effluent.

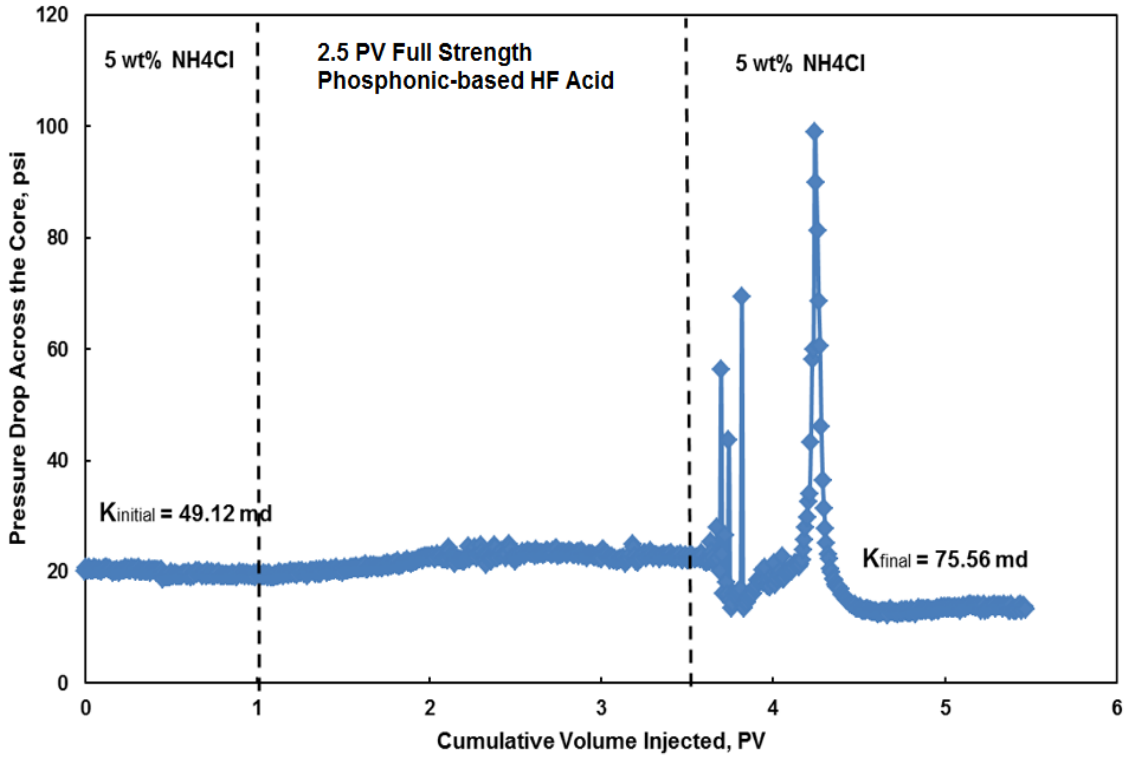

Fig. 52—Pressure drop across the Berea core treated by 2.5 PV of full strength phosphonic-based HF acid without preflush at 2 cm^3/min and 250°F.

The coreflood effluent samples were analyzed by ICP to determine the concentration of key cations. **Fig. 53** shows the concentrations of key cations as a function of cumulative injected volume. Large amount of Fe, Al, Si, Mg and Ca were removed by the phosphonic-based HF acid system, and the concentration of ions keep on increasing with the injection of acid, and reach their highest after 2.5 PV of acids. The highest concentrations of Si and Al were 3,768 and 5,499 mg/l respectively. The concentration of Si was lower than that of Al; this may be attributed to the secondary reaction of alumino-silicates with HF, which dissolved more aluminum at higher temperatures. Besides, the Ca concentration increased with the injection of acid to 1,522 mg/l, this indicates that Ca did not precipitate in the form of CaF_2 when main acid was injected. It was clear from the results that the studied acid did dissolve some minerals from the Berea cores. However, too much injection of the main acid can damage the cores.

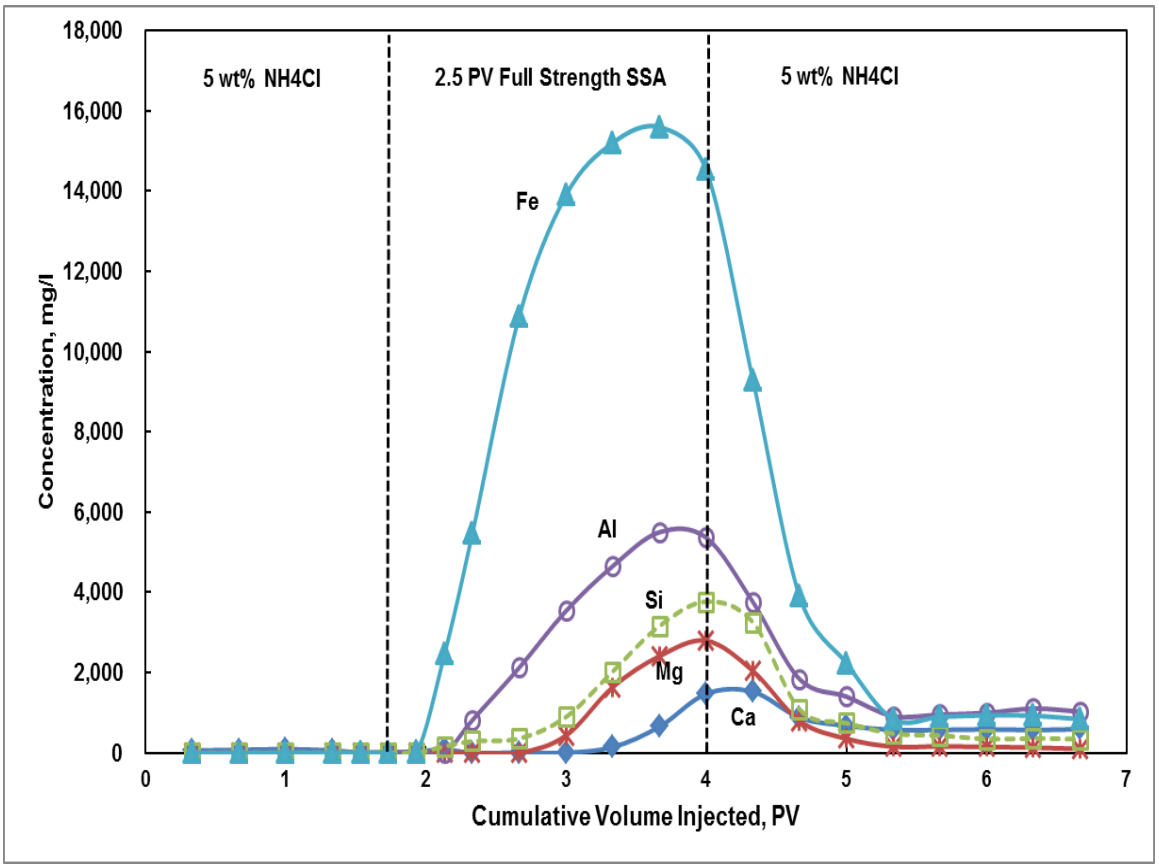

Fig. 53—Analysis of coreflood effluent samples for Berea sandstone core treated without preflush and 2.5 PV of full strength phosphonic-based HF as main flush at 300°F and 2 cm^3/min.

A coreflood experiment was also carried out using Berea sandstone cores to investigate the impact of HF concentration. 3 PV of half strength phosphonic-based HF acid was injected at 300°F with the flow rate of 2 cm^3/min. The ICP analysis of effluent samples is shown in **Fig. 54**. Compared with coreflood experiment using full strength phosphonic-based HF acid under the same conditions, less amount of Fe was dissolved into the solution, and the concentration of Ca also increased with the injection of acid. The highest concentration of Si and Al were 2,522 mg/l, and 2,348 mg/l respectively,

which were both much lower than that in full strength phosphonic-based HF acid test. So it can be concluded that a higher concentration of HF is more effective in dissolving the alumino-silicates.

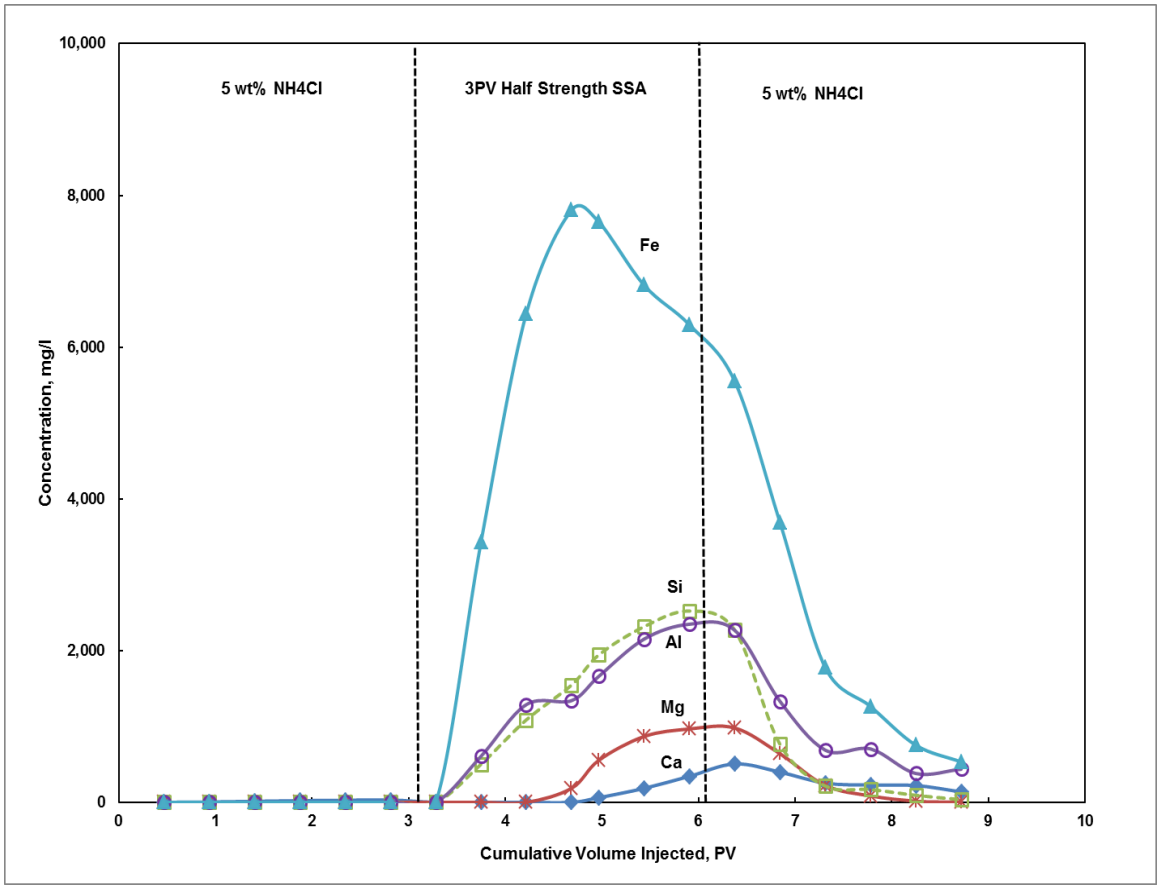

Fig. 54—Analysis of coreflood effluent samples for Berea sandstone core treated without preflush and 3 PV of half strength phosphonic-based HF acid as main flush at 300°F and 2 cm^3/min.

Stimulation of Bandera Sandstone Using phosphonic-based HF Acid

To investigate the effect of mineralogy on the performance of the phosphonic-based HF acid system, a coreflood experiment was conducted on Bandera sandstone core, which has different mineralogy with Berea sandstone cores, at 300°F with flow rate of 2 cm^3/min. the pressure drop increased from an initial value of 27 psi during flowing 5 wt% NH_4Cl brine solution to 531 psi after injection of 2 PV studied full strength phosphonic-based HF acid, **Fig. 55**.

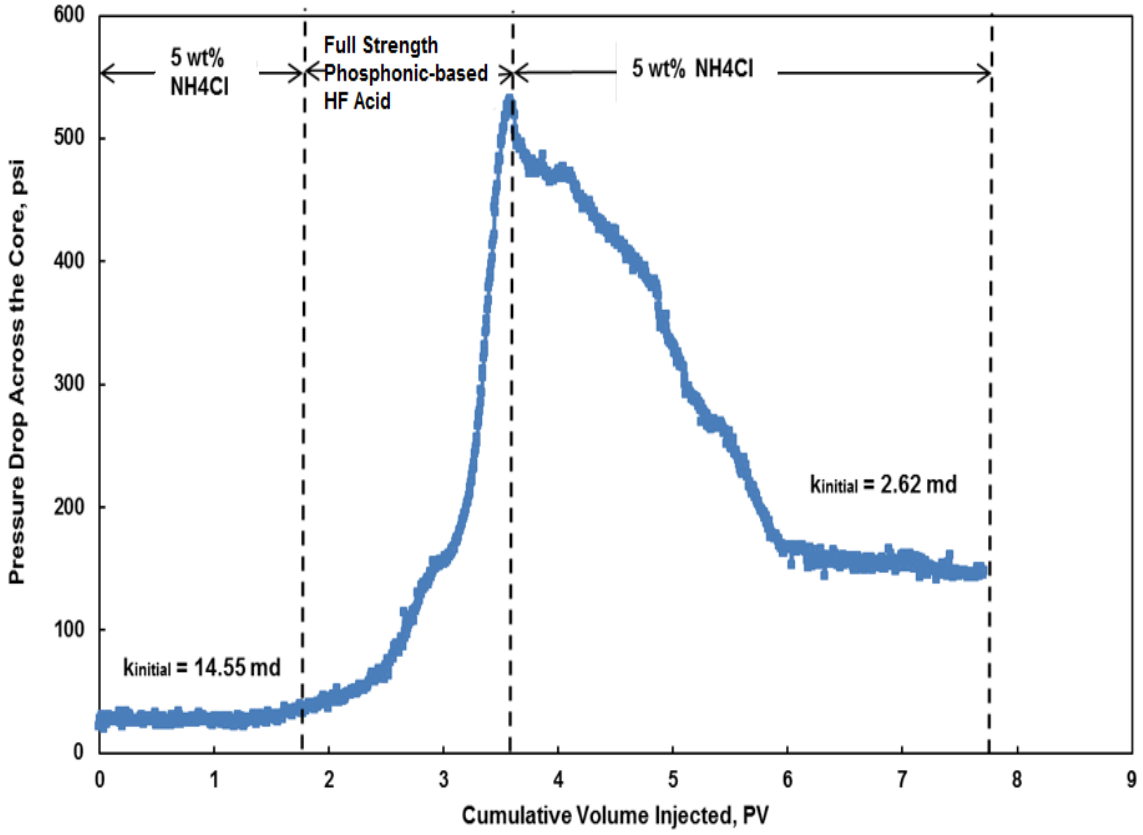

Fig. 55—Pressure drop across the Bandera core treated by 2 PV of full strength phosphonic-based HF acid without preflush at 2 cm^3/min and 300°F

The pressure drop across the core started to increase gradually, showing fines migration and/or precipitation inside the core. The fines migration can be attributed to the high content of illite in this core, and relative high concentration of HCl in the full strength phosphonic-based HF acid, HCl was incompatible with the illite and caused fines migration. After injecting the acids, the core was flowed through with 5 wt% NH_4Cl brine solution until the pressure drop across the core stabilized. Finally, the permeability decreased from 14.55 md to 2.62 md, which showing the damage caused by the injection of full strength phosphonic-based HF acid.

Fig. 40 shows the concentrations of Ca, Si, Al, and Mg in the coreflood effluent samples, the calcium and magnesium concentration dropped to almost zero when main acid was injected without preflushing the core. The source of calcium in the Bandera sandstone core is dolomite, and calcium feldspar (Table. 2). The decreased calcium concentration in the effluent samples can be attributed to the precipitation of calcium fluoride (CaF_2). And the decreasing calcium concentration also can be attributed to the precipitation of $CaSiF_6$, which is from the reaction of fluosilic acid with the calcium, the precipitate inside the core caused formation damage. These results indicated the necessary of preflush the core before HF treatment, especially when the amount of calcium in the core was high, 16 wt% dolomite in Bandera sandstone cores.

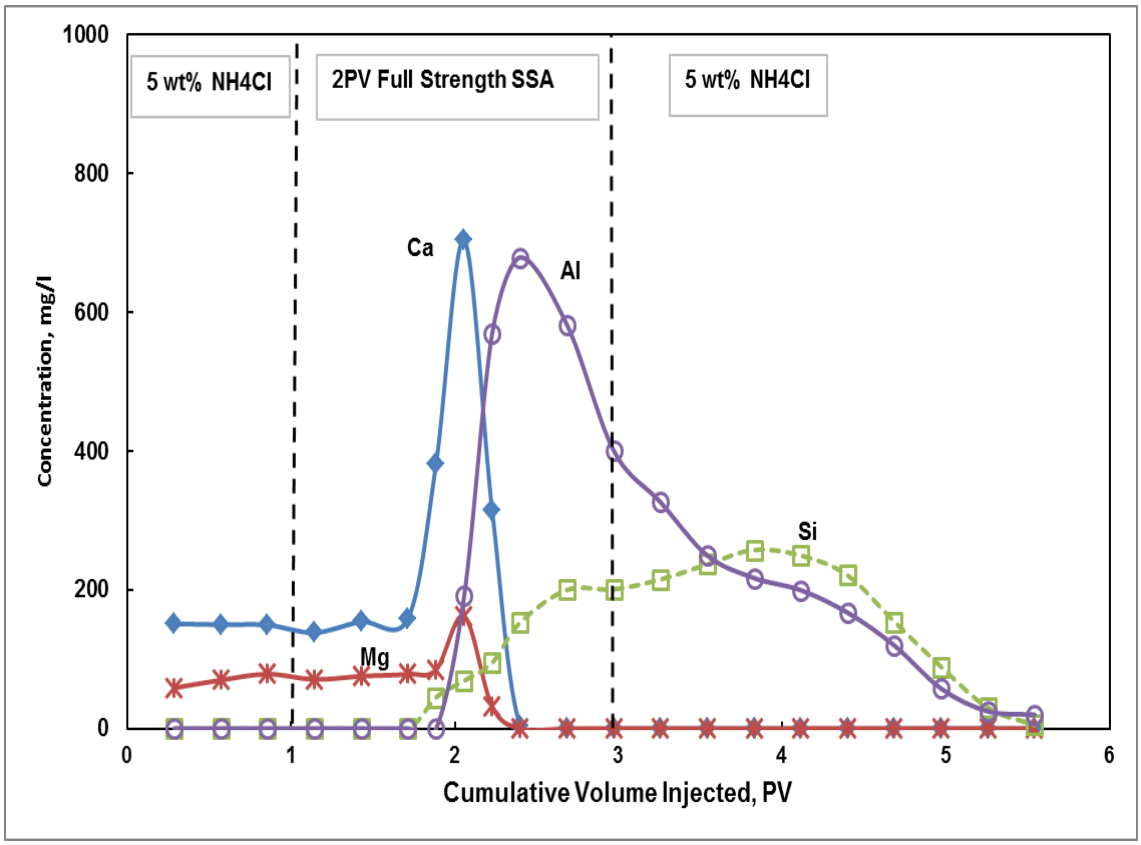

Fig. 56—Ions concentrations in the coreflood effluent samples for Bandera sandstone core treated by 2 PV of full strength phosphonic-based HF acid without preflush at 2 cm^3/min and 300°F

Coreflood Experiments on Berea Sandstone Cores Using Phosphonic-based HF Acid under Different Temperatures

Three different core flood experiments were conducted on Berea sandstone cores at 150, 250, and 300°F, respectively. Details regarding the coreflood experiment were listed in **Table 15**.

TABLE 15—Coreflood experiments on Berea sandstone cores at different temperatures				
Temperature, °F	$K_{initial}$, md	K_{final}, md	$K_{initial}/K_{final}$	Preflush
150	23.9	46.6	1.95	No
250	31.8	51.2	1.61	No
300	49.1	75.6	1.48	No

Ions concentrations in effluent samples collected during coreflood experiments were shown in **Figs. 57 to 59**. For all three temperatures, large amount of Fe were dissolved into the solution, the concentration of Fe increased very fast with the injection of acid.

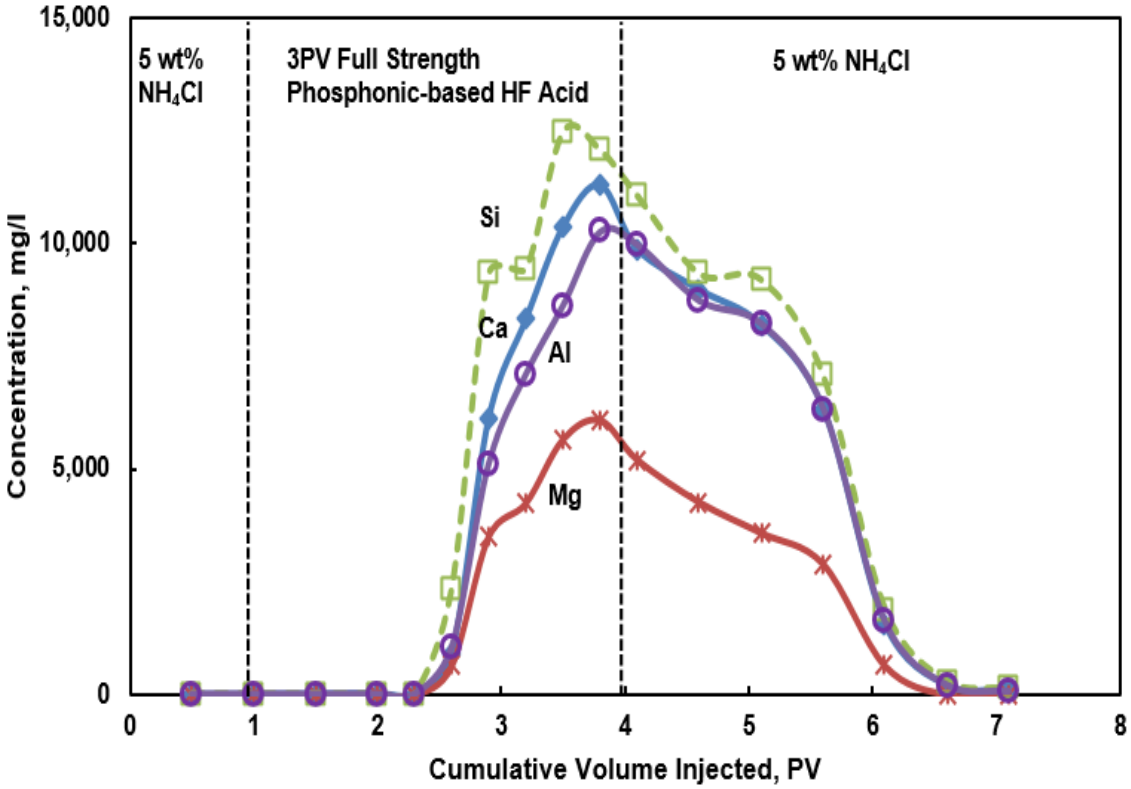

Fig. 57—Analysis of coreflood effluent samples for Berea sandstone core treated without preflush and 3PV of full strength phosphonic-based HF acid as main flush at 150°F and 3 cm^3/min

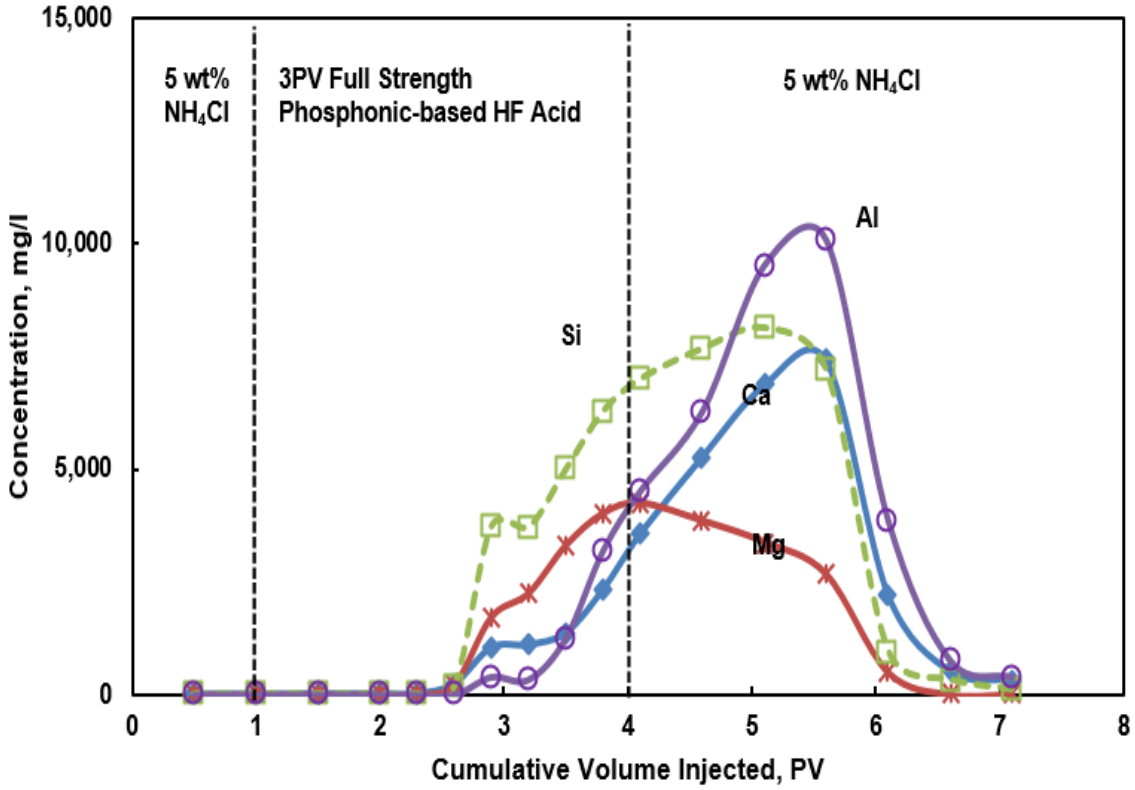

Fig. 58—Analysis of coreflood effluent samples for Berea sandstone core treated without preflush and 3PV of full strength phosphonic-based HF acid as main flush at 250°F and 3 cm^3/min.

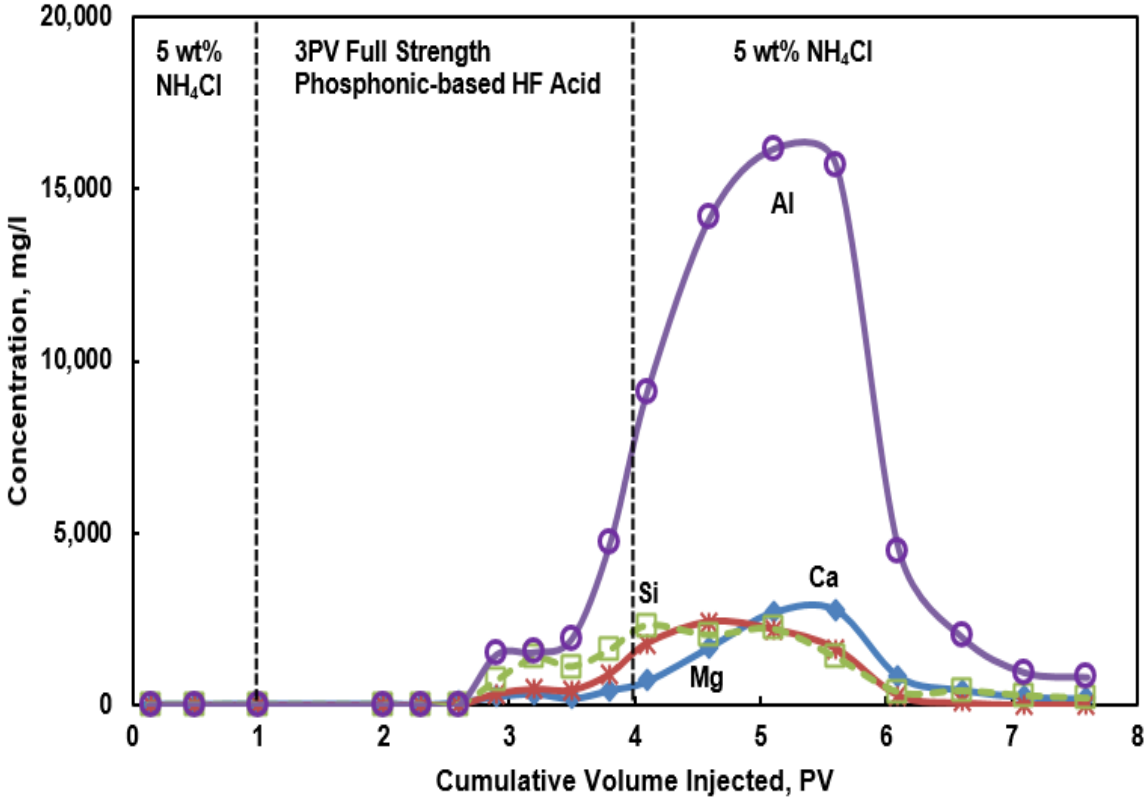

Fig. 59—Analysis of coreflood effluent samples for Berea sandstone core treated without preflush and 3PV of full strength phosphonic-based HF acid as main flush at 300 °F and 3 cm^3/min

For tests at 150°F, all ions concentration increased with the injection of acid, and more silicon were dissolved from Berea cores than aluminum. Besides, the Ca concentration increased with the injection of acid to as high as 11,295 mg/l, this indicates that Ca did not precipitate in the form of CaF_2 when main acid was injected. For the coreflood experiment at 250°F, the ions concentration increased relative slowly than that in the test at 150°F. The highest concentration of Si was 8,160 mg/l, which was less than that in coreflood experiment at 150°F. And more aluminum was dissolved from

cores than silicon. For the coreflood experiment at 300°F, the highest concentration of Al was 16,161 mg/l, which are much higher than the other two tests. However, the highest silicon concentration was only 2,308 mg/l, which was much less than the values in the other two experiments. The source of aluminum is feldspars and clay minerals. Therefore, this trend of Aluminum concentration can be attributed to the secondary reaction of aluminosilicates with HF, which dissolved more aluminum at higher temperatures. Physical examination of the core after the treatment at 300°F indicated that the acid caused deconsolidation of the cores at inlet site. Precipitate was noted in the core effluent, that indicated that the acid cause fine migration at high temperature. It was clear from the results that the studied acid did dissolve some minerals from the Berea cores.

Effect of Preflush on the Stimulation of Bandera Sandstone Using Phosphonic-based HF Acid

The Bandera sandstone cores contained 16 wt% dolomite and 10 wt% illite. Based on literature review, using HCl/HF acids in sandstones that contain sensitive clay (illite) can cause damage to those formations. Therefore, calcium carbonate in Bandera sandstone cores should be removed with preflush to avoid $CaSiF_6$ and CaF_2 precipitates. The objectives of this section are to investigate the effectiveness of three different organic acids in removing calcium in Bandera sandstone cores, and to identify the volume of required preflush of GLDA to prevent the precipitation during injecting the main flush.

Coreflood experiments were performed on the Bandera sandstone cores at 2 cm^3/min and 300°F using 0.6M GLDA, 0.6M HEDTA at pH 4, and 9 wt% formic acid. From the pressure drop performance across the core, the three fluids were compatible with the Bandera sandstone cores.

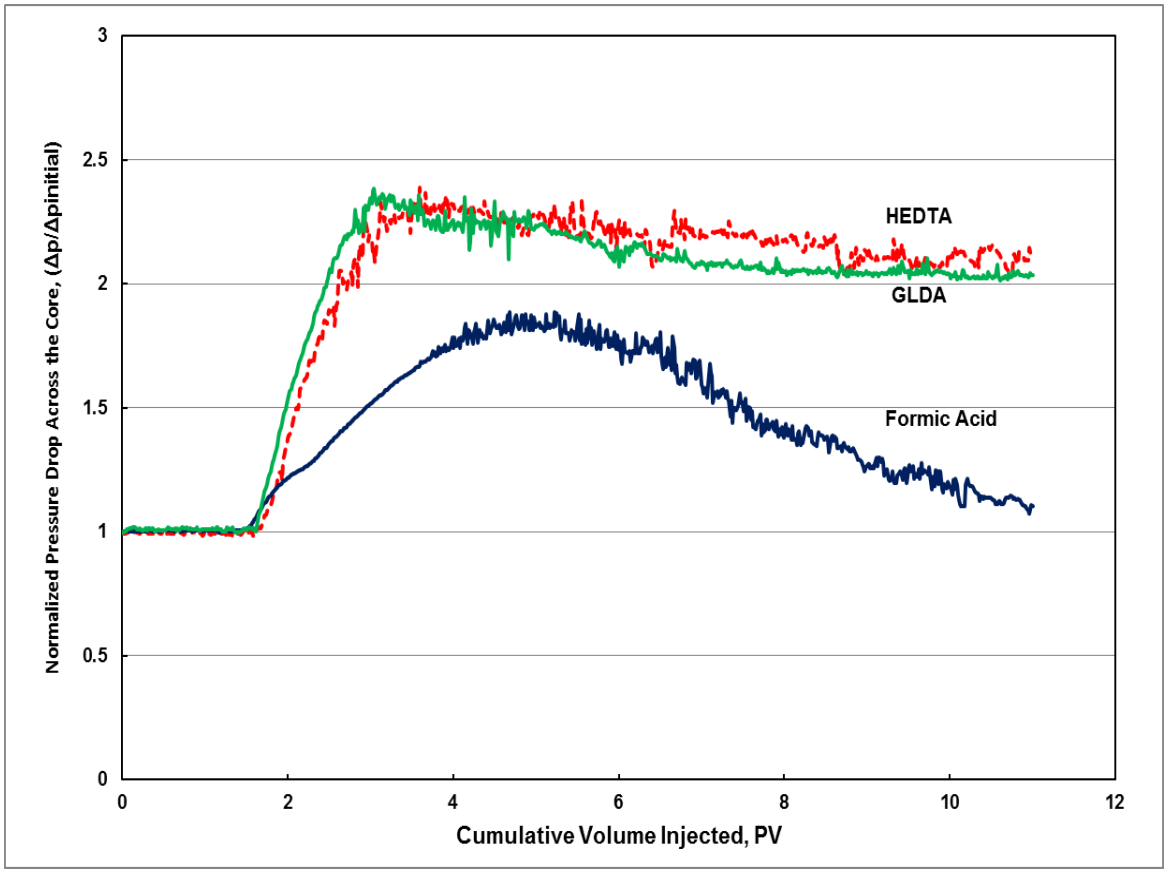

Fig. 60—Pressure drop across the Bandera cores treated by 0.6M GLDA (pH = 3.8), 0.6M HEDTA (pH = 3.8), and 9 wt% formic acid (pH = 1.75) at 2 cm^3/min and 300°F.

Fig. 60 shows the normalized pressure drop across the core for GLDA, HEDTA, and formic acid. The three acids are compatible with Bandera sandstone, and the increase in the pressure drop across the core was due to the increase in viscosity of the fluid inside the core. The normalized pressure drop across the core was almost the same for the GLDA and HEDTA until 2 PV, while it was much greater than that of formic acid. After 2 PV the normalized pressure drop for formic acid was greater than that for GLDA and HEDTA. The amount of dissolved cations was the highest in the case of formic acid. Therefore, the normalized pressure drop across the core was highest.

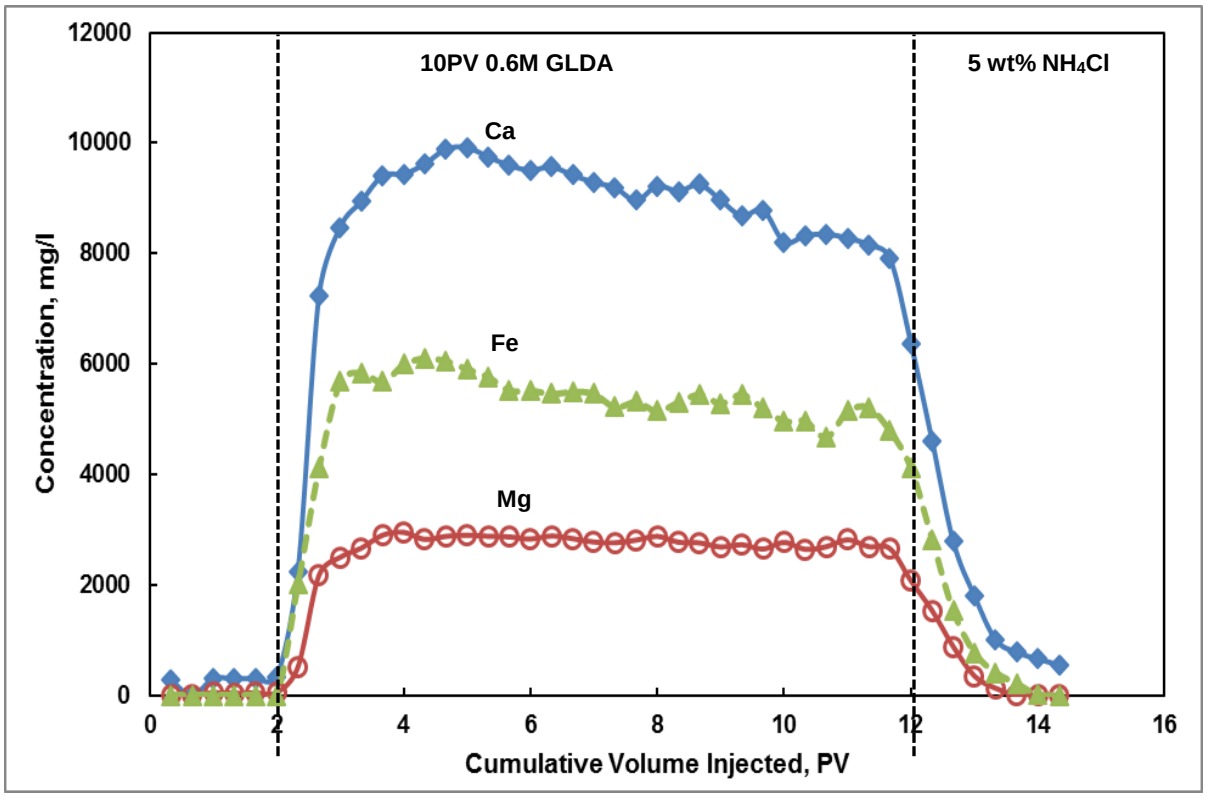

Fig. 61—Analysis of coreflood effluent samples for Bandera sandstone core treated with 10 PV of 0.6M GLDA (pH = 3.8) at 300°F and 2 cm^3/min.

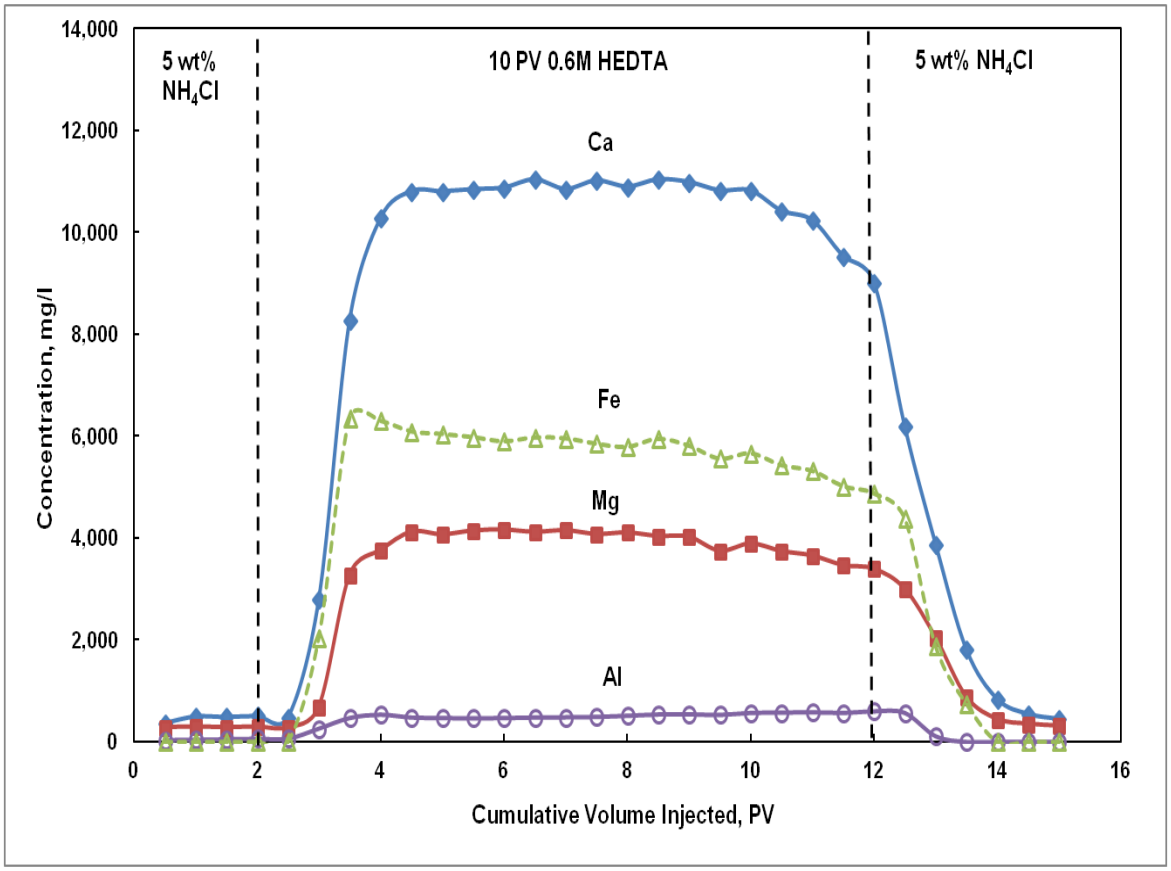

Fig. 62—Analysis of coreflood effluent samples for Bandera sandstone core treated with 10PV of 0.6M HEDTA (pH = 4) at 300°F and 2 cm^3/min.

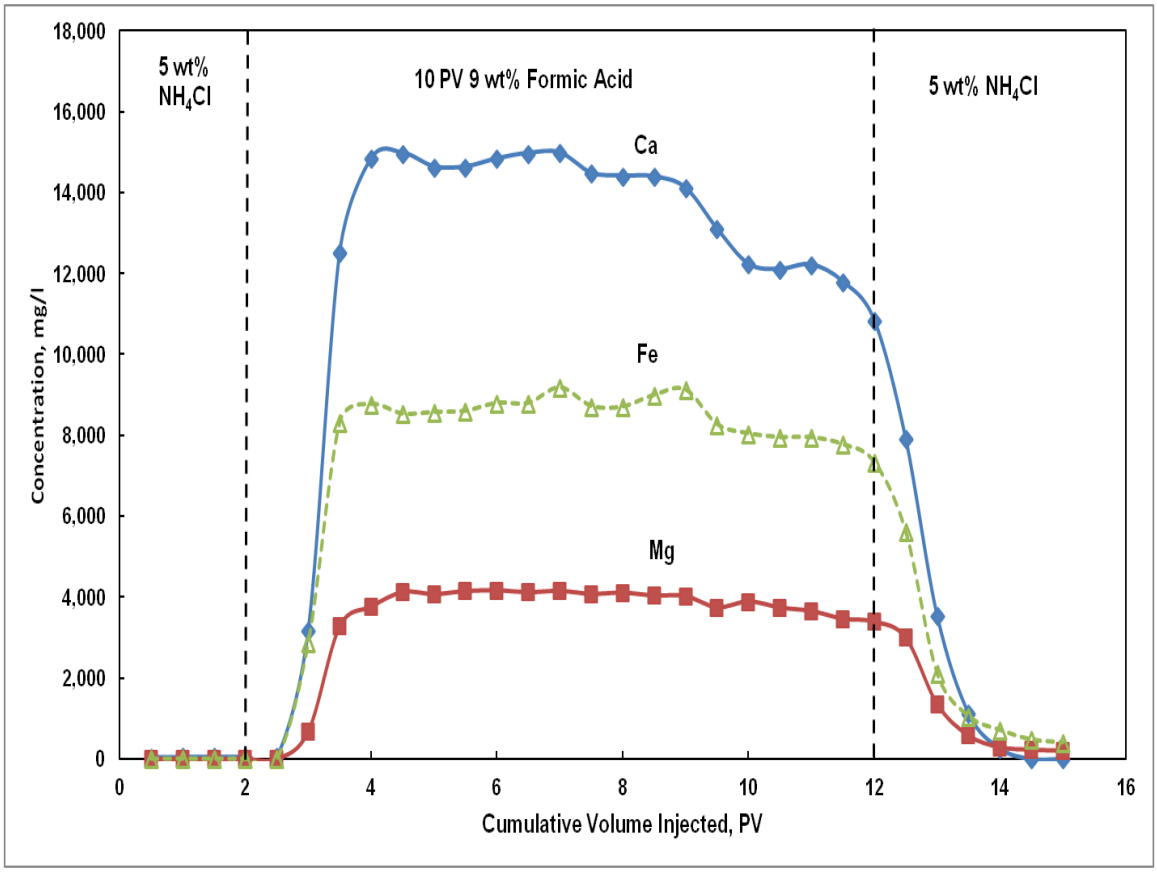

Fig. 63—Analysis of coreflood effluent samples for Bandera sandstone core treated with 10PV of 9 wt% formic acid (pH =1.75) at 300°F and 2 cm^3/min.

Figs. 61 to 63 showed the coreflood effluent analysis for Bandera sandstone cores treated by 0.6M GLDA, 0.6M HEDTA and 9 wt% formic acid at 300°F with a flow rate of 2 cm^3/min. Based on the coreflood experiments, formic acid dissolve more calcium than HETDA and GLDA, therefore, 9 wt% formic acids were better than the other two acids in removing carbonates from Bandera sandstone cores. The total amount of dissolved calcium, iron, and magnesium were the highest for formic acid, then HEDTA and then GLDA.

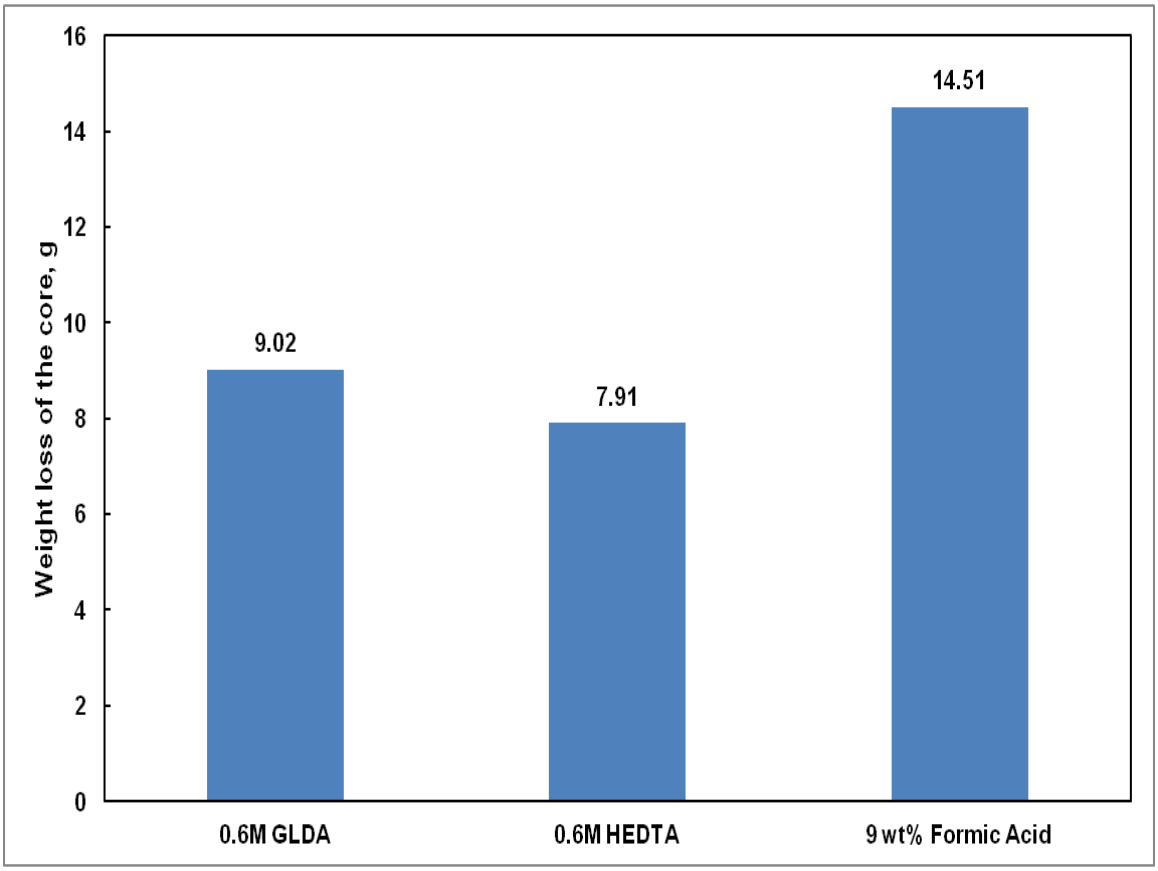

Fig. 64—Weight loss of Bandera cores after the coreflood experiments using 0.6M GLDA (pH = 3.8), 0.6M HEDTA (pH = 3.8), and 9 wt% formic acid (pH =1.75) at 2 cm^3/min and 300°F.

The weight loss of the core, **Fig. 64**, confirmed that 9 wt% formic acids were better than HEDTA and GLDA in dissolving calcium, iron, and magnesium from Bandera sandstone cores. The weight loss of the core was 9.02, 7.91 and 14.51 g for GLDA, HEDTA, and formic acid, respectively. **Fig. 65** showed the permeability ratio for HEDTA, GLDA and 9 wt% formic acids. The permeability ratio for formic acid was

2.11, which was higher than that of GLDA and HEDTA; it was 1.46 for GLDA and 1.26 for HEDTA. Formic acid dissolved more calcium than HEDTA and GLDA, and enhanced the Bandera core permeability better than the other two.

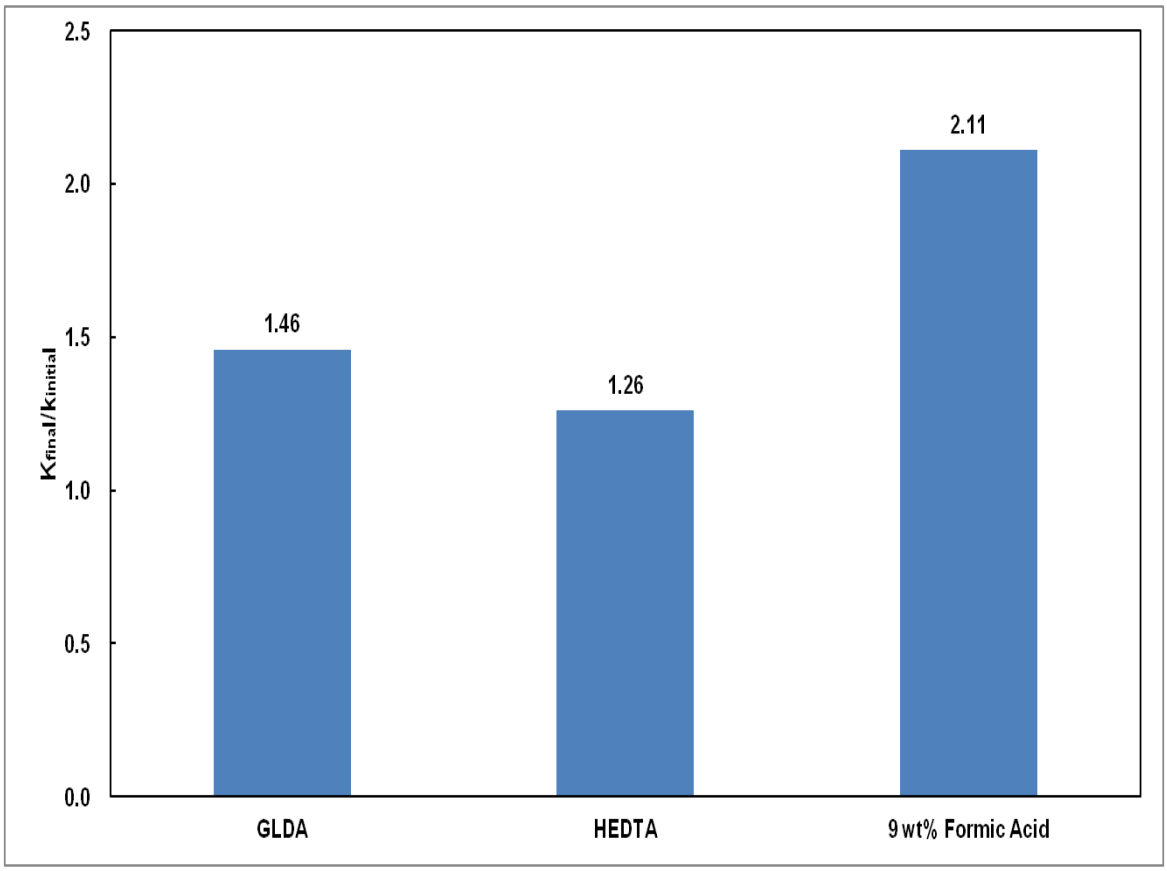

Fig. 65—Comparison between 0.6M GLDA (pH = 3.8), 0.6 M HEDTA (pH = 3.8), and 9 wt% formic Acid (pH =1.75) in stimulating Bandera sandstone cores.

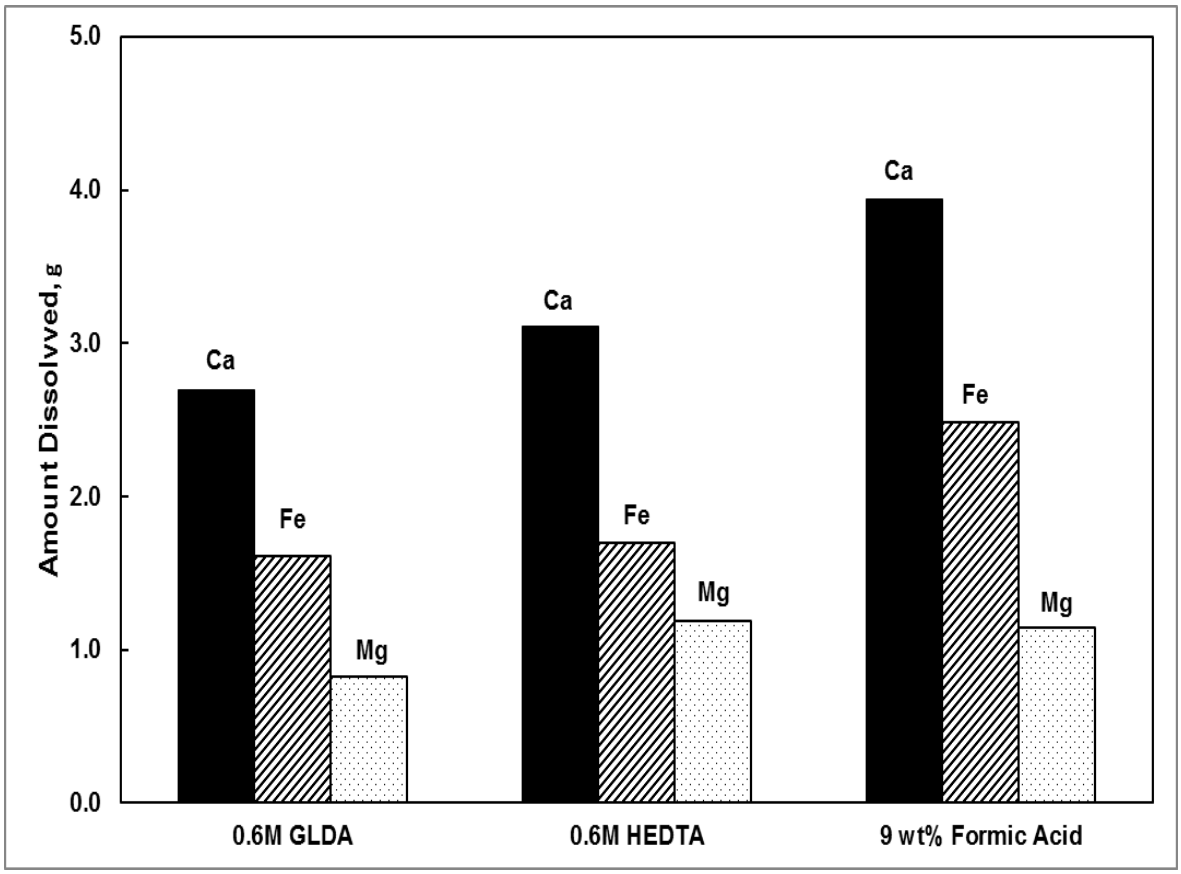

Fig. 66—Amount of different cations, calcium, iron, and magnesium, in the coreflood effluent for Bandera cores treated by 0.6M GLDA (pH = 3.8), 0.6 M HEDTA (pH = 3.8), and 9 wt% formic Acid (pH =1.75) at 2 cm^3/min and 300°F.

The amount of calcium was 3.94 g in the case of 9 wt% formic acids, 3.11 g for HEDTA and 2.69 g for GLDA, as shown in **Fig. 66**. Chelating agents are big source of sodium, although chelating agents can be used effectively to remove the carbonate minerals in the Bandera sandstone cores, it will precipitate sodium fluosilicates and the tetra sodium salts when HF-based acid are used as the main acid to stimulate Bandera

sandstone cores. Therefore, 9 wt% formic acids were used to preflush the Bandera sandstone core before the main acid injection.

A coreflood experiment was also conducted using 0.6M GLDA (pH = 3.8) on Bandera sandstone cores at 300°F to investigate the effect of soak time on the stimulation. The core was saturated with 5 wt% NH_4Cl brine solution, and then 5 PV GLDA injected, and then shut-in the system, the chelate agent was soaked for 2 hours inside the core. The permeability of the core increased with 1.12 improvement factor ($k_{final}/k_{initial}$) after treatment. To investigate if most of carbonate minerals inside the core has been chelated, 3 PV GLDA was injected followed by the postflush of 6 PV of 5 wt% NH_4Cl brine. **Fig. 67** showed the concentrations of Ca, Mg and Fe as a function of cumulative volume injected into the core. The results indicated that main ion concentrations increased greatly after 2 hours soaking time, which gave the acid more time to react with various minerals that are present in the core. However, the concentration of Ca, Fe, and Mg were 10,000, 6,000, and 3,000 mg/l, respectively, when GLDA was injected again after the 5 wt% NH_4Cl brine postflush, which were still very high. Therefore, it can be concluded that a large volume of GLDA is needed to remove carbonate minerals from Bandera sandstone.

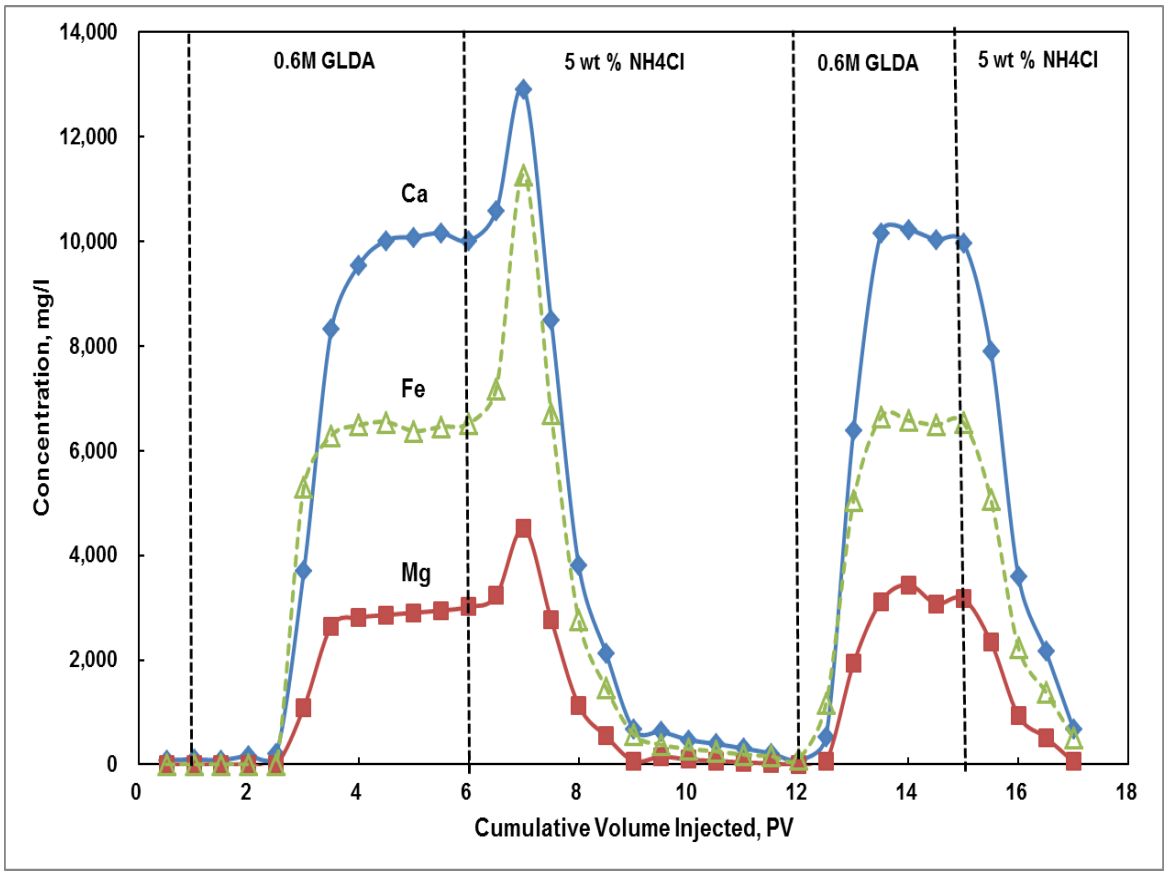

Fig. 67—Analysis of coreflood effluent samples for Bandera sandstone core treated with 5 PV of 0.6M GLDA (pH =3.8) at 300°F and 2 cm^3/min. Shut in 2 hours after 5 PV GLDA.

Stimulating Berea Sandstone Cores with Preflush Using Phosphonic-based HF Acid and 12:3 Mud Acid

To compare the efficiency of the full strength phosphonic-based HF acid and the conventional 12:3 mud acid treatments, coreflood tests were conducted on Berea sandstone cores. The treatment design schedule included a 4 pore volume (PV) of 10 wt% HCl preflush and was followed by the main acid with 3 PV of full strength

phosphonic-based HF acid or 12:3 mud acid and a postflush of 5 wt% NH_4Cl until the pressure drop across the core was stabilized. To prevent corrosion, 2 vol% corrosion inhibitor and 1.0 vol% intensifier were added into HCl, and 1.5 vol% corrosion inhibitor and 2.0 vol% intensifier were added into the full strength phosphonic-based HF acid and 12:3 mud acid, respectively. The flow rate was kept at 2 cm^3/min, and the temperature was 300°F.

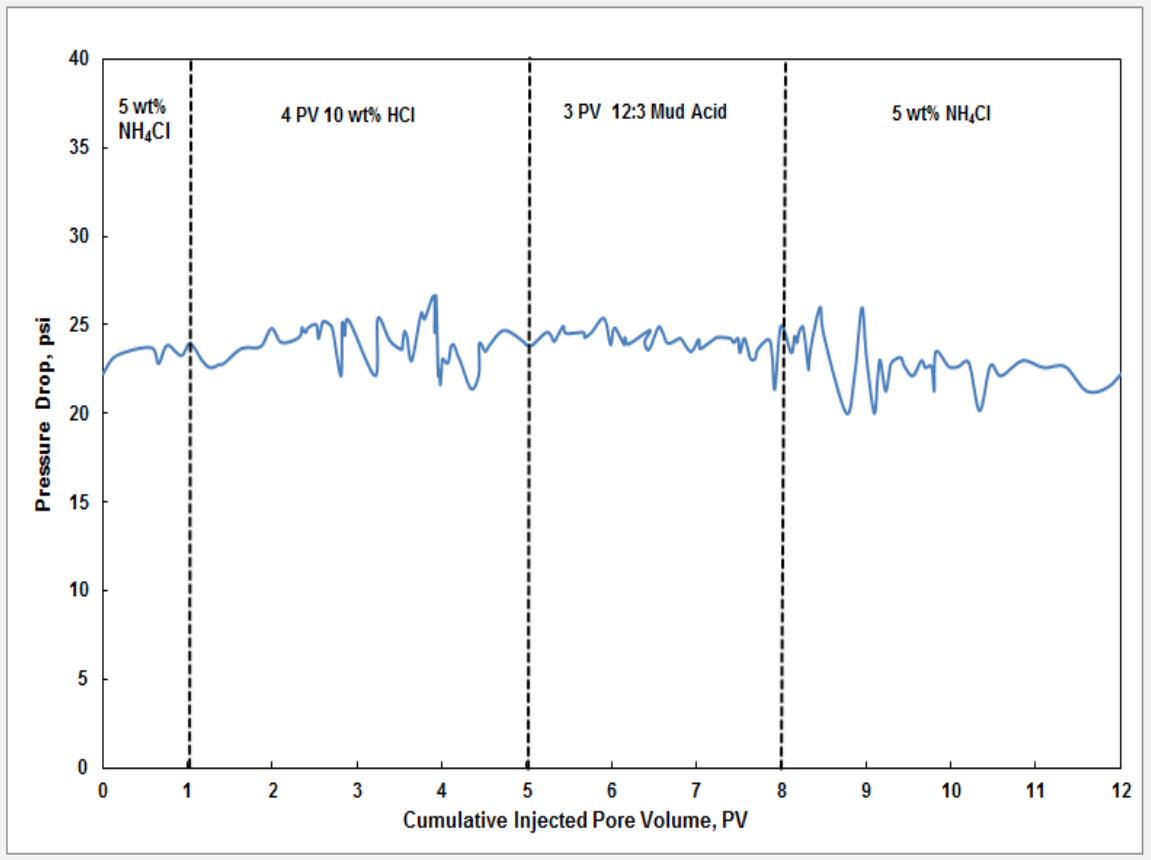

Fig. 68—Pressure drop in the Berea coreflood experiment with 3 PV of 12:3 mud acid in the main flush at 300°F.

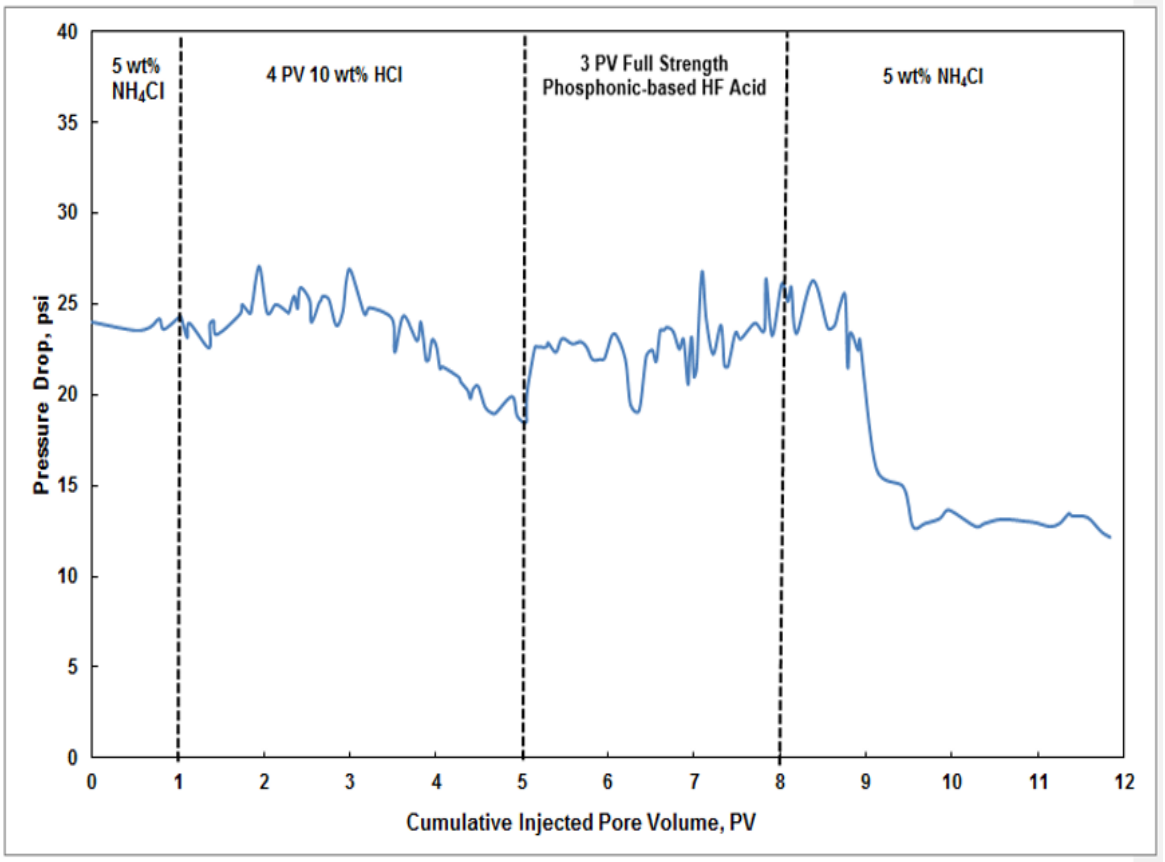

Fig. 69—Pressure drop across the core in the Berea coreflood experiment with 3 PV of full strength phosphonic-based HF acid as the main acid at 300°F.

Figs. 68 to 69 show the pressure drop across the core, the results indicated that the permeability of Berea sandstone cores increased from 26.2 to 72.8 md when 3 PV of full strength phosphonic-based HF acid was used in the main acid treatment. No obvious improvement was observed when 12:3 mud acid was used in the main acid. A significant permeability improvement was observed for treatments using the phosphonic-based acid system.

CT scan was also performed to the cores before and after the coreflood experiment. For the CT images, each pixel has a relative value of linear attenuation coefficient after image reconstruction. CT number is converted by the attenuation coefficient and can be used as the indicator of the change of density and porosity (Akin and Kovscek 2003). **Figs. 70 and 71** show the CT number across the Berea cores before and after the coreflood test at 300°F with the flow rate of 2 cm^3/min.

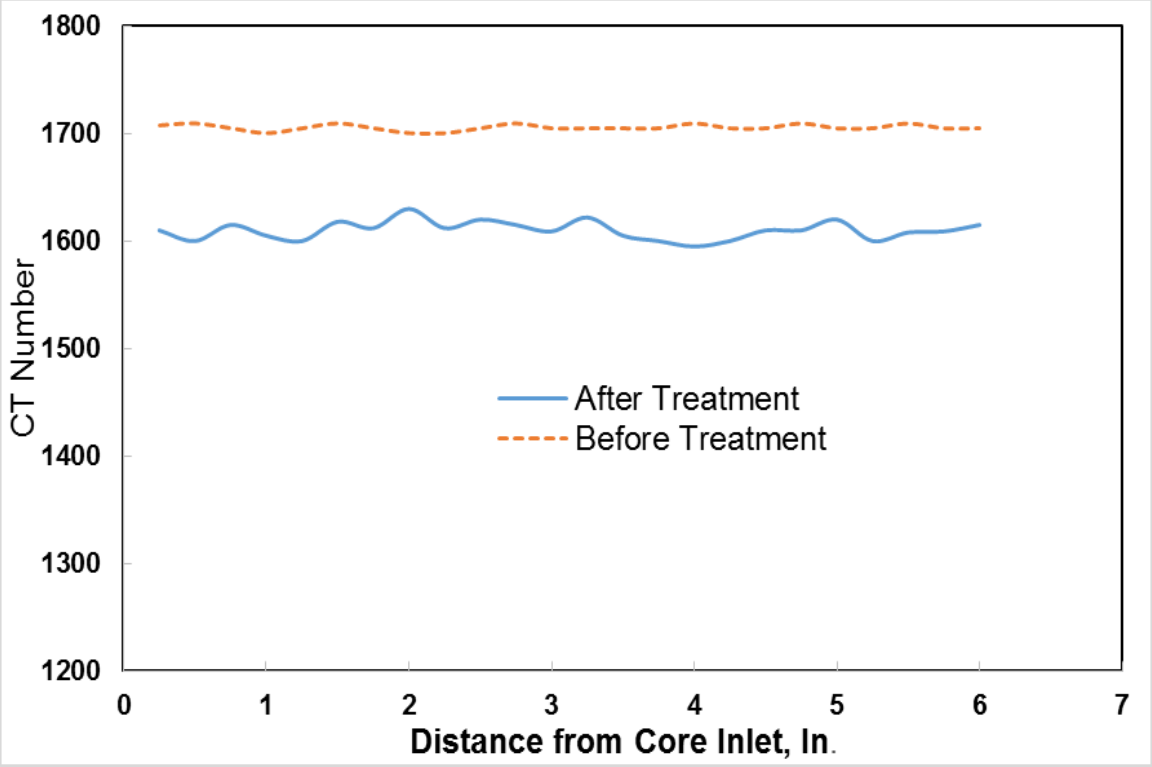

Fig. 70—CT number across the Berea sandstone core before and after the acid treatment using HCl as a preflush and 3 PV of full strength phosphonic-based HF acid as the main flush at 300°F and 2 cm^3/min.

CT number decrease was observed in coreflood experiment with full strength phosphonic-based HF acid (Fig. 69). The decrease in the CT number indicated an increase in the core porosity after the treatment, which confirms the effectiveness of full strength phosphonic-based HF acid in stimulating the Berea sandstone core.

The CT number is related to the bulk density as shown in **Eq. 13** (Akin and Kovscek 2003).

$$\rho_{bulk} = aCTN + b \quad \text{.....(13)}$$

Where ρ_{bulk} is the bulk density, *CTN* represents the CT number, *a* is the slope, and *b* is the intercept of the linear relation between *CTN* and the bulk density.

The results show that the core with full strength phosphonic-based HF acid in the main acid has a lower CT number than the core with 12:3 mud acid in the main acid, which means that the core with the full strength phosphonic-based HF acid in the main acid has a higher porosity than the core with 12:3 mud acid in the main acid. This results indicate that full strength phosphonic-based HF acid has much better performance than 12:3 mud acid in stimulating Berea sandstone cores at 300°F.

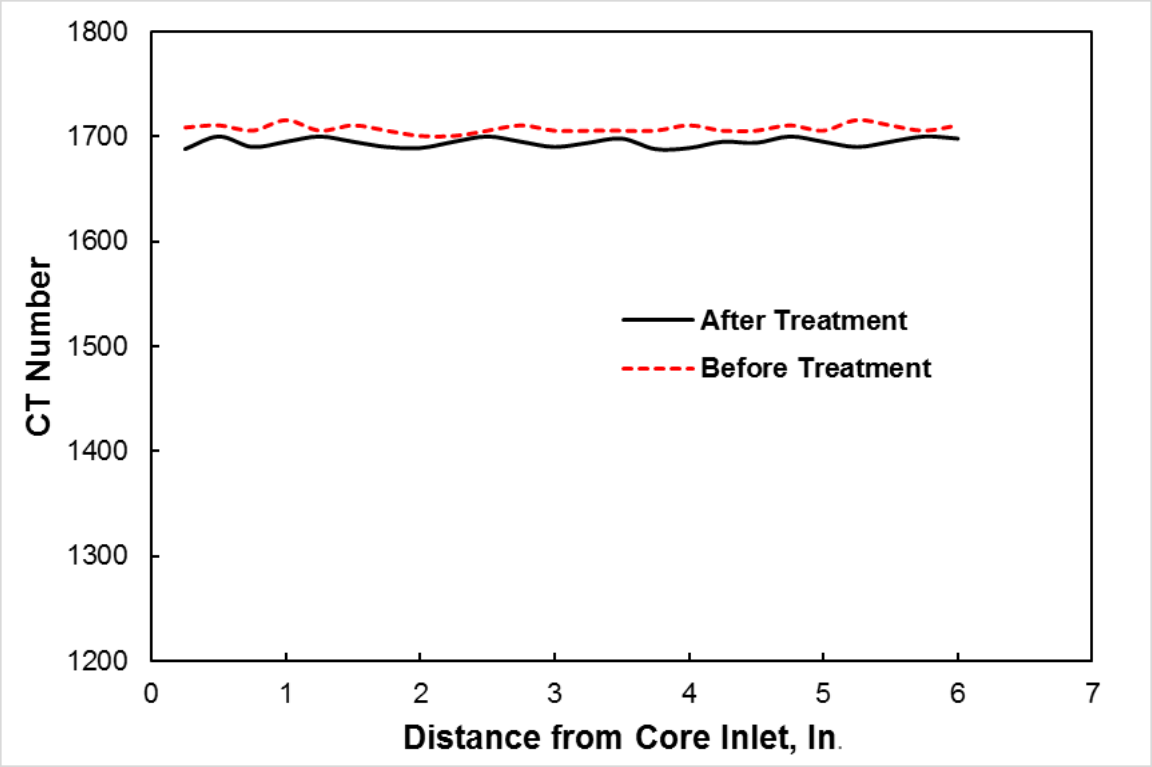

Fig. 71—CT number across the Berea sandstone core before and after the acid treatment using HCl as a preflush and 3 PV of 12:3 mud acid as the main flush at 300°F and 2 cm^3/min.

Concentrations of ions in the core effluent samples collected during coreflood tests are shown in **Figs. 72 and 73**. The results show that, in the preflush stage, most of the Ca was dissolved with 4 PV of the 10 wt% HCl injection in both cases. Only trace amounts of Ca was detected after the 4 PV of HCl injection. Therefore, 4 PV of 10 wt% HCl preflush was sufficient to remove the Ca.

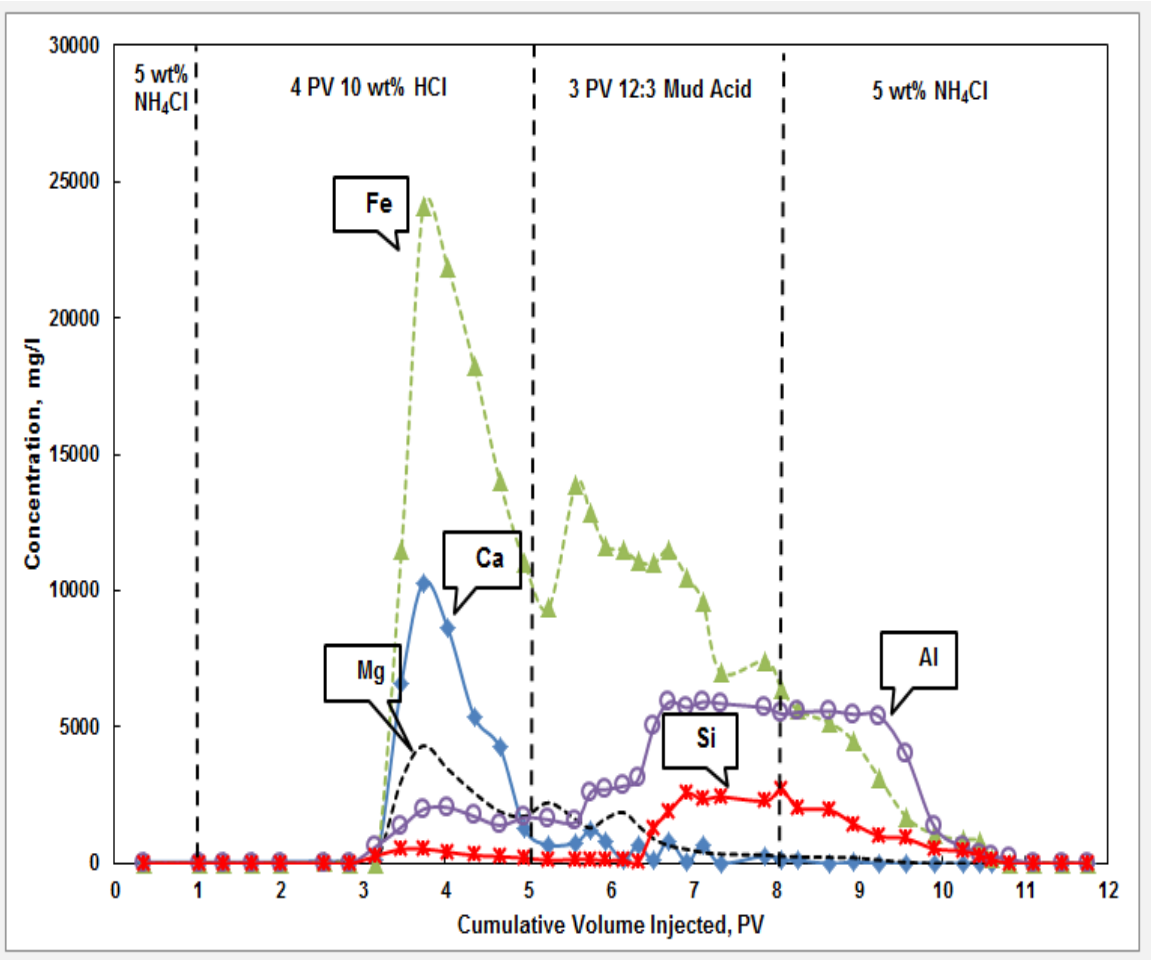

Fig. 72—Ion concentrations in the effluent samples from the Berea coreflood experiment with 3 PV of 12:3 mud acid in the main flush at 300°F.

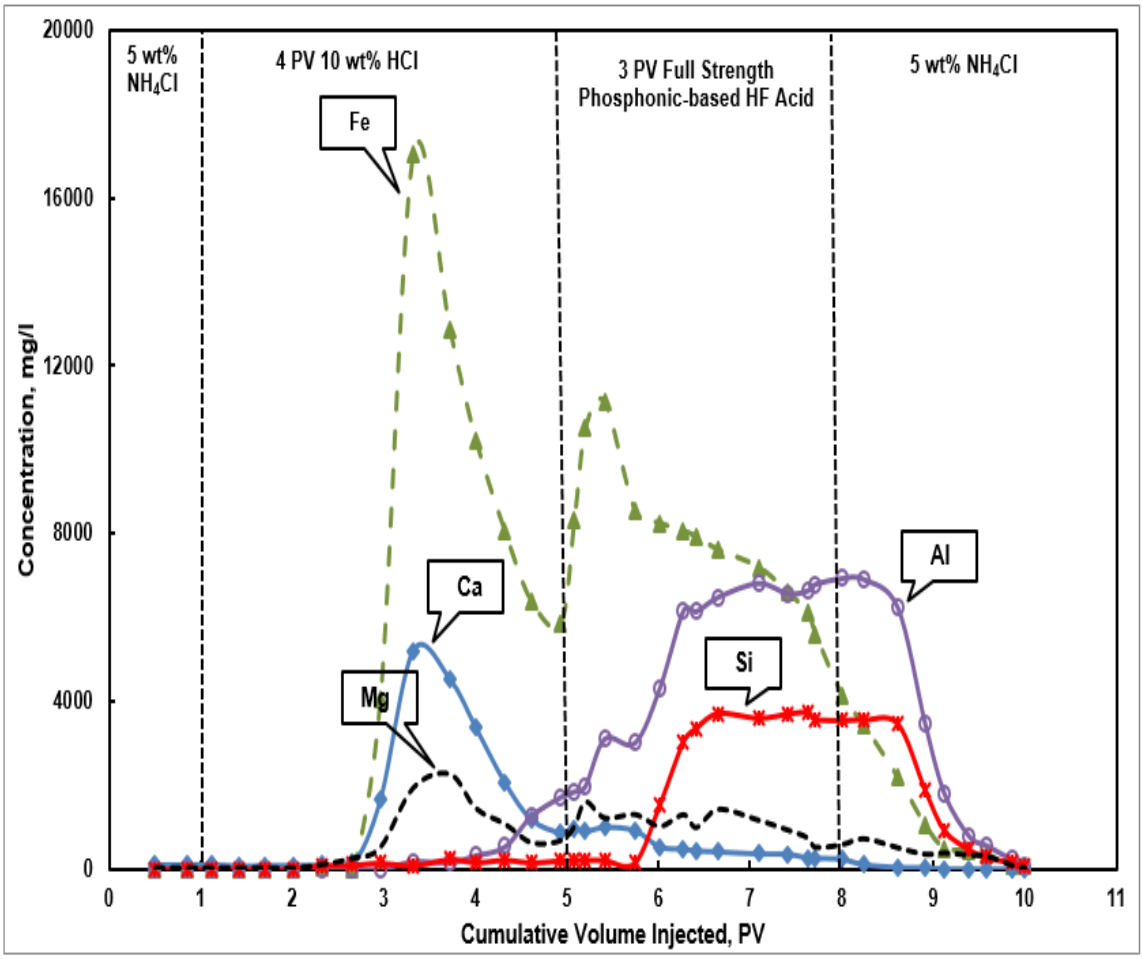

Fig. 73—Ion concentrations in the effluent samples from the Berea coreflood experiment with 3 PV of full strength phosphonic-based HF acid in the main flush at 300°F.

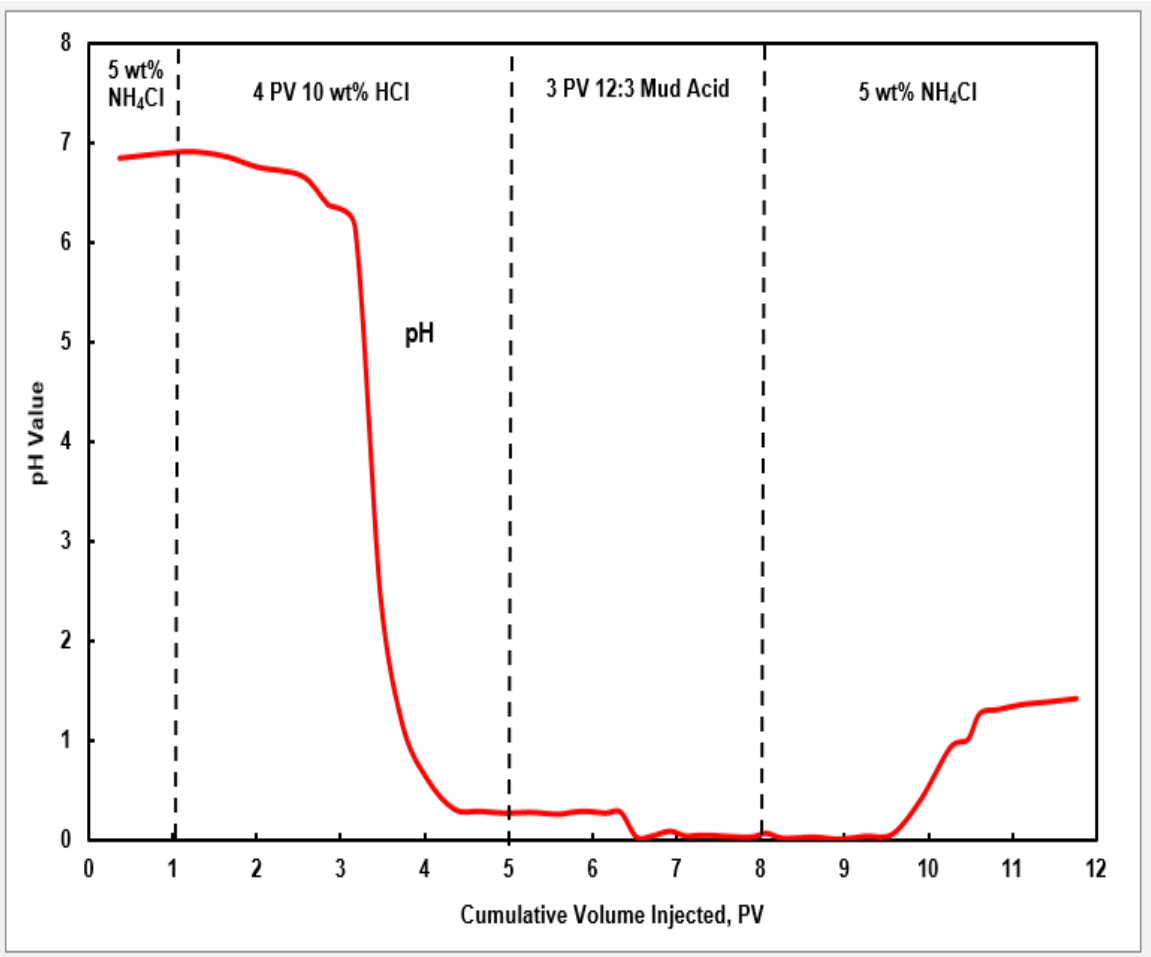

Fig. 74—pH values of the effluent samples from the Berea coreflood experiment with 3 PV of 12:3 mud acid in the main flush at 300°F.

The pH values of the effluent samples were measured (**Figs. 74 and 75**), and the results showed that the pH values of the effluent samples were near 2 when the phosphonic-based acid was used as the main acid. The pH values were higher than that of the effluent samples when the 12:3 mud acid was applied in main stage. As discussed previously, the chelation properties of the phosphonic acid, which is a function of

deprotonation of the organic ligand, would be promoted by the high pH (Atkari et al, 1996).

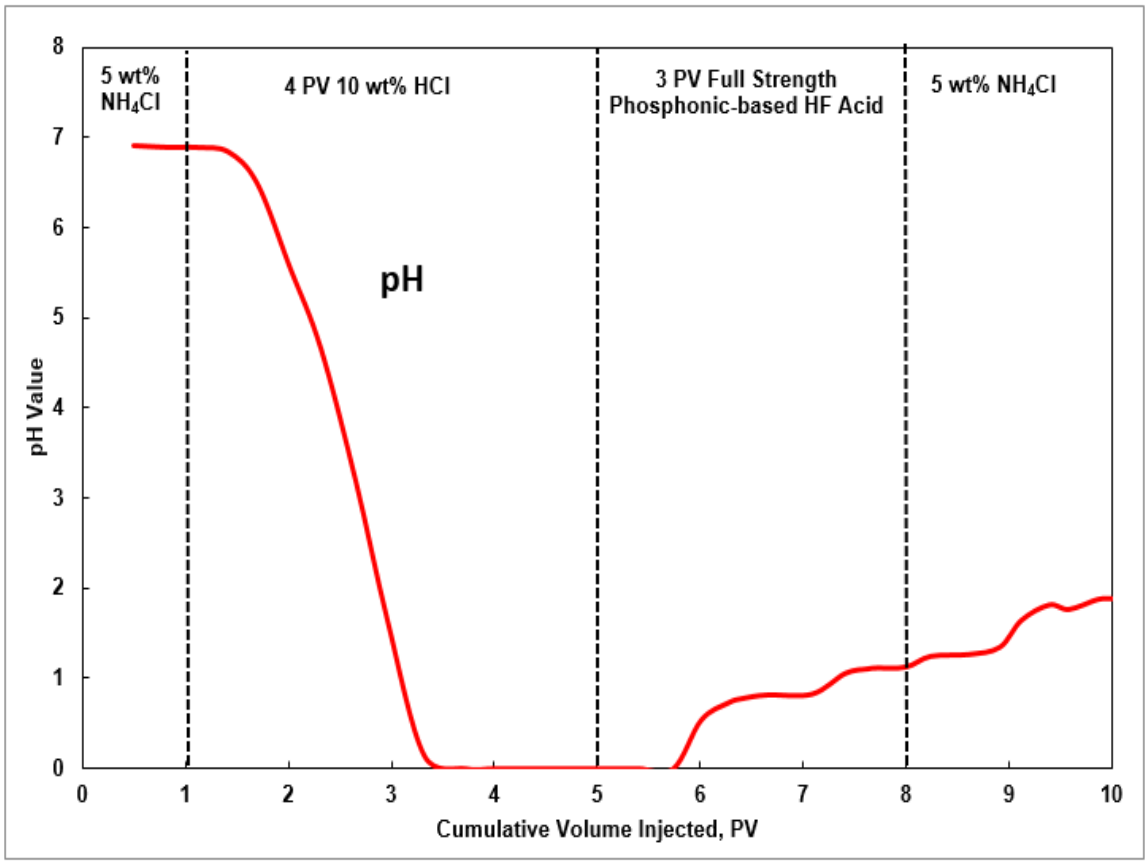

Fig. 75—pH values of the effluent samples from the Berea coreflood experiment with 3 PV of full strength phosphonic-based HF acid in the main flush at 300°F.

The phosphorus concentration of the effluent samples was almost equal to the original phosphorus concentration in the fresh phosphonic-based acid system (**Fig. 76**); this indicates that the chelating properties of the phosphoric-based acid system in the

main flush stage can chelate metal ions in the solution, which can prevent further precipitation formation effectively.

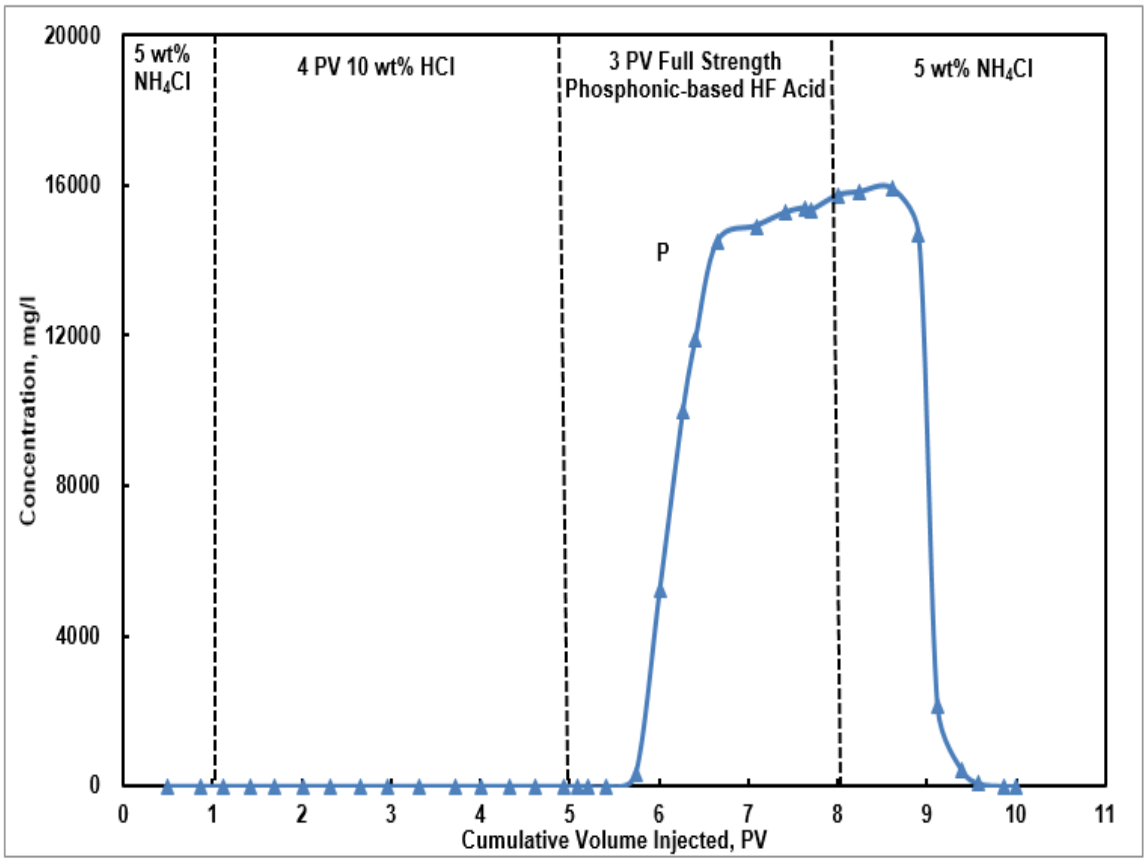

Fig. 76—Phosphorus concentrations of the effluent samples from the Berea coreflood experiment with 3 PV of full strength phosphonic-based HF acid in the main flush at 300°F.

In the main flush stage, less Si was detected in the effluent samples when using 12:3 mud acid mixtures than when using the phosphonic-based acid system. This might

be attributed to the precipitation of silicon caused by the secondary reaction between fluosilicic acid and aluminosilicates. All of these results indicate that the phosphonic-based acid can mitigate the secondary reaction effectively at high temperatures, which is also effective in preventing fluoride precipitation. Therefore, this phosphonic-based acid system has a much better performance than the 12:3 mud acid in the Berea coreflood test at 300°F.

Conclusions

Three different organic acids were compared to remove carbonates in Bandera sandstone cores. Based on the results obtained from this study, the following conclusions can be drawn:

1. This acid system enhanced the permeability of Berea sandstone cores, and the optimum injection volume is 2.5 PV to keep the integrity of the cores at 2 cm^3/min and 300°F.

2. This acid system damaged Bandera sandstone cores severely at 300°F, preflushing the core can minimize the damage caused by the main acid.

3. GLDA and HEDTA and 9 wt% formic acid solutions were compatible with Bandera sandstone cores at low pH value, and 9 wt% formic acid was much more effective in remove carbonate in Bandera sandstone cores.

4. Phosphonic-based HF acid can mitigate the secondary reaction effectively at high temperatures, and is effective in preventing fluoride precipitation. Therefore,

phosphonic-based HF acid has a much better performance than regular mud acid in the Berea coreflood test at 300ºF.

CHAPTER V

CONCLUSIONS

In this study, the interactions between phosphonic-based HF acid systems with clay minerals were examined. Solubility tests and coreflood experiments were conducted to evaluate the performance of the phosphonic-based HF acid on sandstone acidizing. Through this research, it was determined that:

1. The concentration of Si decreased in the spent acid after full strength phosphonic-based HF acid reacted with clay minerals at 302ºF. This indicated that secondary precipitation had occurred. The 19F NMR results at high temperature also demonstrated the occurrence of a secondary reaction, which became fast at high temperatures.
2. 19F NMR results indicated that each fluoro complex had distinct 19F chemical shifts. AlF_3, AlF_2^+, and AlF^{2+} were detected in the spent acid due to the low acid (H^+) concentration. AlF_3 precipitated in the phosphonic-based acid when it reacted with the chlorite mineral at room temperature and 302°F. No AlF3 precipitate was identified by SEM and EDS after kaolinite, bentonite, and illite reacted with phosphonic-based acid under similar conditions.
3. ^{31}P NMR was able to determine the phosphorus species present in the live and spent acid solutions. The results showed that the phosphonic acid in the phosphonic-based HF acid mixtures was effective in preventing fluoride precipitation.

4. ^{27}Al NMR was not an effective tool to characterize the aluminum complexes in the spent acid. All ^{27}Al chemical shifts of all of the Al complexes were approximately the same.
5. This acid system enhanced the permeability of Berea sandstone cores, and the optimum injection volume is 2.5 PV to keep the integrity of the cores at 2 cm^3/min and 300°F.
6. This acid system damaged Bandera sandstone cores severely at 300°F, preflushing the core can minimize the damage caused by the main acid.
7. GLDA and HEDTA and 9 wt% formic acid solutions were compatible with Bandera sandstone cores at low pH value, and 9 wt% formic acid was much more effective in remove carbonate in Bandera sandstone cores.
8. Phosphonic-based HF acid can mitigate the secondary reaction effectively at high temperatures, and is effective in preventing fluoride precipitation. Therefore, phosphonic-based HF acid has a much better performance than regular mud acid in the Berea coreflood test at 300ºF.

REFERENCES

Abrams, A., Scheuerman, R.F., Templeton, C.C., Richardson, E.A. 1983. Higher-pH Acid Stimulation Systems. J. Pet Tech **35** (12): 2175-2184. SPE-7892-PA. http://dx.doi.org/10.2118/7892-PA.

Alonso, C., Morato, A., Medina, F., et al. 2000. Preparation and Characterization of Different Phases of Aluminum Trifluoride. *Chem. Mater.* **12** (4): 1148-1155. DOI**:** 10.1021/cm991195g.

Al-Dahlan, M.N., Nasr-El-Din, H.A., and Al-Qahtani, A. A. 2001. Evaluation of Retarded HF Acid Systems. Paper SPE 65032 presented at the SPE International Symposium on Oil Field Chemistry, Houston, Texas, 13-16 February. http://dx.doi.org/10.2118/65032-MS.

Al-Harbi, B.G., Al-Khaldi M.H., and Al-Dossary K.A. 2011. Interactions of Organic-HF Systems with Aluminosilicates: Lab Testing and Field Recommendations. Paper SPE 144100 presented at European Formation Damage Conference, Noordwijk, The Netherlands, 7-10 June. http://dx.doi.org/10.2118/144100-MS.

Al-Harbi, B.G., Al-Dahlan, M.N., Khaldi, M.H. 2012. Aluminum and Iron Precipitation During Sandstone Acidizing Using Organic-HF Acids. Paper SPE 151781 presented at the SPE International Symposium and Exhibition on Formation Damage Control, Lafayette, Louisiana, 15-17 February. http://dx.doi.org/10.2118/151781-MS.

Al-Harbi, B.G., Al-Dahlan M.N., Al-Khaldi M.H. 2013. Evaluation of Organic Hydrofluoric Acid Mixtures for Sandstone Acidizing. Paper SPE 16967

presented at the International Petroleum Technology Conference, Beijing, China, 26-28 March. http://dx.doi.org/10.2523/16967-MS.

Ali, A.H.A, Frenier, W.W., Xiao, Z., and Ziauddin, M. 2002. Chelating Agent-Based Fluids for Optimal Stimulation of High-Temperature Wells. Paper SPE 77366 presented at the SPE Annual Technical Conference and Exhibition, San Antonio, Texas, 29 September- 2 October. DOI: 10.2188/77366-MS.

Ali, S.A, Ermel, E., Clarke, J. et al. 2008. Stimulation of High-Temperature Sandstone Formations from West Africa with Chelating Agent-Based Fluids. SPE Prod & Oper **23** (1): 32-38. SPE-93805-PA. http://dx.doi.org/10.2118/93805-PA.

Akin, S. and Kovscek, A.R. 2003. Computed tomography in petroleum engineering research. *Geol. Soc. London Spec. Publ.*, **215** (12): 23-38, http://dx.doi.org/10.1144/GSL.SP.2003.215.01.03.

Amaefule, J.O., Kersey, D.G., Norman, D.L., and Shannon, P.M. 1988. Advances in Formation Damage Assessment and Control Strategies. CIM Paper 88-39-65 presented at the 39th Annual Technical Meeting of Petroleum Society of CIM and Canadian Gas Processors Association, Calgary, Alberta, June 12-16. DOI:10.2118/88-39-65.

Atkari, K., Kiss, T., Bertani, R., et al. 1996. Interactions of Aluminum (III) with Phosphates. *Inorg. Chem*. **35** (24): 7089-7094. DOI: 10.1016/S0010-8545(01)00467-2.

Bertaux, J. 1989. Treatment-Fluid Selection for Sandstone Acidizing: Permeability Impairment in Potassic Mineral Sandstone. *SPE Prod Eng* **4** (1): 41-48. http://dx.doi.org/10.2118/15884-PA.

Bodor, A., Tóth, I., Bányai, I. et al. 2000. 19F NMR Study of the Equilibria and Dynamics of the Al3+/F- System. Inorg. Chem. **39** (12): 2530-2537. http://dx.doi.org/10.1021/ic991248w.

Bodor, A., Toth, I., Banyai, I., et al. 2003. Studies of equilibrium, structure, and dynamics in the aqueous Al(III)-oxalate-fluoride system by potentiometry, ^{13}C and ^{19}F NMR spectroscopy. *Geochim et Cosmochim. Acta* **67** (15): 2793-2803. DOI: 10.1016/S0016-7037(03)00099-1.

Buijse, M., de Boer, P., Breukel, B., and Burgos, G. 2004. Organic Acids in Carbonate Acidizing. SPE *Production & Facilities* **19** (3): 128-134. SPE-82211-PA. DOI: 10.2118/82211-PA.

Cade-Menun, B.J. 2005. Characterizing phosphorus in environmental and agricultural samples by 31P nuclear magnetic resonance spectroscopy. Talanta **66** (2): 359–371. http://dx.doi.org/10.1016/j.talanta.2004.12.024.

Chang, F., Nasr-El-Din, H. A., Lindvig, T., and Qiu, X.W. 2008. Matrix Acidizing of Carbonate Reservoirs Using Organic Acids and Mixture of HCl and Organic Acids. Paper SPE 116601 presented at the Annual Technical Conference and Exhibition. Denver, Colorado, USA.

Civan, F. 2000. *Reservoir Formation Damage: Fundamentals, Modeling, Assessment, and Mitigation*. Houston, Texas: Gulf Publishing Company.

Di Lullo, G. and Rae, P. 1996. A New Acid for True Stimulation of Sandstone Reservoirs. Paper SPE 37015 presented at the SPE Asia Pacific Oil and Gas Conference, Adelaide, Australia, 28-31 October.http://dx.doi.org/10.2118/37015-MS.

Dungan, C.H., Van Wazer, J.R. 1970. Compilation of Reported 19F NMR Chemical Shifts 1951 to Mid-1967. Appendix I. New York: Wiley-Interscience, USA.

Economides, M.J. and Nolte, K.G. 2000. *Reservoir Stimulation*. Reservoir Stimulation: Prentice Hall. Original Edition.

Finney WF, Wilson E, Callender A, Morris MD, Beck LW. 2006. Reexamination of hexafluorosilicate hydrolysis by 19F NMR and pH measurement. Envir. Sci. Technol. **40** (8): 2572-2577. http://dx.doi.org/10.1021/es052295s.

Fredd, C.N. and Fogler, H.S. 1998. The Influence of Chelating Agents on the Kinetics of Calcite Dissolution. J. Colloid. Interface. Sci, **204** (1): 187-197. DOI: 10.1006/jcis.1998.5535.

Frenier, W., Wilson, D., Crump, D. et al. 2000. Use of Highly-Soluble Chelating Agents in Well Stimulation Services. Paper SPE 63242 presented at the SPE Annual Technical Conference and Exhibition, Dallas, Texas, USA, 1-4 October. http://dx.doi.org/10.2118/63242-MS.

Frenier, W.W., Brady, M., Al-Harthy, S., Arangath, R., Chan, K.S., Flamant, N. and Samuel, M. 2004. Hot Oil and Gas Well Can Be Stimulated Without Acids. SPE Prod & Fac **19** (4): 189-199. SPE-86522-PA. http://dx.doi.org/10.2118/86522-PA.

Gdanski, R.D. 1985. AlCl3 Retards HF Acid for More Effective Stimulation. Oil & Gas J. **83** (43): 111-115.

Gdanski, R.D.1999. Kinetics of the Secondary Reactions of Hydrofluoric Acid on Alumino-silicates. SPE Prod & Oper **14** (4): 260-268. SPE-59094-PA. http://dx.doi.org/10.2118/59094-PA.

Gdanski, R.D. 1998. Kinetics of the Tertiary Reactions of Hydrofluoric Acid on Alumino-silicates, SPE Prod & Oper **13** (2): 75-80. SPE-31076-PA. http://dx.doi.org/10.2118/31076-PA.

Gdanski, R.D. 2000.Kinetics of the Primary Reaction of HF on Alumino-Silicates. SPE Prod & Oper **15** (4): 279-287. SPE-66564-PA. http://dx.doi.org/10.2118/66564-PA.

Gdandski, R.D. and Shuchart, C.E. 1996. Newly Discovered Equilibrium Controls HF Stoichiometry. J. Pet Tech **48** (2): 145-149. SPE-30456-JPT. http://dx.doi.org/10.2118/30456-JPT.

Gdandski, R.D. and Shuchart, C.E. 1997. HF Acid Blends Based on Formation Conditions Eliminate Precipitations Problems. Pet. Eng. Intl 70 (3): 63-66.

Gidley, J.L. 1985. Acidizing Sandstone Formations: A Detailed Examination of Recent Experience. Paper SPE 14164 presented at the SPE Annual Technical Conference and Exhibition, Las Vegas, Nevada, 22- 25 September. http://dx.doi.org/10.2118/14164-MS.

Gumienna-Kontecka, E., Silvagni, R., Lipinski, R., et al. 2002. Bisphosphonate chelating agents; complexation of Fe(III) and Al(III) by 1-phenyl-1-hydroxymethylene bisphosphonate and its analogues. *Inorg. Chim. Acta* **339**: 111-118.

Hartman, R.L., Lecerf, B., Frenier, W.W. et al. 2006. Acid-Sensitive Aluminosilicates: Dissolution Kinetics and Fluid Selection for Matrix-Stimulation Treatments. SPE Prod & Oper **21** (2): 194-204. SPE-82267-PA. http://dx.doi.org/10.2118/82267-PA.

Kalfayan, L.J. and Metcalf, A.S. 2000. Successful Sandstone Acid Design Case Histories: Exceptions to Conventional Wisdom. Paper SPE 63178 presented at the SPE Annual Technical Conference and Exhibition, Dallas, Texas. Oct. 1- 4. DOI: 10.2118/63178-ms.

Lacour S., Deluchat V., Bollinger J.C., Serpaud B. 1998. Complexation of trivalent cations (Al(III), Cr(III), Fe(III)) with two phosphonic acids in the pH range of fresh waters. Talanta, **46** (5): 999–1009. DOI: 10.1016/S0039-9140(97)00369-X.

Mahmoud, M.A., Nasr-El-Din, H. A., and De Wolf, C. A. 2011. Sandstone Acidizing using a New Class of Chelating agents. Paper SPE 139815 presented at the International Symposium on Oil Field Chemistry Conference, Woodlands, TX, 11-13 April.

Martin, A.N. 2004. Stimulating Sandstone Formations with non-HF Treatment System. Paper SPE 90774 presented at the SPE Annual Technical Conference and Exhibition, Houston, Texas, 26-29 September. DOI: 10. 2118/90774-MS.

Martinez, E.J., Girardet, J.L., and Morat, C. 1996. Multinuclear NMR study of Fluoroaluminate Complexes in Aqueous Solution. Inorganic Chemistry **35** (3): 706-710. http://dx.doi.org/10.1021/ic9507575.

McLeod, H.O.: "Matrix Acidizing", JPT (Dec. 1984), p. 2055-2069.

Mungan, N. 1989. Discussion of An Overview of Formation Damage, *J. Petr. Technol*., **41**(11) 1224.

Murray, H.H., 2007. Applied Clay Mineralogy: occurrences, processing, and application of kaolins, bentonites, palygorskite-sepiolite, and common clays. Indiana University, Bloomington, USA.

Moedritzer, K., L. Maier, and L.C.D. Groenweghe. 1962. Phosphorus-31 nuclear magnetic resonance spectra of phosphorus compounds. J. *Chem. Eng. Data* **7**: 307-310.

Nasr-El-Din, H.A., Al-Dahlan, M.N., As-Sadlan, A.M. et al. 2002. Iron Precipitation During Acid Treatments Using HF-Based Acids. Paper SPE 73747 presented at the International Symposium and Exhibition on Formation Damage Control, Lafayette, Louisiana, 20-21 February. http://dx.doi.org/10.2118/73747-MS.

Nwoke, L., et al. 2004. Phosphonic Acid Complex for stimulating HF-Sensitive Reservoirs-a Revolutionary Response. Paper SPE 89415 presented at the SPE/DOE Symposium On Improve Oil Recovery, Tulsa, Oklahoma, 17-21 April. http://dx.doi.org.lib-ezproxy.tamu.edu:2048/10.2118/89415-MS.

Parkinson, M., Munk, T., Brookley, J., Caetano, A., Albuquerque, M., Cohen, D., and Reekie, M. 2010. Stimulation of Multilayered-Carbonate-Content Sandstone

Formations in West Africa Using Chelant-Based Fluids and Mechanical Diversion. Paper SPE 128043 presented at the SPE International Symposium and Exhibition on Formation Damage, Lafayette, Louisiana, 10-12 February. DOI:10.2188/128043-MS.

Portier, S., L. Andre and F. D. Vuataz. 2007. Review on Chemical Stimulation Techniques in Oil Industry and Applications to Geothermal Systems. Deep Heat Mining Association.

Rae, P.J. and Di Lullo, G. 2007. Single Step Matrix Acidizing with HF - Eliminating Preflushes Simplifies the Process, Improves the Results. Paper SPE 107296 presented at the European Formation Damage Conference, Scheveningen, The Netherlands, 30 May – 1 June. http://dx.doi.org/10.2118/107296-MS.

Reyes, E.A., Smith, A., and Beuterbaugh, A. 2013. Propterties and Application of an Alternative Aminopolycarboxylic Acid for Acidizing of Sandstones and Carbonates. Paper SPE 165142 presented at the SPE 10th European Formation Damage Conference & Exhibition, Noordwijk, The Netherlands, 5-7 June. http://dx.doi.org/10.2118/165142-MS.

Ross, D. and Di Lullo, G. 1998. "HV:HF" Acid Treatment, Proven Successful in South America." Paper IBP-SE-076/98 presented at the Rio Oil & Gas Conference, Rio de Janeiro, Brazil, 5-6 October.

Ross, G.J. 1969. Acid dissolution of Chlorites: Release of Magnesium, iron and Aluminum and Mode of Acid Attack. Clays and Clay Minerals **17** (6): 347-354. DOI:10.1346/CCMN.1969.0170604.

Rubini P., Lakatos A., Champmartin D. et al. 2002. Speciation and structural aspects of interactions of Al(III) with small biomolecules. Coord. Chem. Rev. **228** (2): 1797-1806. DOI: 10.1016/S0010-8545(01)00467-2.

Schlumberger 2003. Sand Control Pumping Service. pp. 37-70.

Shuchart, C.E. 1997. Chemical Study of Organic-HF Blends Leads to Improved Fluids. Paper SPE 37281 presented at the International Symposium on Oilfield Chemistry, Houston, 18–21 Feburary. http://dx.doi.org/10.2118/37281-MS.

Shuchart, C.E. and Buster, D.C. 1995. Determination of the Chemistry of HF Acidizing with the Use of 19F NMR Spectroscopy. Paper SPE 28975 presented at the SPE International Symposium on Oilfield Chemistry, San Antonio, TX, 14–17 Feb. http://dx.doi.org/10.2118/28975-MS.

Shuchart, C.E. andGdanski, R.D.1996. Improved Success in Acid Stimulation with a New Organic-HF System. Paper SPE36907 presented at European Petroleum Conference, Milan, Italy, 22-24 October. http://dx.doi.org/10.2118/36907-MS.

Simon, D.E. and Anderson, M.S. 1990. Stability of Clay Minerals in Acid. Paper SPE 19422 presented at the SPE Formation Damage Control Symposium held in Lafayette, Louisiana, 22-23 February. http://dx.doi.org/10.2118/19422-MS.

Sopngwi, J.-J.S., Gauthreaux, A., Kiburz, D.E. et al. 2014. Successful Application of a Differentiated Chelant-Based Hydrofluoric Acid for the Removal of Aluminosilicates, Fines, and Scale in Offshore Reservoirs of the Gulf of Mexico. Paper SPE 168171 presented at the SPE International Symposium and Exhibition

on Formation Damage Control, Lafayette, Louisiana, 26-28 February. http://dx.doi.org/10.2118/168171-MS.

Sur, S.K. and Bryant, R.G. 1996. 19F and 27Al n.m.r. spectroscopic study of the fluoro complexes of aluminum in aqueous solution and in zeolites: Dealumination of zeolites by fluoride ions. Zeolites **16** (2): 118-124. http://dx.doi.org/10.1016/0144-2449(95)00108-5.

Taylor, K.C., Al-Katheeri, M.I., Nasr-El-Din, H.A. et al. 2005. Development and Field Application of a New Measurement Technique for Organic Acid Additives in Stimulation Fluids. SPE J. **10** (2): 152-160. SPE-85081-PA. http://dx.doi.org/10.2118/85081-PA.

Thomas, R.L., Nasr-El-Din, H.A., Lynn, J.D. et al. 2001. Precipitation During the Acidizing of a HT/HP Illitic Sandstone Reservoir in Eastern Saudi Arabia: A Laboratory Study. Paper SPE 71690 presented at the SPE Annual Technical Conference and Exhibition, New Orleans, Louisiana, 30 September-3 October. http://dx.doi.org/10.2118/71690-MS.

Wehunt, C.D., Van Arsdale, H., Warner, J.L., and Ali, S.A.: 1993. Laboratory Acidization of an Eolian Sandstone at 380ºF. Paper SPE 25211 presented at the SPE International Symposium on Oilfield Chemistry held in New Orleans, LA, March 2-3.

Worden, R.H., and Morad, S., 2003. Clay Minerals in sandstones: Controls on formation, distribution and evolution, in Worden, R.H., and Morad, S., eds., Clay mineral cements in sandstones: Oxford, UK, International Association of

Sedimentologists Special Publication 34, Blackwell Science, p. 3-41. DOI: 10.1002/9781444304336.ch1. ISBN: 9781444304336

Yang, F., Nasr-El-Din, H.A., Al-Harbi, B.M. 2012. Acidizing Sandstone Reservoirs Using HF and Formic Acids. Paper SPE 150899 presented at the SPE International Symposium and Exhibition on Formation Damage Control, Lafayette, Louisiana, 15–17 February. http://dx.doi.org/10.2118/150899-MS.